This is to certify that the

dissertation entitled

BIOCHEMICAL GENETICS OF ABSCISIC ACID BIOSYNTHESIS

presented by

Christopher Dale Rock

has been accepted towards fulfillment
of the requirements for

Ph.D. degree in Genetics/Botany

Major professor

Date April 23, 1991

BIOCHEMICAL GENETICS OF ABSCISIC ACID BIOSYNTHESIS

By

Christopher Dale Rock

A DISSERTATION

Submitted to

Michigan State University

in partial fulfillment of the requirements

for the degree of

DOCTOR OF PHILOSOPHY

Program in Genetics

Department of Botany and Plant Pathology

1991

ABSTRACT

BIOCHEMICAL GENETICS OF ABSCISIC ACID BIOSYNTHESIS

by

Christopher Dale Rock

The iron chelators α,α-dipyridyl and *o*-phenanthroline inhibited abscisic acid (ABA) biosynthesis in water-stressed leaves of *Xanthium strumarium*. This supports the hypothesis that a non-heme oxygenase is involved in ABA biosynthesis. The onium-type plant growth retardant FC-907 inhibited ABA biosynthesis, but the anti-transpirant LAB 173711 did not.

ABA-aldehyde and ABA-*trans*-diol were quantified in apple (*Malus domestica*) fruits and leaves. ^{18}O-Labeling experiments established that [^{18}O]ABA-aldehyde was largely unlabeled in the side chain carbonyl group due to exchange of the carbonyl oxygen with water. This can explain the unusual labeling patterns of [^{18}O]ABA in labeling experiments with apple fruits. Based on specific activity of [^{18}O]ABA and [^{18}O]ABA-*trans*-diol, it is concluded that ABA-*trans*-diol is a catabolite of ABA. Results of feeding studies with [$^{2}H_6$]ABA-aldehyde and [$^{2}H_6$]ABA support the biosynthetic relationship ABA-aldehyde --> ABA --> ABA-*trans*-diol. A parallel pathway of *trans*-

ABA biosynthesis is proposed.

ABA and *trans*-ABA biosynthesis and metabolism were investigated in the ABA-deficient mutants of tomato (*Lycopersicon esculentum*), potato (*Solanum tuberosum*), barley (*Hordeum vulgare*) and *Arabidopsis thaliana*. In the tomato, potato, and barley mutants, a high percentage of [^{18}O]ABA and [^{18}O]*trans*-ABA was doubly-labeled in the side chain carboxyl group. Feeding studies in tomato with [$^{2}H_6$]ABA-alcohol and $^{18}O_2$ established that this doubly-carboxyl-labeled [^{18}O]ABA was synthesized from [^{18}O]ABA-alcohol with incorporation of molecular oxygen. ABA-alcohol oxidation was inhibited by carbon monoxide, which indicates the involvement of a cytochrome P-450 monooxygenase. This minor shunt pathway from ABA-aldehyde --> ABA-alcohol --> ABA operates in all species examined and is an important component of ABA biosynthesis in mutants impaired in ABA-aldehyde oxidation.

Analysis of carotenoids established that the *aba* mutant of *Arabidopsis* is impaired in epoxy-carotenoid biosynthesis. This result supports the hypothesis that ABA is synthesized from xanthophylls via oxidative cleavage of the epoxy-carotenoids violaxanthin and neoxanthin. *Trans*-ABA biosynthesis was less

affected than ABA biosynthesis in the *aba* genotypes. Feeding experiments suggest that *trans*-xanthoxin may be a precursor to ABA in *Arabidopsis*.

The xanthophyll cycle was utilized to specifically ^{18}O label the epoxy group of violaxanthin in spinach (*Spinacia oleracea*) leaves. Subsequent ABA biosynthesis resulted in ^{18}O incorporation specifically into the 1'-hydroxyl group of [^{18}O]ABA. This supports the precursor role of violaxanthin in ABA biosynthesis.

Dedicated to my mother

ACKNOWLEDGEMENTS

I would like to thank those who helped me in my work; Jan Zeevaart, Doug Gage, Tim Heath, and Kate Noon. I would also like to thank my committee members, Andrew Hanson, Hans Kende, John Ohlrogge, and Chris Somerville. I wish to thank Austen D. Warburton for his support and guidance since my father's death. And thanks to my friends, and especially Amy, for helping me through a challenging and rewarding time of my life.

Having pried through the strata, analyzed to a hair, counsel'd

with doctors and calculated close,

I find no sweeter fat than sticks to my own bones.

Walt Whitman

"Song of Myself"

Leaves of Grass

TABLE OF CONTENTS

Page

Appe

Appe

Appe

Appe

Page

LIST OF TABLES

Ta

4.1

4.2.

4.3.

4.4.

4.5.

Table Page

Tab

Table Page

Table Page

LIST OF FIGURES

LIST OF ABBREVIATIONS

ABA	(S)-(+)-abscisic acid
ABA-GE	ß-D-glucopyranosyl abscisate
ABA-*trans*-diol	1',4'-*trans*-ABA-diol
C	Celsius
Ci	Curie(s)
cv	cultivar
E	einstein
ECD	electron capture detection
EI	electron impact mass spectrometry
FAB	fast atom bombardment
FID	flame ionization detection
flc	*flacca*
fr	fresh
GC or GLC	gas-liquid chromatography
h	hour(s)

^2H	deuterium
^3H	tritium
HPLC	high performance liquid chromatography
K_d	partition coefficient
L	liter
M	molarity (moles per liter)
M^-	odd electron negative molecular ion
M^+	positive molecular ion
Me-	methyl ester derivative
min	minute(s)
MS	mass spectrometry
MS/MS	GLC-NCI-collisionally activated dissociation-tandem mass spectrometry
m/z	mass to charge ratio
N	normal (concentration)
NCI	negative chemical ionization
not	*notabilis*
o	*ortho*
PA	phaseic acid

PCI	positive chemical ionization
%	percent
R_T	retention time
SE	standard error of the mean
SIM	selected ion monitoring
sit	*sitiens*
t	*trans*
tert	*tertiary*
w or wt	weight
UV	ultraviolet radiation
v	volume

CHAPTER 1

INTRODUCTION

subst

of ch

highe

cyano

mamm

includ

promo

stresse

and C

althou

compo

et al., 1

ABA re

Weiler,

regulati

demons

1.1. OVERVIEW

Abscisic acid (ABA; Figure 1.1) is a sesquiterpene plant growth substance which was discovered in 1963 (for comprehensive review of chemical aspects, see Hirai, 1986). ABA has been found in all higher plants examined as well as in eukaryotic algae and cyanobacteria (Hirsch *et al.*, 1989). It has even been identified in mammalian brain (Chen *et al.*, 1988; Le-Page-Degivry *et al.*, 1986).

The physiological roles of ABA in plants are diverse and include: closure of stomata, regulation of growth and development, promotion of seed dormancy, and adaptation to environmental stresses (for review of ABA physiology and metabolism see Zeevaart and Creelman, 1988). The mechanisms of ABA action are unknown, although regulation of gene expression by *trans*-acting factors is one component of ABA signal transduction (Guiltinan *et al.*, 1990; Mundy *et al.*, 1990; Skriver and Mundy, 1990). Identification of a putative ABA receptor has been reported (Hocking *et al.*, 1978; Hornberg and Weiler, 1984) but these reports have not been reproduced. ABA regulation of intracellular calcium concentrations has recently been demonstrated (McAinsh *et al.*, 1990; Schroeder and Hagiwara, 1990;

Gehri

in AB

thalia

signa

Finke

mutar

the A

McC

Figure

Gehring *et al.*, 1990), suggesting that calcium is a second messenger in ABA action. The three ABA-insensitive mutants of *Arabidopsis thaliana* (*abi-1, -2, -3)* are likely to correspond to blocks in the ABA signal transduction pathway(s) (Koornneef *et al.*, 1984, 1989; Finkelstein and Somerville, 1990). The maize *viviparous-1 (vp-1)* mutant is ABA-insensitive and identifies a gene which is involved in the ABA response during seed development (Robichaud *et al.*, 1980; McCarty *et al.*, 1989).

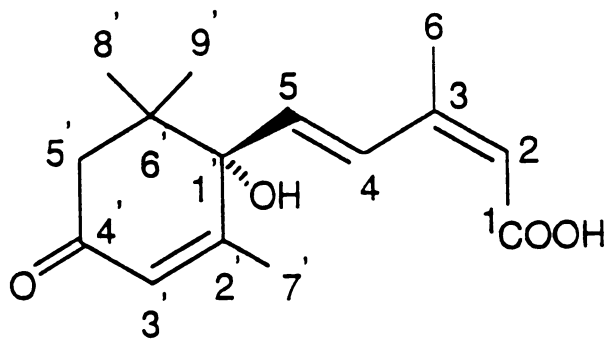

Figure 1.1. The structure of S-(+)-abscisic acid (ABA).

1.2. ABA BIOSYNTHESIS

Although the structure of ABA has been known for 25 years, the biosynthetic pathway has still not been fully elucidated. Two possible pathways are: the "direct" pathway involving a C_{15} precursor derived from cyclization of farnesyl pyrophosphate, or the "indirect" pathway involving epoxy-carotenoids and xanthoxin as intermediates. Some phytopathogenic fungi synthesize ABA via a direct pathway (Neill *et al.*, 1984; Okamoto *et al.*, 1988) which involves ionylidene derivatives. In higher plants the evidence for the direct pathway is low level incorporation of mevalonic acid into ABA (Milborrow, 1974; Hartung *et al.*, 1981; Cowan and Railton, 1987). These data are not inconsistent with the indirect pathway hypothesis. The evidence for the indirect pathway is more substantial: a) The *viviparous* mutants of maize are blocked in the early stages of carotenoid biosynthesis and are ABA-deficient (Figure 1.2; Moore and Smith, 1985; Neill *et al.*, 1986). b) The carotenoid biosynthesis inhibitors fluridone and norflurazon also inhibit ABA biosynthesis (Moore and Smith, 1984; Henson, 1984; Quarrie and Lister, 1984; Gamble and Mullet, 1986). c) $^{18}O_2$-Labeling experiments with

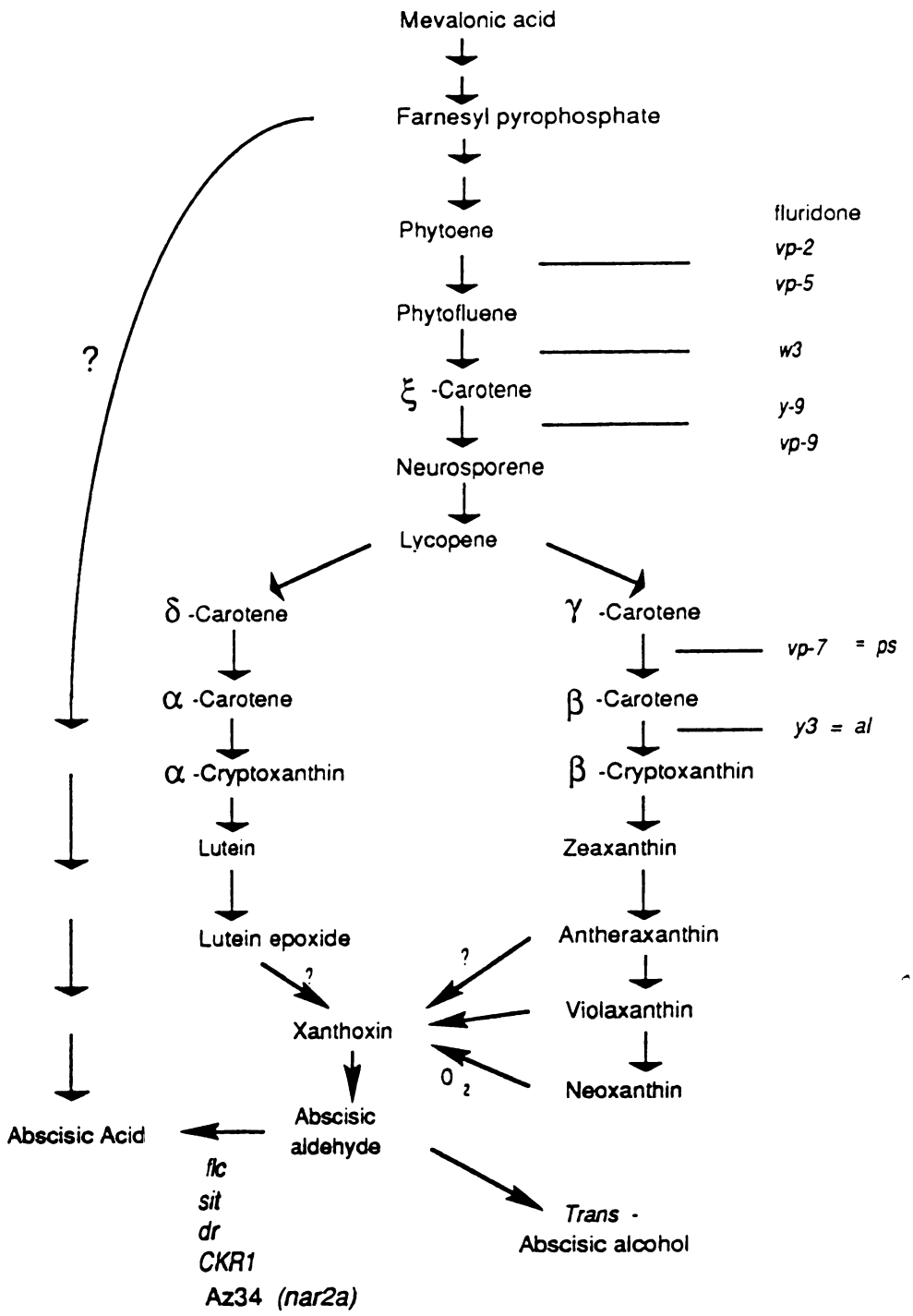

Figure 1.2. Proposed pathways to ABA, showing characterized biosynthetic mutants.

water-stressed leaves show ^{18}O incorporation into the side chain carboxyl group of ABA, but little incorporation in the ring oxygen positions (Creelman *et al.*, 1987; Zeevaart *et al.*, 1989), indicating that there is a large ABA precursor pool (presumably xanthophylls) which contains oxygens on the ring. d) Xanthoxin, a C_{15}-breakdown product of epoxy-carotenoids, is found in plants (Parry *et al.*, 1990) and is readily converted to ABA *in vivo* (Taylor and Burden, 1973; Parry *et al.*, 1988) and by cell-free plant extracts (Sindhu and Walton, 1988; Sindhu *et al.*, 1990). e) Most recently, a 1:1 correlation on a molar basis between decreases in *trans*-violaxanthin and 9'-*cis*-neoxanthin levels and concomitant increases in ABA and its catabolites has been shown for dark-grown, water-stressed bean leaves (Li and Walton, 1990; Parry *et al.*, 1990).

There are ABA-deficient chlorophyll-containing mutants in potato (Quarrie, 1982), tomato (Tal and Nevo, 1973; Parry *et al.*, 1988; Taylor *et al.*, 1988; Sindhu and Walton, 1988), barley (Walker-Simmons *et al.* 1989), *Arabidopsis thaliana* (Koornneef *et al.*, 1982; Koornneef, 1985), pea (Wang *et al.*, 1984), maize (Neill *et al.*, 1986) and *Nicotiana plumbaginifolia* (Parry *et al.*, 1991). The *flacca* and *sitiens* of tomato, *droopy* potato, the molybenum cofactor mutant

Az34 (*nar2*) of barley and the recently discovered wilty mutant of *N. plumbaginifolia, CKR1*, are blocked in ABA-aldehyde oxidation (Taylor *et al.*, 1988; Duckham *et al.*, 1989; Walker-Simmons *et al.*, 1989; Sindhu *et al.*, 1990; Parry *et al.*, 1991); the *flacca* and *sitiens* mutants and the wilty *Nicotiana* mutant accumulate *trans*-ABA-alcohol as a result of the biosynthetic block (Figure 1.2; Linforth *et al.*, 1987; Taylor *et al.*, 1988; Parry *et al.*, 1991). The *wilty* mutant of pea can accumulate ABA in response to water stress (Wang *et al.*, 1984) and it is therefore unclear whether it is an ABA biosynthetic mutant.

1.3. STATEMENT OF PURPOSE

The goal of the research presented in this dissertation was to elucidate the biosynthetic pathway of ABA in higher plants. Toward this end, three approaches were used: 1) Experiments aimed at identifying inhibitors of ABA biosynthesis; 2) Feeding of stable isotopes ($^{18}O_2$, [^{2}H]-labeled ABA precursors) and analysis of labeled ABA by mass spectrometry to study ABA biosynthesis *in vivo*; and 3) characterization of ABA biosynthesis in the ABA-deficient mutants of

tomat

Cher

Cowa

Creel

Duck

Finke

Gamb

Gehri

Guild

tomato, potato, barley, and *Arabidopsis thaliana*.

1.4. LITERATURE CITED

Chen FSC, MacTaggart JM, Wang LCH, Westly JC (1988) Analysis of abscisic acid in the brains of rodents and ruminants. Agric Biol Chem **52**: 1273-1274

Cowan AK, Railton ID (1987) The biosynthesis of abscisic acid in a cell-free system from embryos of *Hordeum vulgare*. J Plant Physiol **131**: 423-431

Creelman RA, Gage DA, Stults JT, Zeevaart JAD (1987) Abscisic acid biosynthesis in leaves and roots of *Xanthium strumarium*. Plant Physiol **85**: 726-732

Duckham SC, Taylor IB, Linforth RST, Al-Naieb RJ, Marples BA, Bowman WR (1989) The metabolism of *cis* ABA-aldehyde by the wilty mutants of potato, pea and *Arabidopsis thaliana*. J Exp Bot **40**: 901-905

Finkelstein RR, Somerville CR (1990) Three classes of abscisic acid (ABA)-insensitive mutations of *Arabidopsis* define genes that control overlapping subsets of ABA responses. Plant Physiol **94**: 1172-1179

Gamble PE, Mullet JE (1986) Inhibition of carotenoid accumulation and abscisic acid biosynthesis in fluridone-treated dark-grown barley. Eur J Biochem **160**: 117-121

Gehring CA, Irving HR, Parish RW (1990) Effects of auxin and abscisic acid on cytosolic calcium and pH in plant cells. Proc Natl Acad Sci USA **87**: 9645-9649

Guiltinan MJ, Marcotte WR, Quatrano RS (1990) A plant leucine zipper protein that recognizes an abscisic acid response element. Science **250**: 267-271

Ha

He

Hi

Hi

Ho

Ho

Ko

Ko

Ko

Ko

Hartung W, Heilmann B, Gimmler H (1981) Do chloroplasts play a role in abscisic acid synthesis? Plant Sci Lett **22**: 235-242

Henson IE (1984) Inhibition of abscisic acid accumulation in seedling shoots of pearl millet (*Pennisetum americanum* L. Leeke) following induction of chlorosis by norflurazon. Z Pflanzenphysiol **114**: 35-43

Hirai N (1986) Abscisic acid. *In* N Takahashi, ed, Chemistry of Plant Hormones. Boca Raton, FL, CRC Press, pp 201-248

Hirsch R, Hartung W, Gimmler H (1989) Abscisic acid content of algae under stress. Bot Acta **102**: 326-334

Hocking TJ, Clapham J, Cattell KJ (1978) Abscisic acid binding to subcellular fractions from leaves of *Vicia faba*. Planta **138**: 303-304

Hornberg C, Weiler EW (1984) High-affinity binding sites for abscisic acid on the plasmalemma of *Vicia faba* guard cells. Nature **310**: 321-324

Koornneef M (1985) Genetic aspects of abscisic acid. *In* J King, ed, Plant Gene Research. Berlin, Springer, pp 35-54

Koornneef M, Hanhart CJ, Hilhorst HMW, Karssen CM (1989) *In vivo* inhibition of seed development and reserve protein accumulation in recombinants of abscisic acid biosynthesis and responsiveness mutants of *Arabidopsis thaliana* Plant Physiol **90**: 463-469

Koornneef M, Jorna ML, Brinkhorst-van der Swan DLC, Karssen CM (1982) The isolation of abscisic acid (ABA) deficient mutants by selection of induced revertants in non-germinating gibberellin sensitive lines of *Arabidopsis thaliana* (L.) Heynh. Theor Appl Genet **61**: 385-393

Koornneef M, Reuling G, Karssen CM (1984) The isolation and characterization of abscisic acid-insensitive mutants of *Arabidopsis thaliana*. Physiol Plant **61**: 377-383

Le Pa

Li Y, V

Linfor

McAi

McC

Milbo

Moor

Moor

Mund

Neill

Neill

Le Page-Degivry M-T, Bidard J-N, Rouvier E, Bulard C, Lazdunski M (1986) Presence of abscisic acid, a phytohormone, in the mammalian brain. Proc Natl Acad Sci USA **83**: 1155-1158

Li Y, Walton DC (1990) Violaxanthin is an abscisic acid precursor in water-stressed dark-grown bean leaves. Plant Physiol **92**: 551-559

Linforth RST, Bowman WR, Griffin DA, Marples BA, Taylor IB (1987) 2-*trans*-ABA-alcohol accumulation in the wilty tomato mutants *flacca* and *sitiens*. Plant Cell Environ **10**: 599-606

McAinsh MR, Brownlee C, Hetherington AM (1990) Abscisic acid-induced elevation of guard cell cytosolic Ca^{2+} precedes stomatal closure. Nature **343**: 186-188

McCarty DR, Carson CB, Stinard PS, Robertson DS (1989) Molecular analysis of *viviparous-1*: an abscisic acid-insensitive mutant of maize. Plant Cell **1**: 523-532

Milborrow BV (1974) Biosynthesis of abscisic acid by a cell-free system. Phytochemistry **13**: 131-136

Moore R, Smith JD (1984) Growth, graviresponsiveness and abscisic acid content of *Zea mays* seedlings treated with fluridone. Planta **162**: 342-344

Moore R, Smith JD (1985) Graviresponsiveness and abscisic acid content of roots of carotenoid-deficient mutants of *Zea mays* L. Planta **164**: 126-128

Mundy J, Yamaguchi-Shinozaki K, Chua N-H (1990) Nuclear proteins bind conserved elements in the abscisic acid-responsive promoter of a rice *rab* gene. Proc Natl Acad Sci USA **87**: 1406-1410

Neill SJ, Horgan R, Parry AD (1986) The carotenoid and abscisic acid content of viviparous kernels and seedlings of *Zea mays* L. Planta **169**: 87-96

Neill SJ, Horgan R, Walton DC (1984) Biosynthesis of abscisic acid.

Okar

Parr

Parr

Parr

Parr

Quar

Quar

Robi

Schr

Skrive

In A Crozier, JR Hillman, eds, The Biosynthesis and Metabolism of Plant Hormones. Soc Exper Biol Seminar Ser **23**, Cambridge, Cambridge University Press, pp 43-70

Okamoto M, Hirai N, Koshimizu K (1988) Biosynthesis of abscisic acid. Mem Coll Agric Kyoto Univ **132**: 79-115

Parry AD, Babiano MJ, Horgan R (1990) The role of *cis*-carotenoids in abscisic acid biosynthesis. Planta **182**: 118-128

Parry AD, Blonstein AD, Babiano MJ, King PJ, Horgan R (1991) Abscisic acid metabolism in a wilty mutant of *Nicotiana plumbaginifolia*. Planta **183**: 237-243

Parry AD, Neill SJ, Horgan R (1988) Xanthoxin levels and metabolism in the wild-type and wilty mutants of tomato. Planta **173**: 397-404

Parry AD, Neill SJ, Horgan R (1990) Measurement of xanthoxin in higher plant tissues using ^{13}C labelled internal standards. Phytochemistry **29**: 1033-1039

Quarrie SA (1982) Droopy: a wilty mutant of potato deficient in abscisic acid. Plant Cell Environ **5**: 23-26

Quarrie SA, Lister PG (1984) Evidence of plastid control of abscisic acid accumulation in barley (*Hordeum vulgare* L.). Z Pflanzenphysiol **114**: 295-308

Robichaud CS, Wong J, Sussex IM (1980) Control of *in vitro* growth on viviparous embryo mutants of maize by abscisic acid. Dev Genet **1**: 325-330

Schroeder JI, Hagiwara S (1990) Repetitive increases in cytosolic Ca^{2+} of guard cells by abscisic acid activation of nonselective Ca^{2+} permeable channels. Proc Natl Acad Sci USA **87**: 9305-9309

Skriver K, Mundy J (1990) Gene expression in response to abscisic acid and osmotic stress. Plant Cell **2**: 503-512

Sindhu RK, Griffin DH, Walton DC (1990) Abscisic aldehyde is an intermediate in the enzymatic conversion of xanthoxin to abscisic acid in *Phaseolus vulgaris* L. leaves. Plant Physiol **93**: 689-694

Sindhu RK, Walton DC (1988) Xanthoxin metabolism in cell-free preparations from wild type and wilty mutants of tomato. Plant Physiol **88**: 178-182

Tal M, Nevo Y (1973) Abnormal stomatal behavior and root resistance, and hormonal imbalance in three wilty mutants of tomato. Biochem Genet **8**: 291-300

Taylor HF, Burden RS (1973) Preparation and metabolism of 2-[^{14}C]-*cis,trans*-xanthoxin. J Exp Bot **24**: 873-880

Taylor IB, Linforth RST, Al-Naieb RJ, Bowman WR, Marples BA (1988) The wilty mutants *flacca* and *sitiens* are impaired in the oxidation of ABA-aldehyde to ABA. Plant Cell Environ **11**: 739-745

Wang TL, Donkin ME, Martin ES (1984) The physiology of a wilty pea: abscisic acid production under water stress. J Exp Bot **35**: 1222-1232

Walker-Simmons M, Kudra DA, Warner RL (1989) Reduced accumulation of ABA during water stress in a molybdenum cofactor mutant of barley. Plant Physiol **90**: 728-733

Zeevaart JAD, Creelman RA (1988) Metabolism and physiology of abscisic acid. Annu Rev Plant Physiol Plant Mol Biol **39**: 439-473

Zeevaart JAD, Heath TG, Gage DA (1989) Evidence for a universal pathway of abscisic acid biosynthesis in higher plants from ^{18}O incorporation patterns. Plant Physiol **91**: 1594-1601

CHAPTER 2

THE IRON CHELATORS α,α-DIPYRIDYL AND *o*-PHENANTHROLINE, AND THE GROWTH RETARDANT FC-907, INHIBIT ABSCISIC ACID BIOSYNTHESIS

2.1. INTRODUCTION

With the exception of fluridone and norflurazon, which inhibit the early desaturation steps of carotenoid biosynthesis (Böger and Sandmann, 1989) and thereby inhibit the indirect pathway of ABA biosynthesis by decreasing the precursor pool of xanthophylls (Henson, 1984; Quarrie and Lister, 1984; Moore and Smith, 1985; Gamble and Mullet, 1986; Li and Walton, 1987), no inhibitors of ABA biosynthesis in plants have been discovered. Paclobutrazol, an inhibitor of cytochrome P-450 enzymes involved in gibberellin and sterol biosynthesis (Hedden, 1983; Benveniste, 1986), also inhibits ABA biosynthesis in the fungus *Cercospora rosicola* (Norman *et al.*, 1986) but only marginally in apple leaves (Wang *et al.*, 1987).

The present study was undertaken to determine if the iron chelators, α,α-dipyridyl and *o*-phenanthroline (Figure 2.1), which inhibit dioxygenases involved in proline hydroxylation (Holleman, 1967; Chrispeels, 1970) and gibberellin biosynthesis (Hedden and Graebe, 1982; Hedden, 1983), could also inhibit ABA biosynthesis. This would support the hypothesis that a dioxygenase is involved in cleavage of epoxy-carotenoids during ABA biosynthesis (Creelman

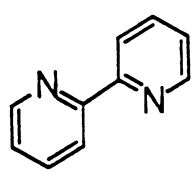

A

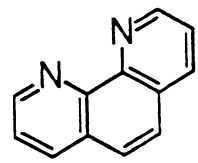

B

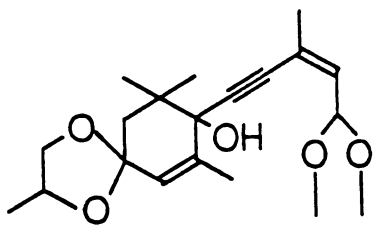

C

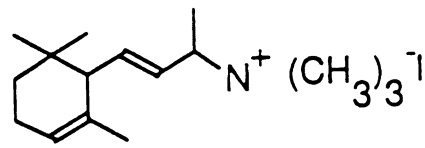

D

Figure 2.1. Structures of α,α-dipyridyl (A), *o*-phenanthroline (B), LAB 173711 (C), FC-907 (D).

et al., 1987). A second hypothesis was tested, *viz*, that ABA structural analogs can inhibit ABA biosynthesis by competitive binding to biosynthetic enzymes, or by a feedback mechanism (Milborrow, 1978).

2.2. MATERIALS AND METHODS

Xanthium strumarium, L., Chicago strain, was grown in a greenhouse under a photoperiod of 20 h to keep the plants in the vegetative state. Growing conditions were as described (Raschke and Zeevaart, 1976). Leaves (average weight 5 g) with petiole were detached using a razor blade and immediately immersed in water for 10 min. Stock solutions of compounds were diluted to various concentrations in 3 mL of water and taken up by leaves through the petioles under dim fluorescent light for 1.5 h. After the solutions were taken up by the leaves, an additional 2 mL of water were taken up for 1 h in darkness, then the blades were detached from the petioles and water-stressed with a hair dryer until 12% of the fresh weight was lost. Leaves were placed in plastic bags and incubated in the dark at room temperature for 4.5 h and frozen.

If PA was to be analyzed, the leaf was bisected through the midrib and one-half of the leaf frozen, while the other half was rehydrated in distilled water for 5 min and incubated in the dark for an additional 4 h and then frozen. ABA and PA were extracted, purified and quantified as described (Zeevaart, 1980). The compound LAB 173711 was the gift of Dr. J. Jung, BASF, D-6703 Limburgerhof, Germany. The compound FC-907 (*N,N,N,*-trimethyl-1-methyl-2',6',6'-trimethylcyclohex-2'-en-1'-yl) prop-2-enylammonium iodide) was the gift of Dr. Y. Kamuro, Tsukuba Research Laboratories, Ibaraki 300-26, Japan. The iron chelators, α,α-dipyridyl and *o*-phenanthroline, were purchased from Aldrich Chemical, Milwaukee, WI.

2.3. RESULTS AND DISCUSSION

2.3.1. Feeding Studies with Iron Chelators

The effects of various concentrations of α,α-dipyridyl on ABA accumulation in water-stressed *Xanthium* leaves are presented in Figure 2.2. There was a clear inhibition of ABA accumulation at high (3.2 mM) concentrations of α,α-dipyridyl. Figure 2.3 presents the

Fig

acc

was

wat

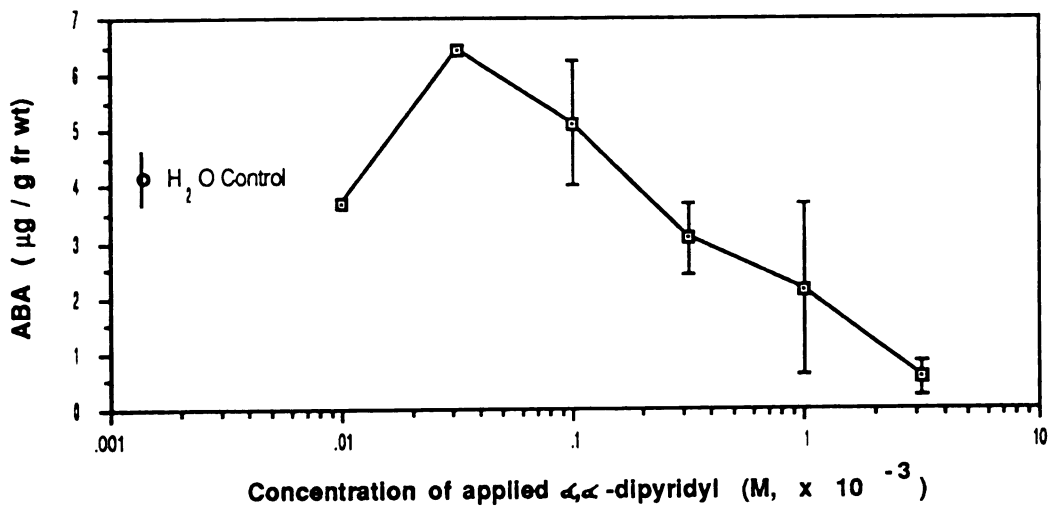

Figure 2.2. The effect of various α,α-dipyridyl concentrations on ABA accumulation in *Xanthium* leaves. A leaf (approximately 5 g fr wt) was fed 3 mL of water or a solution of α,α-dipyridyl, and was then water-stressed for 4.5 h.

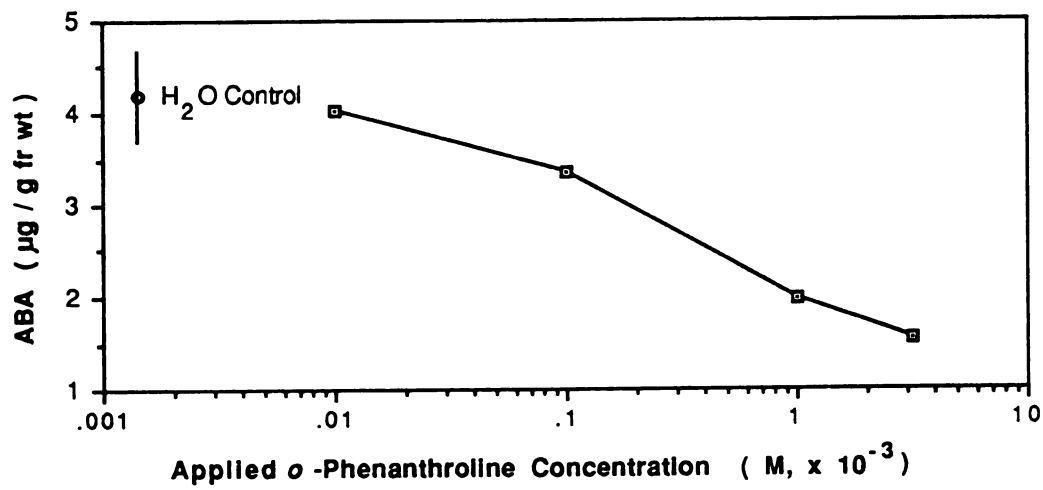

Figure 2.3. The effect of various *o*-phenanthroline concentrations on ABA accumulation in *Xanthium* leaves. Experimental conditions as described in Figure 2.2.

results of a similar experiment with *o*-phenanthroline. Because there are no reports in the literature of heme mono-oxygenase inhibition by α,α-dipyridyl, we interpret these results as evidence for the involvement of a non-heme dioxygenase in ABA biosynthesis. Iron deficiency does not affect the synthesis of violaxanthin (Morales *et al.*, 1990), and carbon monoxide, an inhibitor of heme monooxygenases, does not inhibit zeaxanthin epoxidation (data not shown). Therefore, the most likely ABA biosynthetic step which would involve a dioxygenase would be the cleavage step, where 9-*cis*-violaxanthin or 9'-*cis*-neoxanthin is cleaved to xanthoxin and a C_{25}-apocarotenal with insertion of O_2. This hypothesis is analogous to the cleavage enzyme which synthesizes vitamin A (retinal) from ß-carotene in animals (Ganguly and Sastry, 1985) and ß-carotene oxidase of *Microcystis* (Jüttner and Hoflächer, 1985). Evidence in support of the cleavage enzyme hypothesis, aside from the circumstantial evidence for the indirect pathway of ABA biosynthesis (Li and Walton, 1990; Parry *et al.*, 1990, Chapter 5), is the incorporation of ^{18}O from $^{18}O_2$ into the side chain carboxyl group of ABA during stress-induced ABA biosynthesis (Creelman *et al.*, 1987), and the observation that carbon monoxide, a specific inhibitor of

heme monooxygenases, does not inhibit stress-induced ABA biosynthesis (data not shown; see Chapter 4).

It has been shown that α,α-dipyridyl causes increases in seedling hypocotyl elongation rates (Barnett, 1970; Lang, 1976). It was proposed that hydroxyproline synthesis in the cell wall might play a causal role in cell wall extensibility and elongation. However, Lang (1976) showed that light-induced inhibition of radish hypocotyl elongation did not result in increased hydroxyproline deposition in the cell wall and suggested that the effect of α,α-dipyridyl on elongation may be unrelated to its inhibition of hydroxyproline biosynthesis. In light of the results of Figures 2.2 and 2.3, which show inhibition of ABA biosynthesis by α,α-dipyridyl and *o*-phenanthroline, we hypothesize that inhibition of ABA biosynthesis by iron chelators may result in stimulation of hypocotyl elongation. Bensen *et al.* (1988) have shown that increased levels of ABA result in inhibition of soybean hypocotyl elongation; it follows that reduced levels of ABA associated with inhibition of ABA biosynthesis may enhance elongation. This hypothesis is supported by experiments with rice coleoptiles; treatment with fluridone caused an increase in growth rate (Hoffmann and Kende, 1990). However, this

interpretation is complicated by the involvement of ethylene in hypocotyl elongation. The ethylene-forming enzyme requires iron and ascorbate for activity (Ververdis and John, 1991) and is inhibited *in vivo* by *o*-phenanthroline (H. Kende, personal communication).

2.3.2. Feeding Studies with LAB 173711

The effect of various LAB 173711 concentrations on stress-induced ABA accumulation in *Xanthium* leaves is shown in Figure 2.4. There was little inhibition of ABA accumulation, even at high (3.2 mM) concentrations of LAB 173711. When leaves were re-hydrated for 4 h after the water stress treatment, ABA levels decreased and PA levels increased about 2 fold at all LAB173711 concentrations tested (data not shown). This suggests that LAB 173711 did not inhibit ABA hydroxylation or other metabolic processes in general. LAB 173711 has been shown to have ABA-like activity in physiological processes such as stomatal closing and promotion of senescence (Jung and Grossmann, 1985; Schubert *et al.*, 1991). If LAB 173711 has an inhibitory effect on ABA biosynthesis, it is a subtle one, based on the inconclusive data of Figure 2.4. A feedback mechanism which down-regulates ABA biosynthesis at high ABA concentrations has been proposed

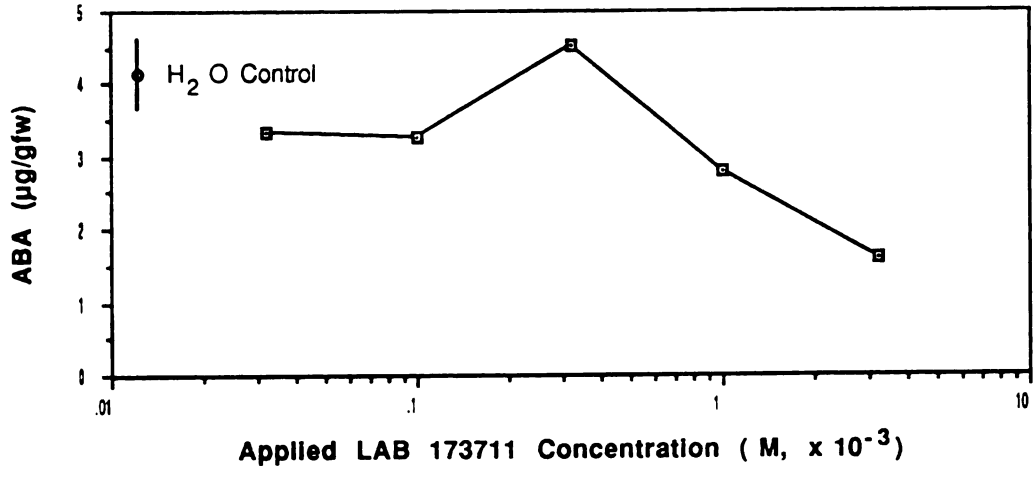

Figure 2.4. The effect of various LAB 173711 concentrations of ABA accumulation in *Xanthium* leaves. Experimental conditions as described in Figure 2.2.

(Milborrow, 1978). If LAB 173711 functions as an ABA analog which can interact with an ABA-receptor, then its effect at high concentrations may be due to feedback inhibition of ABA biosynthesis.

2.3.3. Feeding Studies with FC-907

The compound FC 907 (Figure 2.1D) is an onium type plant growth retardant (Haruta *et al.*, 1974) similar to other quaternary ammonium compounds such as AMO-1618 and chlorocholine chloride (CCC), which inhibit *ent*-kaurene synthetase activity A (Hedden, 1983). FC-907 also inhibits gibberellin biosynthesis in fungi (Hedden *et al.*, 1977). Figure 2.5 shows the effects of various concentrations of FC 907 on ABA accumulation in water-stressed *Xanthium* leaves. There is an inhibitory effect on ABA biosynthesis at the highest (3.2 mM) concentration of FC 907. It is unknown whether the inhibition of ABA accumulation is due to a specific effect on ABA biosynthesis, or to a more general inhibition of metabolism.

In the inhibition studies described here, the extent of uptake and the final intracellular concentrations of compounds were unknown. This may account for the variability in ABA accumulation at low concentrations of inhibiting compounds compared with

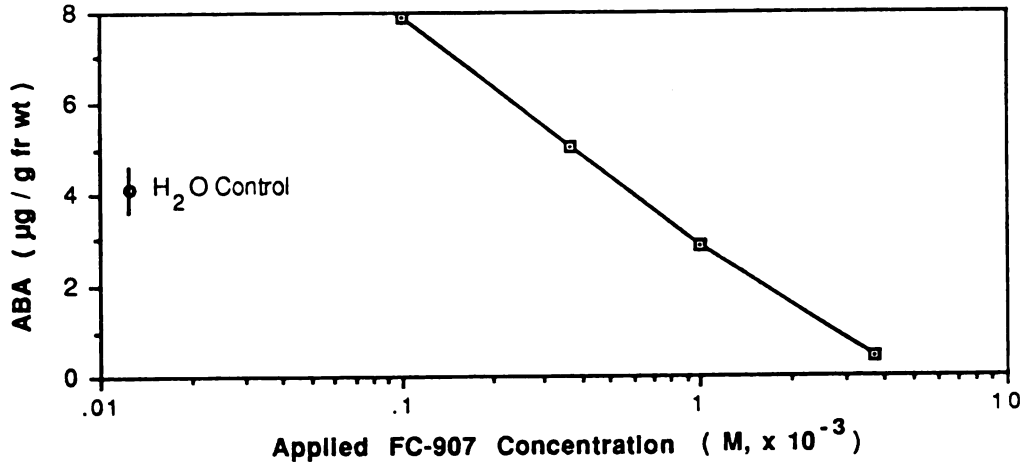

Figure 2.5. The effect of various concentrations of FC-907 on ABA accumulation in *Xanthium* leaves. Experimental conditions as described in Figure 2.2.

control leaves which took up water (Figures 2.2-2.5). Ultimately the mechanism of ABA biosynthesis inhibition can only be resolved *in vitro* with purified ABA biosynthetic enzymes.

2.4. LITERATURE CITED

Barnett NM (1970) Dipyridyl-induced cell elongation and inhibition of cell wall hydroxyproline biosynthesis. Plant Physiol **45**: 188-191

Bensen RJ, Boyer JS, Mullet JE (1988) Water deficit-induced changes in abscisic acid, growth, polysomes, and translatable RNA in soybean hypocotyls. Plant Physiol **88**: 289-294.

Benviste P (1986) Sterol biosynthesis. Annu Rev Plant Physiol **37**: 275-308

Chrispeels MJ (1970) Synthesis and secretion of hydroxyproline-containing macromolecules in carrots. II. *In vivo* conversion of peptidyl proline to peptidyl hydroxyproline. Plant Physiol **45**: 223-227

Creelman RA, Gage DA, Stults JT, Zeevaart JAD (1987) Abscisic acid biosynthesis in leaves and roots of *Xanthium strumarium*. Plant Physiol **85**: 726-732

Ganguly J, Sastry PS (1985) Mechanism of conversion of ß-carotene into vitamin A: central cleavage versus random cleavage. Wld Rev Nutr Diet **45**: 198-220

Haruta H, Yagi H, Iwata T, Tamura S (1974) Syntheses and plant growth retardant activities of trimethyl-ammonium compounds containing a terpenoid moiety. Agr Biol Chem **38**: 141-148

Hedden P (1983) *In vitro* metabolism of gibberellins. *In* A Crozier, ed, The Biochemistry and Physiology of Gibberellins, Vol. I. New York, Praeger, pp 99-149

Hedden P, Graebe JE (1982) Cofactor requirements for the soluble oxidases in the metabolism of the C_{20}-gibberellins. J Plant Growth Regul **1**: 105-116

Hedden P, Phinney BO, MacMillan J, Sponsel VM (1977) Metabolism of kaurenoids by *Gibberella fujikuroi* in the presence of the plant growth retardant, *N,N,N,*-trimethyl-1-methyl-2',6',6'-trimethylcyclohex-2'-en-1'-yl) prop-2-enylammonium iodide. Phytochemistry **16**: 1913-1917

Henson IE (1984) Inhibition of abscisic acid accumulation in seedling shoots of pearl millet (*Pennisetum americanum* [L.] Leeke) following induction of chlorosis by norflurazon. Z Pflanzenphysiol **114**: 35-43

Hoffmann S, Kende H (1990) The role of ABA in the growth of rice coleoptiles. Plant Physiol **93**: S71.

Holleman J (1967) Direct incorporation of hydroxyproline into protein of sycamore cells incubated at growth-inhibitory levels of hydroxyproline. Proc Natl Acad Sci USA **57**: 50-54

Jung J, Grossmann K (1985) Effectiveness of new terpenoid derivatives, abscisic acid and its methyl ester on transpiration and leaf senescence of barley. J Plant Physiol **121**: 361-367

Jüttner F, Hoflächler B (1985) Evidence of ß-carotene 7,8(7',8') oxygenase (ß-cyclocitral, crocetindial generating) in *Microcystis*. Arch Microbiol **141**: 337-343

Lang W (1976) Biosynthesis of extensin during normal and light-inhibited elongation of radish hypocotyls. Z Pflanzenphysiol **78**: 228-235

Li Y, Walton DC (1987) Xanthophylls and abscisic acid biosynthesis

in water-stressed bean leaves. Plant Physiol **85**: 910-915

Li Y, Walton DC (1990) Violaxanthin is an abscisic acid precursor in water-stressed dark-grown bean leaves. Plant Physiol **92**: 551-559

Milborrow BV (1978) Abscisic acid. *In* DS Letham, PB Goodwin, TJV Higgins, eds, Phytohormones and Related Compounds: A Comprehensive Treatise, Vol 1. Elsevier/North-Holland, New York, pp 295-347

Morales F, Abadía A, Abadía J (1990) Characterization of the xanthophyll cycle and other photosynthetic pigment changes induced by iron deficiency in sugarbeet (*Beta vulgaris* L.) Plant Physiol **94**: 607-613

Moore R, Smith JD (1984) Growth, graviresponsiveness and abscisic acid content of *Zea mays* seedlings treated with fluridone. Planta **162**: 342-344

Norman SM, Bennett RD, Poling SM, Maier VP, Nelson MD (1986) Paclobutrazole inhibits abscisic acid biosynthesis in *Cercospora rosicola*. Plant Physiol **80**: 122-125

Parry AD, Babiano MJ, Horgan R (1990) The role of *cis*-carotenoids in abscisic acid biosynthesis. Planta **182**: 118-128

Quarrie SA, Lister PG (1984) Evidence of plastid control of abscisic acid accumulation in barley (*Hordeum vulgare* L.). Z Pflanzenphysiol **114**: 295-308

Raschke K, Zeevaart JAD (1976) Abscisic acid content, transpiration, and stomatal conductance as related to leaf age in plants of *Xanthium strumarium* L. Plant Physiol **58**: 169-174

Sandmann G, Böger P (1989) Inhibition of carotenoid biosynthesis by herbicides. *In* P Böger, G Sandmann, eds, Target Sites of Herbicide Action. CRC Press, Boca Raton, FL, pp 25-44

Schubert J, Röser K, Grossmann K, Sauter H, Jung J (1991) Transpiration-inhibiting abscisic acid analogs. J Plant Growth Regul **10**: 27-32

Ververdis P, John P (1991) Complete recovery *in vitro* of ethylene-forming enzyme activity. Phytochemistry **30**: 725-727.

Wang SY, Sun T, Ji ZL, Faust M (1987) Effect of paclobutrazole on water stress-induced abscisic acid in apple seedling leaves. Plant Physiol **84**: 1051-1054

Zeevaart JAD (1980) Changes in the levels of abscisic acid and its metabolites in excised leaf blades of *Xanthium strumarium* during and after water stress. Plant Physiol **66**: 672-678

CHAPTER 3

ABSCISIC (ABA)-ALDEHYDE IS A PRECURSOR TO, AND 1', 4'-*TRANS*-DIOL A CATABOLITE OF, ABA IN APPLE

Plant Phy
0032-0889

M

Previous
shown that
synthesize
the " -hydr
Zeevaart
1601. It w
with the m
ABA biosy
trans-ABA-
and measu
tandem ma
bryde ABA
precursor t
of °C in the
of °C from
ments with
precursor-p
trans-diol
fruits and le
per gram f
respectiven
nanograms
10-fold lowe
was conjug
leaves ABA
pathways fo
in fruits and

Evidence
biosynthes
mutants of
specific inh
biosynthes
from 10
biosynthes
pool that co
Li and Wa
amount and
grown dea

Supported
AC
DE
Ana
Ma

Plant Physiol. (1990) 93, 915–923
0032-0889/90/93/0915/09/$01.00/0

Received for publication December 7, 1989
Accepted March 19, 1990

Abscisic (ABA)-Aldehyde Is a Precursor to, and 1′,4′-*trans*-ABA-Diol a Catabolite of, ABA in Apple[1]

Christopher D. Rock and Jan A. D. Zeevaart*

Michigan State University-Department of Energy Plant Research Laboratory, Michigan State University, East Lansing, Michigan 48824-1312

ABSTRACT

Previous ^{18}O labeling studies of abscisic acid (ABA) have shown that apple (*Malus domestica* Borkh. cv Granny Smith) fruits synthesize a majority of [^{18}O]ABA with the label incorporated in the 1′-hydroxyl position and unlabeled in the carboxyl group (JAD Zeevaart, TG Heath, DA Gage [1989] Plant Physiol 91: 1594–1601). It was proposed that exchange of ^{18}O in the side chain with the medium occurred at an aldehyde intermediate stage of ABA biosynthesis. We have isolated ABA-aldehyde and 1′-4′-*trans*-ABA-diol (ABA-*trans*-diol) from ^{18}O-labeled apple fruit tissue and measured the extent and position of ^{18}O incorporation by tandem mass spectrometry. ^{18}O-Labeling patterns of ABA-aldehyde, ABA-*trans*-diol, and ABA indicate that ABA-aldehyde is a precursor to, and ABA-*trans*-diol a catabolite of, ABA. Exchange of ^{18}O in the carbonyl of ABA-aldehyde can be the cause of loss of ^{18}O from the side chain of [^{18}O]ABA. Results of feeding experiments with deuterated substrates provide further support for the precursor-product relationship of ABA-aldehyde → ABA → ABA-*trans*-diol. The ABA-aldehyde and ABA-*trans*-diol contents of fruits and leaves were low, approximately 1 and 0.02 nanograms per gram fresh weight for ABA-aldehyde and ABA-*trans*-diol, respectively, while ABA levels in fruits ranged from 10 to 200 nanograms per gram fresh weight. ABA biosynthesis was about 10-fold lower in fruits than in leaves. In fruits, the majority of ABA was conjugated to β-D-glucopyranosyl abscisate, whereas in leaves ABA was mainly hydroxylated to phaseic acid. Parallel pathways for ABA and *trans*-ABA biosynthesis and conjugation in fruits and leaves are proposed.

Evidence now strongly favors the indirect pathway of ABA biosynthesis from carotenoids. First, carotenoid biosynthetic mutants of maize are ABA-deficient (18), and fluridone, a specific inhibitor of carotenoid biosynthesis, inhibits ABA biosynthesis (8, 13). Second, heavy oxygen is incorporated from $^{18}O_2$ into the side chain of ABA during stress-induced biosynthesis, suggesting oxidative cleavage of a large precursor pool that contains oxygen functions on the ring (6, 7). Third, Li and Walton (14) have provided evidence that 9-*cis*-violaxanthin and 9′-*cis*-neoxanthin are precursors to ABA in dark-grown bean leaves. They showed a reduction in the levels of these two xanthophylls during water stress, with a concomitant increase in ABA and its catabolites PA[2] and dihydrophaseic acid, on a mole:mole basis. In contrast to higher plants, fungi synthesize ABA through α- and γ-ionylidene intermediates (29).

Xanthoxin is an apocarotenoid and a probable intermediate in ABA biosynthesis (22, 24). ABA-aldehyde has been postulated as the immediate precursor of ABA because the ABA-deficient tomato mutants *flacca* and *sitiens* are unable to convert xanthoxin or ABA-aldehyde to ABA *in vivo* (21, 25) or *in vitro* (23). ABA-*trans*-diol is an endogenous compound of plants and has been proposed as both a precursor to (20, 21), and a catabolite of ABA (26).

Zeevaart *et al.* (30) reported that ripe avocado and apple fruits, in contrast to stressed leaves, incorporated ^{18}O predominantly into the 1′-hydroxyl position of ABA. The apparent conflict of these results with the indirect pathway was reconciled by hypothesizing an exchange of ^{18}O label in the side chain carbonyl with water at an aldehyde intermediate stage of ABA biosynthesis. The present work was undertaken to determine if ABA-aldehyde is an endogenous compound in apple and could be the cause of the unusual ABA ^{18}O-labeling patterns in fruits. We also investigated the role of ABA-*trans*-diol in ABA biosynthesis.

MATERIALS AND METHODS

Plant Material

Young, fully expanded apple (*Malus domestica* Borkh. cv Mutsu) leaves were frozen in liquid N_2, or allowed to lose 12% fresh weight and subsequently incubated in 20% $^{18}O_2$:80% N_2 (v/v) for 12 or 24 h as previously described (7). The cultivars Granny Smith and Mutsu were used in post-harvest apple fruit experiments. Immature apple fruits were approximately 110 d post-anthesis. Alternatively, Mutsu apple fruits stored approximately 150 d under hypobaric conditions (0.05 atm at 0 °C to prevent ripening) were used. Cortical tissue (skin and core excised) was frozen or sliced into wedges and incubated with $^{18}O_2$ or exposed to air for 48

[1] Supported by the U.S. Department of Energy under contract DE-AC02-76ERO-1338, by the National Institutes of Health grant DRR00480 to the MSU-NIH Mass Spectrometry Facility, by National Science Foundation grant DMB-8703847 to J. A. D. Z., and by a Monsanto Graduate Fellowship to C. D. R.

[2] Abbreviations: PA, phaseic acid; ABA-GE, β-D-glucopyranosyl abscisate; ABA-*trans*-diol, 1′-4′-*trans*-ABA-diol; ECD, electron capture detection; EI, electron impact; FID, flame ionization detection; fr, fresh; M^-, odd electron negative molecular ion; Me-, methyl ester; MS-MS, GLC-NCI-collisionally activated dissociation-tandem mass spectroscopy; NCI, negative chemical ionization; PCI, positive chemical ionization; SIM, selected ion monitoring; *t-*, *trans*.

h before freezing. O_2 consumption and ethylene evolution were measured as described elsewhere (6, 12).

For feeding experiments, a 10 μM solution of deuterated substrate (approximately 2 μg/g fresh weight) in 2% (w/v) KCl plus 0.05% (v/v) Tween 20 (1) was vacuum-infiltrated and incubated at room temperature in the dark for 24 or 48 h. Control tissue was autoclaved for 20 min before incubation with substrate for 48 h.

Extraction and Purification of Metabolites

Frozen tissue was extracted overnight at 4 °C in acetone plus 0.01% (w/v) 2,6-di-*tert*-butyl-4-methylphenol and 0.25% (v/v) glacial acetic acid. The extract was drawn off and the tissue homogenized in an additional volume of extraction solvent with a Polytron (Brinkmann Instruments). The homogenate was filtered and 30 mL 1.0 M phosphate buffer (pH 8.3) was added to the combined fractions. The acetone was evaporated using a rotary evaporator at 35 °C and the aqueous extract adjusted to pH 7.2 with 6 N KOH. The extracts were filtered through a cellulose membrane to remove precipitates. With leaf extracts, Chl and lipids were removed by partitioning one to three times with an equal volume of hexanes. Measurement of the partition coefficient of an ABA-aldehyde standard indicated less than 8% loss from the aqueous fraction by partitioning with one volume of hexanes, and greater than 90% extraction of ABA-aldehyde from the aqueous fraction with one volume of ethyl acetate or diethyl ether (data not shown). The aqueous extract was partitioned three times with an equal volume of ethyl acetate to give the neutral fraction containing ABA-aldehyde. The aqueous phase was adjusted to pH 3.0 with 6 N HCl and partitioned four times with one volume of ethyl acetate to give the acidic fraction containing ABA, ABA-*trans*-diol, PA, and a portion of the ABA-GE (4). The organic fractions were taken to dryness under vacuum or N_2, and were further purified by HPLC.

ABA, ABA-GE, and PA in the acidic fraction were separated by reverse phase HPLC as previously described (6, 30). ABA-*trans*-diol coeluted with ABA and *t*-ABA from 23.5 to 26.5 min. The ethanol from the eluates was evaporated and the remaining water was removed by lyophilization. ABA-aldehyde from leaf neutral fractions was also purified using the same reverse phase HPLC conditions as described above; it eluted from 21 to 25 min. The ethanol was evaporated and an equal volume of 1.0 M phosphate buffer (pH 8.3) was added; the ABA-aldehyde was then partitioned four times into equal volumes of diethyl ether and dried under N_2 for normal phase HPLC. Apple fruit extracts did not require reverse phase HPLC for ABA-aldehyde purification.

The ABA plus ABA-*trans*-diol fraction was methylated with ethereal diazomethane and purified by normal phase HPLC with a μPorasil 30 × 0.4 cm column (Waters Associates). Elution was with a gradient of ethyl acetate in hexanes from 10 to 50% in 20 min at 2.0 mL/min. UV absorbance was monitored at 270 nm. Me-ABA was collected from 14.9 to 17.6 min, and Me-ABA-*trans*-diol from 18.8 to 21 min.

The fraction containing ABA-GE and PA was hydrolyzed with 2 N NH_4OH for 2 h at 60 °C to yield free ABA. The samples were dried, methylated and purified by the same HPLC system as for Me-ABA and Me-ABA-*trans*-diol, except a gradient of 10 to 60% ethyl acetate in hexanes in 10 min was used. Me-ABA and Me-*t*-ABA were collected from 12 to 13.8 min, and Me-PA from 14.5 to 16.5 min. ABA-aldehyde was purified using the same conditions, except UV absorbance was monitored at 282 nm. ABA-aldehyde was collected from 14.5 to 16.5 min. ABA-alcohol fractions were also collected from 18.5 to 21 min.

Quantifications

ABA-aldehyde and ABA-*trans*-diol were quantified by the method of isotope dilution (17) using deuterium-labeled internal standards. [$^2H_6$]ABA-aldehyde was synthesized by exchange of the ring hydrogens of ABA-alcohol in 1 N NaOD for 2 d, followed by oxidation in chloroform with manganese oxide IV (10) to [$^2H_6$]ABA-aldehyde. [$^2H_7$]ABA-*trans*-diol was synthesized by reduction of [$^2H_6$]ABA with sodium borodeuteride (11) and purified by reverse phase semipreparative HPLC. Deuterated standards were quantified by GLC-FID and GLC-ECD for ABA-aldehyde and Me-ABA-*trans*-diol, respectively, using standard curves of the unlabeled compounds. Quantification of ABA-aldehyde and Me-ABA-*trans*-diol standards was confirmed by UV absorbance in ethanol at 285 and 262 nm, using a molar extinction coefficient of 25,000 and 20,000, respectively (11) (C.D. Rock, unpublished observations). As determined by GLC-NCI-MS, the [$^2H_6$]ABA-aldehyde internal standard contained trace amounts of unlabeled ABA-aldehyde and was 56% hexadeutero-labeled. The [$^2H_7$]ABA-*trans*-diol was 60% heptadeutero-labeled with a trace of unlabeled compound. A calibration curve was made using various amounts of unlabeled and [$^2H_6$]ABA-aldehyde. A linear NCI-SIM response for m/z = 248 and 254 was observed when molar ratios of unlabeled ABA-aldehyde to [$^2H_6$]ABA-aldehyde were greater than 0.2, indicating that reliable measurements could be made when deuterated standard was added to extracts within a factor of five of the endogenous concentration of compound.

ABA, ABA-GE, and PA were quantified by GLC-ECD and addition of ^{3}H-labeled standards to correct for losses during extraction and purification (5). Percent recoveries for ABA and PA averaged approximately 50%, and typically 15% for ABA-GE because only a small fraction partitioned into the organic phase (4). In experiments with apple leaves where the entire extract was lyophilized instead of partitioned, ABA-GE recoveries were typically 50%.

MS

GLC-NCI-MS and GLC-NCI-SIM were performed on a JEOL AX-505H double focusing mass spectrometer equipped with a Hewlett-Packard 5890 gas chromatograph and a direct source inlet. The column used was a DB-1 capillary (30 m × 0.25 mm, film thickness 1.0 μm; or 30 m × 0.326 mm, film thickness 0.25 μm; J&W Scientific, Inc., Rancho Cordova, CA) injected in splitless mode with He as the carrier gas (flow rate 2.5 mL/min). GLC conditions were: oven temperature programmed from 50 to 180 °C at 35 °C/min, followed immediately by a temperature gradient from 180 to 260 °C at

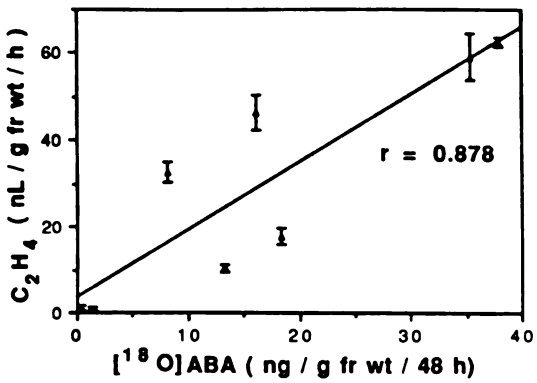

Figure 1. Relationship between the rate of ethylene evolution and ABA biosynthesis in Mutsu apple fruit. Cortical tissue from postharvest apples of varying degrees of ripeness was incubated 48 h under $^{18}O_2$. The content of [^{18}O]ABA was calculated from ABA levels measured by GLC-ECD multiplied by the percentage of [^{18}O]ABA enrichment in the same samples measured by GLC-NCI-SIM of M^-. Ethylene measurements ± SE.

10 °C/min. Methane was used as the reagent gas for NCI and PCI.

MS-MS was performed on a Finnegan TSQ 70 triple quadrupole mass spectrometer as described (30) with modifications. The collision energy in the second quadrupole was 9 eV for ABA-aldehyde, 2 eV for Me-ABA-*trans*-diol, and 3 eV for Me-ABA with an O_2 pressure of 0.19 Pa.

For analysis of mass spectral data, ion intensity values were normalized by subtracting the naturally abundant ^{13}C and ^{18}O isotope contributions. To express ^{18}O label incorporation into the side chain of ABA and metabolites as a percentage of total ^{18}O incorporation, the relative abundance of M^-, $(M + 2)^-$, $(M + 4)^-$, and $(M + 6)^-$ was measured by GLC-NCI-SIM and the percent of total [^{18}O]ABA for each M^- calculated. The percent ^{18}O enrichment of the side chain was measured by MS-MS. The product of these two measurements for each respective M^- yields the incorporation into the side chain as a percent of total ^{18}O incorporation.

The amount of ^2H-labeled product synthesized in feeding experiments was calculated from the ratio of deuterated to endogenous metabolite measured by GLC-SIM and multiplied by the amount of the endogenous compound measured by GLC-ECD of control tissue frozen at the beginning of the experiment. The extent of ^2H exchange by [^{2}H]ABA-GE during hydrolysis was small (data not shown), and resulted in a slight underestimation of [^{2}H]ABA-GE quantities in feeding experiments.

Chemicals

$^{18}O_2$ (97–98% enrichment) was purchased from Cambridge Isotopes Laboratories (Woburn, MA). Synthetic (±)-ABA-aldehyde and (±)-ABA-alcohol were gifts of Dr. M. Soukup, Hoffmann-LaRoche Inc., Basel, Switzerland.

RESULTS

ABA Biosynthesis in Fruits and Leaves

The relationship between ethylene evolution and ABA biosynthesis as measured by ^{18}O incorporation in postharvest Mutsu fruit tissue is shown in Figure 1. Although the data do not establish a causal relationship between ethylene production and ABA biosynthesis, the two biosynthetic processes are clearly linked. The postharvest increase in ABA biosynthesis was related to the ripening stage of the fruits. Each fruit began its climacteric at a different time, between 5 and 30 d after harvest, presumably due to the slightly different stage of ripening of each individual fruit. With apple fruits stored under hypobaric conditions, ethylene evolution began immediately after removal from storage and thus the fruits were synchronized with respect to ABA biosynthesis (data not shown). A correlation between the climacteric and ABA levels has been reported in avocado fruits (2).

Results on the biosynthesis and catabolism of ABA in fruits and water-stressed leaves are shown in Table I. Fruit tissue had a 10-fold lower rate of ABA biosynthesis than stressed leaves on a fresh weight basis. ABA levels averaged 200 ng/g fresh weight in these fruits and decreased about 70% during the labeling period with a concomitant increase in ABA-GE. In stressed leaves the ABA content was initially 360 ng/g fresh weight and increased approximately 50% during 24 h under $^{18}O_2$. No *t*-ABA was detected in these samples, although some postharvest apple fruits did contain significant amounts of *t*-ABA, as has been reported (3).

In fruit, [^{18}O]ABA was metabolized to [^{18}O]ABA-GE to a much greater extent than it was to [^{18}O]PA, whereas leaves metabolized a larger percentage of ABA to PA than to ABA-GE (Table I). As measured by MS-MS, [^{18}O]ABA-GE (as Me-ABA) did not lose ^{18}O from the carboxyl group during purification or hydrolysis, as evident from the equal ^{18}O enrichment in the side chain of ABA and ABA-GE from the same samples (data not shown). The 4′-keto group of ABA exchanges with water under basic conditions (9), thus [^{18}O]ABA-GE 4′-keto label was lost during hydrolysis and the values of [^{18}O]ABA-GE in Table I are therefore underestimated. In fruits, relatively more [^{18}O]*t*-ABA-GE than [^{18}O]

Table I. *Biosynthesis and Catabolism of ABA in Mutsu Fruit and Leaves under $^{18}O_2$*

Amounts of [^{18}O]ABA and [^{18}O]metabolites synthesized were calculated from the levels measured by GLC-ECD and multiplied by the percent ^{18}O enrichment as determined by GLC-NCI-SIM of the M^- (Me-ABA, m/z = 280, 282, 284; Me-PA, m/z = 296, 298, 300, 302). No *t*-ABA was detected in these samples.

^{18}O-Labeled Compound	Fruit 48 h $^{18}O_2$	Stressed Leaves 24 h $^{18}O_2$
	ng/g fresh wt/time	
ABA	29.8 ± 6.9[a]	313.0 ± 58.5
PA	0.2 ± 0.1	69.4 ± 14.6
ABA-GE	0.5 ± 0.3	19.8 ± 6.1
t-ABA-GE	3.0 ± 1.3	3.0 ± 0.7

[a] Average of three experiments ± SE.

Table II. Er
Leaf immatu
Except for
prepared as

Tissue

Stressed lea
12 h
24 h
Immature

Mature
5 d post
28 d pos
150 d st
Not perf

ABA-GE
Table I
In Table
leaves imm
of the tota
O atoms
fraction of
all cases ex
completely
of ABA fro
and turnov
on the mag
in an alden
leaves the
the precurs
proximately
24 h see
was almost
dochmylabe
total O
column 1
an aldehyd
carbonyl ox
In immat
molecules
stressed lea
leaves com
these fruits
turned over
the side cha
sion to AB
1. In matu
contained
O exchan
Table II.

Table II. *Extent of ABA Functional Group ^{18}O-Labeling in Mutsu Leaf, Immature and Mature Fruit Tissues*

Except for column 3, each class of [^{18}O]ABA molecules is interpreted as having the majority of label in the 1′-hydroxyl group (30).

Tissue/Treatment	Percent of Total [^{18}O]ABA				
	Unlabeled in carboxyl		One ^{18}O atom in carboxyl		
	(M + 2) 1	(M + 4) 2	(M + 2) 3	(M + 4) 4	(M + 6)⁻ 5
Stressed leaf					
12 h $^{18}O_2$	9.9	Trace	89.4	0.4	0.1
24 h $^{18}O_2$	16.4	Trace	81.4	1.5	0.3
Immature fruit, 48 h $^{18}O_2$					
	42.8	Trace	52.9	0.9	3.3
	30.6	0.1	62.6	2.7	4.0
Mature fruit, 48 h $^{18}O_2$					
5 d postharvest	61.2	0.3	6.8	31.1	0.3
28 d postharvest	64.8	0.6	5.4	29.2	ND[a]
150 d storage[b]	15.1	23.6	17.9	17.8	25.3

[a] Not detected [b] Stored under hypobaric conditions

ABA-GE was synthesized: the converse was true for leaves (Table I).

In Table II the various classes of labeled ABA from stressed leaves, immature and mature fruits are expressed as percent of the total [^{18}O]ABA. The class of [^{18}O]ABA containing two ^{18}O atoms in the carboxyl group (30) represented a negligible fraction of total [^{18}O]ABA and is not included in Table II. In all cases examined [^{18}O]ABA not labeled in the carboxyl was completely labeled at the 1′-hydroxyl position. Two aspects of ABA biosynthesis are demonstrated in Table II: the size and turnover of the precursor pool containing oxygen atoms on the ring, and the extent of the proposed carbonyl exchange in an aldehyde which is a precursor to ABA (30). In stressed leaves, the ABA synthesized over 24 h only slightly depleted the precursor pool containing the ring oxygens of ABA (approximately 18% of [^{18}O]ABA contained ^{18}O on the ring after 24 h; see columns 1 + 4 + 5). It can be inferred that there was almost complete exchange of the side chain ^{18}O in a doubly-labeled aldehyde intermediate, because the percent of total [^{18}O]ABA in column 4 is only one-tenth of that in column 1 (Table II). These two classes would be identical at an aldehyde precursor stage before exchange of the side chain carbonyl oxygen with water.

In immature fruit, a larger percentage of ^{18}O-labeled ABA molecules contained ^{18}O atoms on the ring as compared to stressed leaves (approximately 35% compared with < 18% for leaves; combine columns 1, 4, and 5). This suggests that in these fruits the precursor pool containing oxygens on the ring turned over quickly. As in leaves, the proposed exchange of the side chain ^{18}O of an aldehyde intermediate before conversion to ABA was almost complete (compare columns 4 and 1). In mature fruit the majority of labeled ABA molecules contained ^{18}O on the ring. As in the other tissues examined, ^{18}O exchange of an aldehyde precursor was substantial (Table II).

ABA-Aldehyde and ABA-*trans*-Diol in Apple Fruits and Leaves

ABA-aldehyde and ABA-*trans*-diol were present in both fruit and leaf tissues. Figure 2 shows mass spectra of ^{18}O labeled ABA-aldehyde and *t*-ABA-aldehyde isomers separated by GLC. Isomerization, if it occurs *in vivo*, is slow because the two isomers have significantly different ^{18}O enrichment. ABA-aldehyde was synthesized and/or metabolized more quickly than *t*-ABA-aldehyde, as evidenced by the greater ^{18}O enrichment of the *cis* isomer than that of the *trans* isomer (Fig. 2). On the other hand, in three ^{18}O labeling experiments, ABA-*trans*-diol averaged 10% ^{18}O enrichment, while ABA from the same extracts averaged 38% ^{18}O incorporation. Therefore, synthesis and/or turnover of the ABA pool was faster than that of the ABA-*trans*-diol pool in these fruits.

The fragmentation pathways by NCI of ABA-aldehyde and

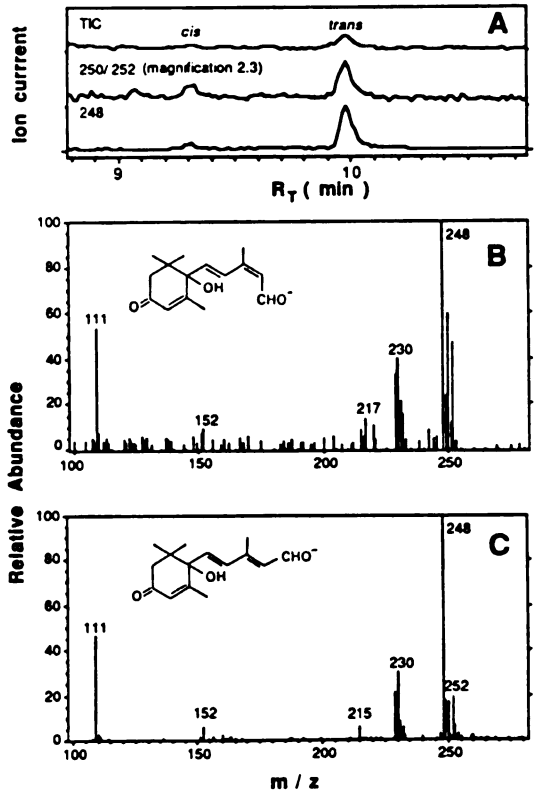

Figure 2. GLC-NCI-MS of apple fruit ABA-aldehyde synthesized under $^{18}O_2$. Granny Smith cortical tissue was incubated for 48 h under $^{18}O_2$. (A) Ion chromatogram with profile of total ion current (TIC), ABA-aldehyde isomer M^- m/z = 248, and ^{18}O-enriched (M + 2)⁻ and (M + 4)⁻, m/z = 250, 252. (B) Mass spectrum of ABA-aldehyde, showing ^{18}O enrichment. R_T = 9 min 18 s. (C) Mass spectrum of *t*-ABA-aldehyde. R_T = 10 min.

Relative abundance

Figure 3

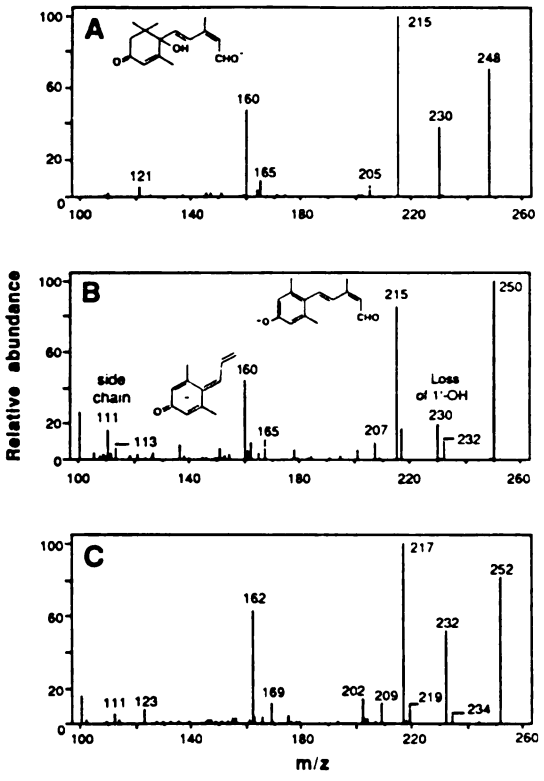

Figure 3. MS-MS of ABA-aldehyde containing zero, one, or two ^{18}O atoms. MS-MS was performed on the sample of Figure 2 to determine the position and extent of ^{18}O incorporation into ABA-aldehyde. ABA-aldehyde and *t*-ABA-aldehyde were not separated by the GLC method employed, so that spectra are of a mixture of ABA-aldehyde isomers. (A) Unlabeled ABA-aldehyde with M^- inset; (B) singly ^{18}O-labeled ABA-aldehydes with fragmentation products inset; (C) doubly ^{18}O-labeled ABA aldehydes.

Me-ABA-*trans*-diol are analogous to those of Me-ABA (19); (C.D. Rock and T.G. Heath, unpublished observations). Figure 3 shows MS-MS spectra obtained from parent M^- of ABA-aldehyde containing zero, one or two ^{18}O atoms. The ion at m/z = 230 corresponds to loss of the 1'-hydroxyl group as water; m/z = 215 has lost the 1'-hydroxyl and a *gem*-methyl group from position C-8' or C-9' as methanol. Two other diagnostic ions are m/z = 160, which contains the 4' keto group, and m/z = 111, which corresponds to the side chain. Measurement of isotope intensities of these ions allows determination of ^{18}O enrichment at each oxygen function of ABA-aldehyde when the parent ions $(M + 2)^-$ (m/z = 250) and $(M + 4)^-$ (m/z = 252) are analyzed by MS-MS.

It is apparent that the side chain carbonyl was only partially ^{18}O-labeled in the $(M + 2)^-$ and $(M + 4)^-$ species (see m/z = 111 and 113; 160 and 162; 215, 217 and 219). The 1'-hydroxyl was predominantly ^{18}O labeled in both the $(M + 2)^-$ and $(M + 4)^-$ species (loss of 20 atomic mass units as $H_2{}^{18}O$; see m/z 230, 232, 234), and the 4' keto group was partially labeled in the $(M + 2)^-$ and completely labeled in the $(M + 4)^-$ species (see m/z = 162). Thus, the [^{18}O]ABA-aldehyde pool consisted of molecules with ^{18}O at each oxygen function, the majority of the molecules containing ^{18}O in the 1'-hydroxyl group. The ^{18}O incorporation pattern of ABA-aldehyde is correlated with that of [^{18}O]ABA in fruits in which there is lack of label in the side chain and predominant ^{18}O-labeling of the 1'-hydroxyl oxygen (Table II).

In model experiments with synthetic ABA-aldehyde it was established that the carbonyl oxygen of ABA-aldehyde exchanges with H_2O with a half-life of approximately 9 min (± 2 SE, $n = 9$), but does not exchange ^{18}O carbonyl label when dissolved in ethyl acetate (data not shown). Rapid workup and phase partitioning of aqueous extracts from ^{18}O-labeled tissue may have allowed retention of some label in the carbonyl oxygen of ABA-aldehyde from ^{18}O-labeled samples (Fig. 3, Table III).

In Table III the percent ^{18}O-enrichment in the side chain is compared between ABA-aldehyde, ABA, and ABA-*trans*-diol extracted from the same sample and analyzed by MS-MS. The law of mass action supports a precursor role for species which have a higher specific activity of ^{18}O label than the product, assuming biosynthetic precursor pools are homogeneous and the label does not exchange with the medium. The second assumption is true for the carboxyl and 1'-hydroxyl groups of ABA (6), but not for the carbonyl of ABA-aldehyde, which exchanges oxygen with water (see above). The 4'-keto group of ABA can slowly exchange with water with a half-life of days (6). ABA-*trans*-diol can slowly exchange the 1'-hydroxyl with water, but not the 4'-hydroxyl (27). Because each compound can exchange some oxygen function with water, the ^{18}O labeled $(M + 4)^-$ pools are converted to the $(M + 2)^-$ pools for each compound. Thus, the weighted average of side chain enrichment (factoring in the relative abundance of each M^-) is presented in Table III. Taking into account the loss of

Table III. *^{18}O Incorporation in the Side Chain of ABA-Aldehyde, ABA-trans-Diol and ABA Extracted from the Same Fruit Sample after 48 h under $^{18}O_2$*

Percent side chain enrichment was calculated from intensities of daughter ions measured by MS-MS and GLC-NCI-SIM of ^{18}O-enriched M^- (Me-ABA m/z = 280, 282, 284; Me-ABA-*trans*-diol m/z = 282, 284; ABA-aldehyde m/z = 250, 252). ABA-aldehyde was measured as a mixture of *cis*- and *trans*-isomers. Experiments 1 to 4 were performed with post-harvest Granny Smith cortex tissue, experiment 5 with Mutsu cortex from fruits stored under hypobaric conditions.

Experiment	Percent of ^{18}O-Labeled Molecules Containing ^{18}O in the Side Chain		
	ABA-aldehydes	ABA	ABA-*trans*-diol
1	18.2	10.6	6.1
2	13.6	16.0	4.1
3	10.5	71.8	5.5
4	NA[a]	42.0	25.5
5	NA	59.4	35.2

[a] Not analyzed.

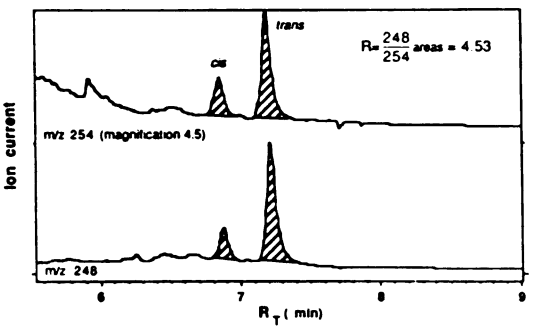

Figure 4. GLC-NCI-SIM chromatogram of ABA-aldehyde from Mutsu fruit with [$^2H_6$]ABA-aldehyde internal standard. The sum of the ABA-aldehyde plus *t*-ABA-aldehyde peak areas gave a ratio of unlabeled to [$^2H_6$]ABA-aldehyde, from which the amount of unknown endogenous ABA-aldehyde was calculated.

^{18}O label from the ABA-aldehyde side chain carbonyl due to exchange with the medium, a precursor role of ABA-aldehyde for ABA can be inferred. In one experiment the side chain label of ABA-aldehyde was actually higher than that of ABA. In all cases the side chain specific activity of Me-ABA (percent ^{18}O in side chain of total ^{18}O) was greater than that of Me-ABA-*trans*-diol. Thus, these data suggest that ABA is a precursor to ABA-*trans*-diol.

Quantification of ABA-Aldehyde and ABA-*trans*-Diol

The method of isotope dilution of deuterated internal standards (17) was used to quantify ABA-aldehyde and ABA-*trans*-diol. Retention and stability of deuterium label during extraction and purification procedures were confirmed by dissolving deuterium-labeled compounds in 0.2 M phosphate buffers, ranging from pH 3.5 to 10, for 6 d at room temperature, followed by partitioning into ethyl acetate and analysis by GLC-MS. There was less than 1% exchange of deuterium for both standards over the range of pHs tested (data not shown). Thus, the internal standards could be used for quantification, provided the standards were added at concentrations less than five times the endogenous sample concentrations to minimize contamination of the nominal mass peak by unlabeled internal standard (see "Materials and Methods").

Figure 4 shows a GLC-NCI-SIM chromatogram for quantification of ABA-aldehyde. The deuterated material eluted from the GLC column about 2 s earlier than the unlabeled compound. The ratio of ABA-aldehyde to *t*-ABA-aldehyde as measured by NCI-SIM was essentially constant, regardless of the actual quantities of isomers present in a stock solution. This suggested that the two isomers were not equally detected by this method. Consequently, both isomers were then analyzed by various GLC detection methods. In Table IV the phenomenon of 'differential ionization' of ABA-aldehyde isomers is illustrated. FID generates a signal based on the mass and organic composition of the compound being measured and is unbiased in the response toward different isomers of similar or identical compounds. Positive ion detection methods (PCI and EI) generally reflected the abundance of ABA-aldehyde versus *t*-ABA-aldehyde isomers, but were relatively less sensitive to ABA-aldehyde than FID. NCI and ECD consistently gave ABA-aldehyde to *t*-ABA-aldehyde isomer ratios which were less than unity, indicating that the two isomers were differentially ionized. The degree of ABA-aldehyde ionization was affected by the pressure of reagent gas (Table IV). The mechanism of this differential ionization is unknown. Thermal isomerization of ABA-aldehyde in the injection port of the gas chromatograph was ruled out as a possible cause of observed isomer ratios (see Fig. 3). Xanthoxin and *t*-xanthoxin ratios were relatively constant regardless of the detection method employed (Table IV), even though the chemical structure is quite similar to that of ABA-aldehyde. NCI was the only mass spectroscopy method tested which was sensitive enough to measure the small amounts of ABA-aldehyde present in plants. It was apparent that ABA-aldehyde isomers could not be quantified by NCI-SIM using a deuterated internal standard because the *cis* isomer was refractory to ionization. The relative amount of *cis* isomer was reflected in the NCI-MS signal at high reagent gas pressure (Table IV). Because the ratio of *cis*- to *trans*-ABA-aldehyde isomers in the deuterated internal standard was known, and the endogenous isomer ratio was similar (Fig. 4), the sum of the two isomer concentrations was used as a measure of total ABA-aldehydes.

In Table V the levels of ABA, ABA-*trans*-diol and ABA-aldehyde plus *t*-ABA-aldehyde in leaves and apple fruit tissue are presented. There was very little ABA-*trans*-diol in either leaves or fruit, and no ABA-alcohol was detected. ABA-aldehyde levels were low in all tissues examined. When ABA-aldehyde concentrations are presented as percent of ABA levels, there is a trend toward relatively higher ABA-aldehyde levels from leaves to mature fruits (Table V).

Feeding Studies with Deuterated Substrates

Table VI summarizes feeding experiments addressing the biosynthetic relationship of putative ABA precursors. [$^2H_6$]ABA-aldehyde and and [$^2H_6$]*t*-ABA-aldehyde were converted to [$^2H_6$]ABA and [$^2H_6$]*t*-ABA, which were further converted

Table IV. *Comparison of cis- and trans-ABA-Aldehyde and -Xanthoxin Isomer Ratios by Various GLC Detection Methods*

An aliquot of a stock solution was chromatographed by GLC using a DB-1 capillary column and the isomers quantified by peak areas of the detector responses. For mass spectrometric detection methods, the total ion current was integrated.

Sample	Ratio of *cis* to *trans* Isomer Areas					
	FID	PCI	EI	NCI_{Low}[a]	NCI_{High}[a]	ECD
ABA-aldehyde	55.4	10.9	2.3	0.5	0.9	1.1
cis- and *trans*-ABA-aldehydes	0.6	0.2	0.2	0.2	0.3	0.2
[$^2H_6$]ABA-aldehydes	5.1	1.1	1.0	0.2	0.4	0.8
cis- and *trans*-xanthoxins	0.3	0.3	0.4	0.3	0.3	0.4

[a] Methane chemical ionization gas pressure was 6.7×10^{-4} and 2.0×10^{-3} Pa for "low" and "high" measurements, respectively.

Table V. *Quantification of ABA, ABA-trans-Diol and cis- plus trans-ABA-Aldehydes in Mutsu Fruit and Leaves*

ABA was quantified by GC-ECD using [^{3}H]ABA as an internal standard. ABA-aldehydes and ABA-*trans*-diol were quantified by isotope dilution using ^{2}H-labeled synthetic standards and measurement by GLC-NCI-SIM of the M^- as shown in Figure 4.

Tissue	Sample			$\frac{\text{ABA-Aldehydes}}{\text{ABA}} \times 100$
	ABA	ABA-*trans*-diol	ABA-aldehydes (*cis* + *trans*)	
	ng/g fr wt			%
Unstressed leaf	362.80[a]	0.02	1.02	0.3
Immature fruit[a]	19.85	NA[b]	0.44	2.2
Mature fruit[c]	5.12	0.01	0.68	13.3

[a] Average of two experiments. [b] Not analyzed. [c] Average of four experiments.

to [$^2H_6$]ABA-GE and [$^2H_6$]*t*-ABA-GE. There was no evidence for isomerization of ABA to *t*-ABA (Table VI, [$^2H_7$]ABA-*trans*-diol feed), or ABA-GE to *t*-ABA-GE ([$^2H_6$]ABA feed) during the incubation. These data can be interpreted as showing a direct conversion of ABA-aldehyde to ABA to ABA-GE, and of *t*-ABA-aldehyde to *t*-ABA to *t*-ABA-GE. The rate of metabolism of *t*-ABA to *t*-ABA-GE appears to be greater than that of ABA to ABA-GE, as indicated by the lower levels of *t*-ABA relative to ABA and higher levels of *t*-ABA-GE than of ABA-GE. A higher rate of conjugation for *t*-ABA than for ABA has been reported for other plants (16). The (−) enantiomer of ABA is conjugated readily (16); thus, a significant proportion of the [^{2}H]ABA-GE product would be (−)-ABA-GE, if (−)-ABA-aldehyde was converted to (−)-ABA. The conclusions reached for conversion of [$^2H_6$]ABA-aldehyde to ABA and ABA-GE isomers also hold for the [$^2H_6$]ABA-alcohol feeding experiment. Assuming the applied compounds entered the cell to equal extents and were not converted to products other than listed in Table VI, it can be concluded that the rate of metabolism of [$^2H_6$]ABA-alcohol was slower than that of [$^2H_6$]ABA-aldehyde.

Conversion of [$^2H_7$]ABA-*trans*-diol to ABA took place; however, this oxidation occurred nonenzymatically as evidenced by the presence of [$^2H_6$]ABA in the autoclaved control feed (see also ref. 27). [$^2H_6$]ABA was enzymatically reduced to [$^2H_6$]ABA-*trans*-diol (Table VI). The extent of this conversion was dependent on the concentration of ABA. When [$^2H_6$]ABA was fed at a concentration approximately 400-fold higher than the endogenous ABA level, the [$^2H_6$]ABA-*trans*-diol produced was about 50 times the endogenous ABA-*trans*-diol content; quantifications of ABA-*trans*-diol also support a concentration dependence on ABA (Table V).

Table VI. *Metabolism of Deuterated Compounds Fed to Mutsu Fruit Tissue*

Plugs of cortex tissue (1.4 cm diameter) were vacuum-infiltrated with 2 mL of a 10 μM solution of substrate (except [$^2H_7$]ABA-*trans*-diol, 2.0 μM). The substrates [$^2H_6$]ABA-aldehyde and [$^2H_6$]ABA-alcohol contained a significant amount of the respective *trans* isomer. The control tissue was autoclaved before addition of substrate for the 48 h incubation period.

Substrate	Product				
	[^{2}H]ABA	[^{2}H]*t*-ABA	[^{2}H]ABA-*trans*-diol	[^{2}H]ABA-GE	[^{2}H]*t*-ABA-GE
			ng/g fresh wt/time		
[$^2H_6$]ABA-aldehyde					
24 h	1.6	0.2		ND	2.6
48 h	1.4	1.1		1.6	8.0
Control	ND[a]	ND		ND	ND
[$^2H_6$]ABA-alcohol					
24 h	0.2	ND		ND	0.3
48 h	0.8	ND		ND	3.4
Control	ND	ND		ND	ND
[$^2H_7$]ABA-*trans*-diol					
24 h	7.1	ND		0.2	0.1
48 h	5.3	ND		3.2	0.1
Control	12.5	ND		ND	ND
[$^2H_6$]ABA					
24 h			0.4	2.0	ND
48 h			0.6	17.3	ND
Control			ND	ND	ND

[a] Not detected.

ABA-Aldeh
a Catabolit

ABA Biosy

DISCUSSION

ABA-Aldehyde as a Precursor to, and ABA-*trans*-Diol as a Catabolite of ABA

Evidence is presented that ABA-aldehyde is the immediate precursor to ABA, and that ABA-*trans*-diol is a catabolite of ABA in apple fruits and leaves, and possibly in all plants. These conclusions are based on the following evidence. (a) Assuming the labeled and unlabeled metabolite pools were in equilibrium, there was greater flux through the ABA-aldehyde pool than the *t*-ABA-aldehyde pool (Fig. 2). These data are consistent with an enzymatic specificity toward the *cis* isomer of ABA, the biologically active isomer in plants (28). There was also greater flux through the ABA *versus* ABA-*trans*-diol pools (data not shown), which supports ABA as a precursor to ABA-*trans*-diol. (b) Precursor-product relationships were established by measurement of ^{18}O specific activity of metabolites extracted from ^{18}O-labeled tissues (Table III), and by feeding studies using deuterated substrates (Table VI). (c) There were low endogenous levels of ABA-aldehyde and ABA-*trans*-diol (Table V) and a concentration dependence of ABA-*trans*-diol on ABA.

ABA-aldehyde has been postulated as a precursor to ABA, because the ABA-deficient *flacca* and *sitiens* mutants of tomato are unable to convert xanthoxin or ABA-aldehyde to ABA *in vivo* (21, 25) or *in vitro* (23). Taylor *et al.* (15, 25) showed that these mutants reduce ABA-aldehyde to *t*-ABA-alcohol, which accumulates to high levels. [$^2H_6$]ABA-alcohol is converted to ABA in apple fruits, but at lower rates than [$^2H_6$]ABA-aldehyde (Table VI).

ABA Biosynthesis in Apple Fruits and Leaves

The qualitative and quantitative data obtained by MS-MS of metabolites from ^{18}O-labeled tissues provide a means to analyze the ABA biosynthetic pathway, especially rates of turnover of precursor pools. Two conclusions can be drawn from Table II regarding the precursor(s) of ABA. (a) Based on ABA biosynthetic capacity of the tissues (Table I), and the turnover rate of the pools as judged by ^{18}O incorporation on the ring of ABA (Table II), the precursor pool containing ring oxygens is large in leaves and much smaller in fruits. (b) In apple, and perhaps in all plants, a significant amount of exchange occurs between the medium and the carbonyl side chain oxygen of an aldehyde precursor to ABA. This carbonyl exchange would give rise to unlabeled ABA synthesized under $^{18}O_2$ in tissues which have a large precursor pool. ABA labeled exclusively in the ring oxygens is observed only in tissues (like apple fruit) which have a small, rapidly depleted violaxanthin precursor pool. This tissue type synthesizes ABA labeled in the ring oxygen functions, but without label in the carboxyl group. The exchange can be at the ABA-aldehyde level (Fig. 3), but could also occur in an aldehyde precursor prior to ABA-aldehyde, such as xanthoxin. Parry *et al.* (21) observed a low amount of ^{18}O incorporation from $^{18}O_2$ into xanthoxin in tomato leaves and suggested that lack of steady state ^{18}O enrichment might be due to carbonyl exchange.

ABA biosynthesis and catabolism in climacteric fruits is under developmental control, in contrast to leaves where turgor pressure is a regulatory signal for ABA metabolism (29). The regulation of ABA biosynthesis and catabolism is different in leaves and fruits; hydroxylation of ABA to PA is a minor pathway in fruits (Table I), but the major catabolic pathway in leaves (Table I) (29). Fruits synthesize relatively more of the *trans* than the *cis* isomer of ABA-GE; in contrast, leaves synthesize more ABA-GE than *t*-ABA-GE (Table I). There is no evidence to support enzymatic isomerization of ABA to *t*-ABA, or of ABA-GE to *t*-ABA-GE (Table VI) (16). We hypothesize that ABA and *t*-ABA biosynthesis and metabolism proceed in parallel from xanthophylls to xanthoxin isomers, through ABA-aldehyde isomers, to the corresponding isomers of ABA and ABA-GE. Both *cis*- and *trans*-xanthoxin isomers are present in plants, and *t*-xanthoxin is converted to *t*-ABA (16, 21, 22). Sindhu and Walton (23) showed that bean leaf extracts convert ABA-aldehyde and *t*-ABA-aldehyde predominantly to ABA and *t*-ABA, respectively. If the levels of ABA-aldehyde plus *t*-ABA-aldehyde are similar in leaves and fruits, but ABA levels are much lower in fruits (Table V), then the latter should contain more *t*-ABA-aldehyde than leaves. The relatively high *t*-ABA-GE levels in fruits are evidence in support of this hypothesis. The large amounts of *t*-ABA found in apple fruits (3) may not have been due to isomerization as proposed, but by a loss of ABA-conjugating activity in these apples. A precise measurement of ABA-aldehyde and *t*-ABA-aldehyde levels would provide further insight into synthesis of ABA and *t*-ABA in plants.

ACKNOWLEDGMENTS

We thank T.G. Heath and Dr. D.A. Gage for assistance with mass spectrometry, Dr. D.R. Dilley and Dr. F.G. Dennis Jr. for providing plant material, and Dr. M. Soukup, Hoffmann-LaRoche, Inc. for providing synthetic ABA-alcohol and ABA-aldehyde.

LITERATURE CITED

1. **Adams DO, Yang SF** (1979) Ethylene biosynthesis: identification of 1-aminocyclopropane-1-carboxylic acid as an intermediate in the conversion of methionine to ethylene. Proc Natl Acad Sci USA **76**: 170–174
2. **Adato I, Gazit S, Blumenfeld A** (1976) Relationship between changes in abscisic acid and ethylene production during ripening of avocado fruits. Aust J Plant Physiol **3**: 555–558
3. **Bangerth F** (1982) Changes in the ratio of *cis-trans* to *trans-trans* abscisic acid during ripening of apple fruits. Planta **155**: 199–203
4. **Boyer GL, Zeevaart JAD** (1982) Isolation and quantitation of β-D-glucopyranosyl abscisate from leaves of *Xanthium* and spinach. Plant Physiol **70**: 227–231
5. **Cornish K, Zeevaart JAD** (1984) Abscisic acid metabolism in relation to water stress and leaf age in *Xanthium strumarium*. Plant Physiol **76**: 1029–1035
6. **Creelman RA, Gage DA, Stults JT, Zeevaart JAD** (1987) Abscisic acid biosynthesis in leaves and roots of *Xanthium strumarium*. Plant Physiol **85**: 726–732
7. **Creelman RA, Zeevaart JAD** (1984) Incorporation of oxygen into abscisic acid and phaseic acid from molecular oxygen. Plant Physiol **75**: 166–169
8. **Gamble PE, Mullet JE** (1986) Inhibition of carotenoid accumulation and abscisic acid biosynthesis in fluridone-treated dark-grown barley. Eur J Biochem **160**: 117–121
9. **Gray RT, Mallaby R, Ryback G, Williams VP** (1974) Mass spectra of methyl abscisate and isotopically labeled analogs. J Chem Soc Perkins Trans **2**: 919–924

Gritter R
Hirai, N
Ikeda, H
Li, Y., W
Li, Y., W
Lubowitz
Hi
Matsuura
Neil, N.J.
Neil, N.J.
Nettles
Okamura,

10. **Gritter RJ, Wallace TJ** (1959) The manganese dioxide oxidation of allylic alcohols. J Org Chem **24**: 1051–1056
11. **Hirai N, Okamoto M, Koshimizu K** (1986) The 1′,4′-*trans*-diol of abscisic acid, a possible precursor of abscisic acid in *Boltrytis cinerea*. Phytochemistry **25**: 1865–1868
12. **Kende H, Hanson AD** (1975) Relationship between ethylene evolution and senescence in morning-glory flower tissue. Plant Physiol **57**: 523–527
13. **Li Y, Walton DC** (1987) Xanthophylls and abscisic acid biosynthesis in water-stressed bean leaves. Plant Physiol **85**: 910–915
14. **Li Y, Walton DC** (1990) Violaxanthin is an ABA precursor in water-stressed dark-grown bean leaves. Plant Physiol **92**: 551–559
15. **Linforth RST, Bowman WR, Griffin DA, Marples BA, Taylor IB** (1987) 2-*trans*-ABA-alcohol accumulation in the wilty tomato mutants *flacca* and *sitiens*. Plant Cell Environ **10**: 599–606
16. **Milborrow BV** (1983) Pathways to and from abscisic acid. *In* FT Addicott, ed, Abscisic Acid. Praeger, New York, pp 79–111
17. **Neill SJ, Horgan R** (1987) Abscisic acid and related compounds. *In* L Rivier, A Crozier, eds, Principles and Practice of Plant Hormone Analysis, Vol 1. Academic, London, pp 111–167
18. **Neill SJ, Horgan R, Parry AD** (1986) The carotenoid and abscisic acid content of viviparous kernels and seedlings of *Zea mays* L. Planta **169**: 87–96
19. **Netting AG, Milborrow BV, Vaughan GT, Lidgard RO** (1988) The fragmentation of methyl abscisate and its 2*E* isomer in methane positive and negative chemical ionization mass spectrometry. Biomed Environ Mass Spectrom **15**: 375–389
20. **Okamoto M, Hirai N, Koshimizu K** (1987) Occurrence and metabolism of 1′,4′-*trans*-diol of abscisic acid. Phytochemistry **26**: 1269–1271
21. **Parry AD, Neill SJ, Horgan R** (1988) Xanthoxin levels and metabolism in the wild-type and wilty mutants of tomato. Planta **173**: 397–404
22. **Sindhu RK, Walton DC** (1987) Conversion of xanthoxin to abscisic acid by cell-free preparations from bean leaves. Plant Physiol **85**: 916–921
23. **Sindhu RK, Walton DC** (1988) Xanthoxin metabolism in cell-free preparations from wild type and wilty mutants of tomato. Plant Physiol **88**: 178–182
24. **Taylor HF, Burden RS** (1972) Xanthoxin, a recently discovered plant growth inhibitor. Proc R Soc Lond Ser B **180**: 317–346
25. **Taylor IB, Linforth RST, Al-Naieb RJ, Bowman WR, Marples BA** (1988) The wilty mutants *flacca* and *sitiens* are impaired in the oxidation of ABA-aldehyde to ABA. Plant Cell Environ **11**: 739–745
26. **Vaughan GT, Milborrow BV** (1987) The occurrence and metabolism of the 1′,4′-diols of abscisic acid. Aust J Plant Physiol **14**: 593–604
27. **Vaughan GT, Milborrow BV** (1988) The stability of the 1′,4′-diols of abscisic acid. Phytochemistry **27**: 339–343
28. **Walton DC** (1983) Structure-activity relationships of abscisic acid analogs and metabolites. *In* FT Addicott, ed, Abscisic Acid. Praeger, New York, pp 113–146
29. **Zeevaart JAD, Creelman RA** (1988) Metabolism and physiology of abscisic acid. Annu Rev Plant Physiol Plant Mol Biol **39**: 439–473
30. **Zeevaart JAD, Heath TG, Gage DA** (1989) Evidence for a universal pathway of abscisic acid biosynthesis in higher plants from ^{18}O incorporation patterns. Plant Physiol **91**: 1594–1601

CHAPTER 4

ABSCISIC (ABA)-ALCOHOL IS AN INTERMEDIATE IN ABA BIOSYNTHESIS IN A SHUNT PATHWAY FROM ABA-ALDEHYDE

defi

alde

the

739-

accu

accu

wate

[^{18}O

muta

ABA

droo

muta

also

^{18}O la

and

expe

doub

with

4.1. ABSTRACT

It has previously been shown that the abscisic acid (ABA) - deficient *flacca* and *sitiens* mutants of tomato are impaired in ABA-aldehyde oxidation and accumulate *trans*-ABA-alcohol as a result of the biosynthetic block (IB Taylor *et al.* [1988] Plant Cell Environ 11: 739-745). Here we report that the *flacca* and *sitiens* mutants accumulate *trans*-ABA and *trans*-ABA-glucose ester, and that this accumulation is due to *trans*-ABA biosynthesis. ^{18}O Labeling of water-stressed wild type and mutant tomato leaves and analysis of [^{18}O]ABA by tandem mass spectrometry shows that the tomato mutants synthesize a significant percentage of their ABA and *trans*-ABA as [^{18}O]ABA with two ^{8}O atoms in the carboxyl group. The *droopy* mutant of potato and the Az34 (*nar2a*) molybdenum cofactor mutant of barley, which are also impaired in ABA-aldehyde oxidation, also synthesize more doubly-carboxyl-labeled ABA than wild type in ^{18}O labeling experiments. The *droopy* mutant accumulates *t*-ABA and *t*-ABA-GE like the *sitiens* mutant. We further show, by feeding experiments in tomato with [$^{2}H_6$]ABA-alcohol and $^{18}O_2$, that this doubly-carboxyl-labeled ABA is synthesized from [^{18}O]ABA-alcohol with incorporation of molecular oxygen. *In vivo* inhibition by carbon

monoxide of [$^2H_6$]ABA-alcohol oxidation establishes the involvement of a cytochrome P-450 monooxygenase. Likewise, CO inhibits the synthesis of doubly-carboxyl-labeled ABA in ^{18}O labeling experiments. This minor shunt pathway from ABA-aldehyde to ABA-alcohol to ABA operates in all plants. For the ABA-deficient mutants impaired in ABA-aldehyde oxidation, this shunt pathway is an important source of ABA and is physiologically significant.

4.2. INTRODUCTION

Much progress has been made recently on the elucidation of the biosynthetic pathway of ABA. The evidence is now conclusive for the "indirect pathway," which proceeds by oxidative cleavage of epoxycarotenoids to xanthoxin, which is sequentially metabolized to ABA-aldehyde and ABA. Xanthoxin and ABA-aldehyde are endogenous compounds of plants (Parry *et al.*, 1988; 1990b; Rock and Zeevaart, 1990a) and the oxidase activities which convert these compounds to ABA have been characterized *in vitro* (Sindhu and Walton, 1988; Sindhu *et al.*, 1990). The *viviparous* mutants of maize are blocked in the early stages of carotenoid biosynthesis and are ABA-deficient (Moore and Smith, 1985; Neill *et al.*, 1986). Fluridone

and norflurazon, specific inhibitors of carotenoid biosynthesis, also inhibit ABA biosynthesis (Gamble and Mullet, 1986). ^{18}O-Labeling experiments show incorporation predominantly into the side chain carboxyl group of ABA, suggesting oxidative cleavage of xanthophylls which contain oxygens on the ring of ABA (Creelman and Zeevaart, 1984; Creelman *et al.*, 1987; Zeevaart *et al.*, 1989). Li and Walton (1990) showed a 1:1 relationship on a molar basis between decreases in violaxanthin and 9'-*cis*-neoxanthin and increases in ABA and the catabolites PA and dihydrophaseic acid in dark-grown water-stressed bean leaves; similar results have been obtained by others (Gamble and Mullet, 1986; Parry *et al.*, 1990a). Rock and Zeevaart (1991) have characterized *aba*, the ABA-deficient mutant of *Arabidopsis thaliana* (Koornneef *et al.*, 1982) as being impaired in epoxy-carotenoid biosynthesis, which provides strong evidence for the indirect pathway of ABA biosynthesis.

There are three non-allelic ABA-deficient mutants of tomato, *not, flc,* and *sit*, which differ in their phenotypic severity of transpiration rates and inability to close their stomata (Tal and Nevo, 1973; Neill and Horgan, 1985). Application of ABA can restore the normal phenotype (Tal and Nevo, 1973; Neill and Horgan, 1985). Feeding studies and enzymology have established that the *flc* and *sit*

mutants are blocked in ABA-aldehyde oxidation (Sindu and Walton, 1988, Sindhu *et al.*, 1990; Taylor *et al.*, 1988). The Az34 (*nar2a*) molybdenum cofactor mutant of barley (Walker-Simmons *et al.*, 1989), the *droopy* mutant of potato (Quarrie, 1982; Duckham *et al.*, 1989), and the *CKR1* mutant of *Nicotiana plubaginifolia* (Parry *et al.*, 1991) have also been characterized as being blocked in ABA-aldehyde oxidation.

Because the *flc* and *sit* mutants accumulate *t*-ABA-alcohol as a result of the ABA-aldehyde oxidase biosynthetic block (Linforth *et al.*, 1987, 1990; Taylor *et al.*, 1988), our observation that the *flc* and *sit* mutants accumulate significant amounts of *t*-ABA-GE (Rock and Zeevaart, 1990b) prompted us to investigate whether ABA-alcohol could be a biosynthetic intermediate between ABA-aldehyde and ABA. Our results confirm this hypothesis and establish the enzyme involved in ABA-alcohol oxidation is a P-450 monooxygenase. This shunt pathway is the source of doubly-carboxyl-labeled ABA observed in $^{18}O_2$ labeling experiments with numerous species (Zeevaart *et al.*, 1989).

4.3

an

fil

we

we

an

C

an

fr

an

(W

ho

Ph

an

Wa

We

4.3. MATERIALS AND METHODS

4.3.1. Plant Material

Seeds of *Lycopersicon esculentum* Mill. cv Rheinlands Ruhm and the near-isogenic mutants *not, flc,* and *sit* were germinated on filter paper under continuous light and transplanted to pots which were subirrigated with half-strength Hoagland's solution. Plants were grown for six to ten weeks in a high humidity growth chamber and maintained on a diurnal cycle of 9 hr light (300 $\mu E \cdot m^{-2} \cdot s^{-1}$), 23° C and 15 hr dark, 20° C. Seeds of *Hordeum vulgare* L. cv Steptoe and the molybdenum cofactor mutant Az34 (*nar2a*) were obtained from Dr. Robert Warner, Washington State University, Pullman, WA and grown for 8 d in vermiculite in a greenhouse, as described (Walker-Simmons *et al.,* 1989). Seeds of heterozygous (*Dr/dr*) and homozygous (*dr/dr*) *droopy* potato (*Solanum tuberosum* L., group *Phureja*) were from Dr. Ian Taylor, University of Nottingham, U.K. and were grown as described for the tomato mutants.

For ABA biosynthesis studies the leaves were harvested and water-stressed by dehydrating with a hair dryer until 14% of the fresh weight was lost. The tissue was incubated under 20% $^{18}O_2$: 80% N_2

(v/v) (Creelman and Zeevaart, 1984) or air at room temperature in the dark for various lengths of time and frozen in liquid N_2.

4.3.2. Feeding Experiments

$[^2H_{3-6}](\pm)$ABA-alcohol and $[^2H_{3-6}](\pm)$ABA-aldehyde (97.2% [w/w]) were synthesized as described (Rock and Zeevaart, 1990a). Leaves of *flc* or *sit* were dipped in a 4×10^{-5} M solution of substrate containing 0.05% (v/v) Tween 20 and 0.2 % (v/v) ethanol, and were immediately placed in an atmosphere containing either 20% $^{18}O_2$: 80% N_2 (v/v) or air plus 10% or 50% (v/v) carbon monoxide, or N_2, and incubated in darkness for 8 h and frozen.

4.3.3. ABA, ABA-GE, and PA Analysis

ABA and catabolites were extracted with acetone plus 0.025% (w/v) 2,6-di-*tert*-butyl-4-methylphenol and 0.25% (v/v) glacial acetic acid, partitioned at pH 3.0 into ethyl acetate, and purified by reverse phase HPLC as described (Rock and Zeevaart, 1991). The *trans* isomers of ABA and ABA-GE had slightly shorter retention times in the HPLC system than the respective *cis* isomers. Samples were methylated with ethereal diazomethane and quantified by GC-NCI-SIM as described (Rock and Zeevaart, 1991). For Me-ABA synthesized from $[^2H_{3-6}]$-labeled compounds, m/z = 278, 283, 284,

285, 286, and 288 were monitored. Corrections were made for the natural abundance of stable isotopes. MS/MS was performed on a Finnegan TSQ-70 triple-quadrupole mass spectrometer as previously described (Rock and Zeevaart, 1990a).

4.3.4. Chemicals

$^{18}O_2$ (97-98% enrichment) was purchased from Cambridge Isotopes Laboratories (Woburn, MA). Carbon monoxide (99.3% pure) was from Scott Specialty Gases (Houston, TX) and was the gift of Dr. Robert Creelman, Department of Biochemistry and Biophysics, Texas A & M University.

4.4. RESULTS

4.4.1. ABA and *Trans*-ABA Biosynthesis in the ABA-Deficient Tomato Mutants

Quantitation of ABA, *t*-ABA and their catabolites ABA-GE, *t*-ABA-GE and PA in unstressed leaves of wild type and mutant tomato is presented in Table 4.1. Consistent with the work of others (Tal and Nevo, 1973; Neill and Horgan, 1985; Linforth *et al.*, 1987), there was a correlation between ABA levels and resistance to wilting in

Table 4.1. Quantitation of ABA, *trans*-ABA and Catabolites from Unstressed Leaves of Wild Type and ABA-Deficient Tomato Mutants

Mutants are listed in order of increasing phenotypic severity (13, 28). ABA and metabolites were quantified by GC-NCI-SIM. Mean of three experiments (± SE).

Genotype	ABA	*t*-ABA	ABA-GE	*t*-ABA-GE	PA[a]
			ng / g fr wt		
Rheinlands Ruhm	290.2 ± 13.0	1.0 ± 0.3	20.5 ± 7.7	22.2 ± 5.9	392.2
Notabilis	239.9 ± 59.8	1.8 ± 0.1	24.0 ± 7.9	24.2 ± 9.0	132.4
Flacca	59.1 ± 9.6	1.2 ± 0.3	2.8 ± 0.8	28.2 ± 8.9	4.7
Sitiens	29.9 ± 7.4	3.5 ± 1.5	2.8 ± 0.5	56.5 ± 15.9	3.7

[a]Average of two experiments

unstressed leaves of the mutants; this correlation also holds for the ABA catabolites ABA-GE and PA (Table 4.1). Furthermore, there is an inverse correlation between *t*-ABA and *t*-ABA-GE accumulation and phenotypic severity of the mutants (Table 4.1). The least severe mutant, *not*, accumulated similar amounts of *t*-ABA and *t*-ABA-GE, taken together, as wild type (Table 4.1). The most severe mutant, *sit*, accumulated the most *t*-ABA and *t*-ABA-GE, while *flc* had intermediate levels between *not* and *sit* (Table 4.1). These results correlate with increased levels of *t*-ABA-alcohol in the *flc* and *sit* mutants (Linforth *et al.*, 1987).

^{18}O-Labeling of ABA *in vivo* and quantitation by MS allows measurement of biosynthetic capacity of the ABA pathway (Zeevaart *et al.*, 1989; Rock and Zeevaart, 1990a, 1991; Rock *et al.*, 1991). Table 4.2 shows quantitation of ^{18}O-labeled ABA, *t*-ABA and catabolites from water-stressed leaves incubated under $^{18}O_2$ for various lengths of time. Consistent with the results in Table 4.1, there was a correlation between phenotypic severity of the mutants and lower ABA biosynthetic capacity (Table 4.2). Furthermore, there was a correlation between phenotypic severity of the mutants and the lack of inhibition of *t*-ABA biosynthesis, as measured by the ratio

Table 4.2. Quantitation of ^{18}O-Labeled ABA, *trans*-ABA and Catabolites from Water-Stressed Leaves of Wild Type and ABA-Deficient Tomato Mutants in $^{18}O_2$ for Various Lengths of Time

Mutants are listed in order of increasing phenotypic severity (13, 28). ABA and metabolites were quantified by GC-NCI-SIM. Average of two experiments.

Genotype/ Time	[^{18}O]ABA	[^{18}O] *t*-ABA	[^{18}O]ABA-GE	[^{18}O] *t*-ABA-GE	[^{18}O]PA	*Cis* Metabolites / *Trans* Metabolites
			ng / g fr wt / time			
Rheinlands Ruhm						
4 h	263.0	2.1	1.6	5.8	105.2	46.8
8 h	323.4	2.2	8.5	8.9	641.9	87.7
23 h	621.6	3.4	64.8	13.9	N.A.[a]	
Notabilis						
4 h	8.2	1.3	0.1	1.7	50.5	19.6
23 h	41.1	0.3	1.7	2.5	170.9	76.3

Table 4.2 (cont'd.)

Flacca						
4 h	3.9	0.3	N.D.[b]	0.8	2.6	5.9
8 h	6.1	0.5	0.1	3.9	16.5	5.1
23 h	11.0	0.5	0.4	5.3	N.A.	
Sitiens						
4 h	1.8	0.5	N.D.	1.0	2.3	2.7
8 h	2.0	0.6	trace	4.3	6.3	1.7

[a]Not analyzed [b]Not detected.

of *cis*-ABA and metabolites to *trans*-ABA and metabolites (Table 4.2). However, *t*-ABA and *t*-ABA-GE biosynthesis, taken together, were still decreased in the mutants by more than 60 percent (Table 4.2).

The fragmentation of Me-ABA by NCI has been elucidated (Netting *et al.*, 1987; Heath *et al.*, 1990). Analysis of [^{18}O]ABA by MS/MS allows measurement of the position and extent of ^{18}O incorporation into the different oxygen functions of ABA (Zeevaart *et al.*, 1989; Rock and Zeevaart, 1990a; Rock *et al.*, 1991). Three phenomena involving the ABA biosynthetic pathway have been characterized by this method. 1) The incorporation of a single ^{18}O atom into the side chain carboxyl group of ABA, with gradual incorporation, over time, of label into the ring oxygens. This was the observation by Creelman *et al.* (1987) which suggested there is a large ABA precursor pool of xanthophylls that turns over slowly and already contains the oxygens on the ring. 2) The loss of side chain carboxyl ^{18}O label in [^{18}O]ABA due to carbonyl oxygen exchange with the medium at an aldehyde (xanthoxin or ABA-aldehyde) stage of biosynthesis. This exchange is proposed to be the mechanism which gives rise to ring-labeled [^{18}O]ABA which is unlabeled in the

side chain carboxyl, as seen in apple fruit (Rock and Zeevaart, 1990a). 3) The phenomenon of doubly-carboxyl-labeled [^{18}O]ABA, which has been observed as a minor biosynthetic product in ^{18}O-labeling experiments with a number of species (Zeevaart *et al.*, 1989).

Figure 4.1 shows MS/MS spectra of [$^{18}O_2$]ABA (parent ion m/z=282) from water-stressed wild type, *flc* and *sit* leaves under $^{18}O_2$ for 8 h. Rheinlands Ruhm wild type showed the typical pattern of labeling; for doubly-labeled ABA the side chain ion (unlabeled m/z= 141) was shifted to m/z = 143, and dehydration of the 1'-hydroxyl group of [$^{18}O_2$]ABA yielded a loss of 20 atomic mass units to m/z = 262. This result shows that incorporation of ^{18}O was predominantly into the side chain carboxyl and 1'-hydroxyl groups. Doubly-carboxyl-labeled ABA, evident by the presence of ions at m/z = 145, was a minor product in wild type leaves (Figure 4.1). However, in [$^{18}O_2$]ABA from *flc* and *sit* the majority of molecules contained both ^{18}O atoms in the side chain carboxyl group, evident by the abundance of ions at m/z = 145 (Figure 4.1).

Table 4.3 presents a quantitative analysis of the labeling patterns of [^{18}O]ABA and [^{18}O]*t*-ABA from wild type and ABA-deficient

Figure 4.1. GC-NCI-MS/MS of [$^{18}O_2$]Me-ABA (m/z = 282) from water-stressed leaves of wild type Rheinlands Ruhm (A), *flacca* (B), and *sitiens* (C) tomato in $^{18}O_2$ for 8 h. Inset: the structure of Me-ABA with asterisks (*) showing the predominant position of ^{18}O atoms.

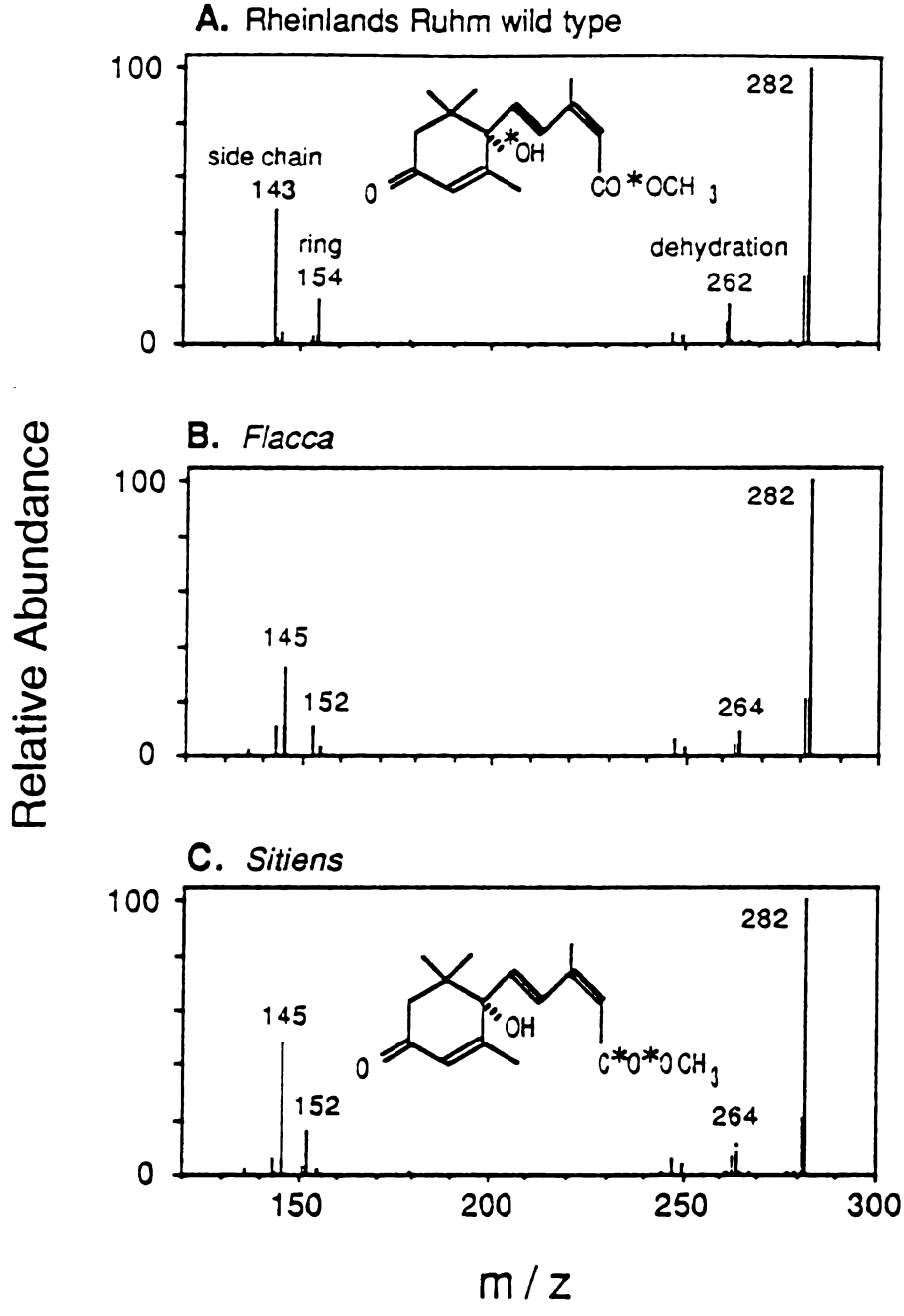
A. Rheinlands Ruhm wild type
100
0
282
side chain
143
ring
154
dehydration
262
OH
CO*OCH 3
B. Flacca
145
152
264
C. Sitiens
C*O*O CH3
Relative Abundance
150
200
250
300
m / z

Table 4.3. Extent and Position of ABA and *trans*-ABA ^{18}O-Labeling in Water Stressed Leaves of Wild Type and ABA-Deficient Mutants of Tomato in $^{18}O_2$ for 4 h

Mutants are listed in order of increasing phenotypic severity (13, 28). All classes of [^{18}O]ABA, except columns 3 and 6, are completely labeled at the 1'-hydroxyl position. Samples were analyzed by GC-NCI-SIM and MS/MS.

	Percent of Total [^{18}O]ABA							
	Unlabeled in Carboxyl		One ^{18}O Atom in Carboxyl			Two ^{18}O Atoms in Carboxyl		
Genotype	One ^{18}O In Ring 1	Two ^{18}O In Ring 2	Zero ^{18}O In Ring 3	One ^{18}O In Ring 4	Two ^{18}O In Ring 5	Zero ^{18}O In Ring 6	One ^{18}O In Ring 7	Doubly-Carboxyl-Labeled ABA
								ng / g fr wt / 4 h
Rheinlands Ruhm								
ABA	1.7	0.1	92.9	3.7	1.2	0.4	trace	1.05
t-ABA	3.1	0.2	81.6	10.0	3.5	1.3	0.2	0.03
Notabilis								
ABA	14.0	0.3	74.0	5.6	N.D.	6.1	N.D.	0.50
t-ABA	12.3	0.2	83.3	3.4	N.D.	0.8	N.D.	0.01
Flacca								
ABA	11.8	0.7	61.9	4.9	1.4	18.2	1.0	0.74
t-ABA	7.4	0.8	70.7	2.5	0.6	17.5	0.5	0.05
Sitiens								
ABA	11.6	0.2	42.3	7.7	3.6	32.0	2.6	0.62
t-ABA	15.0	0.4	67.5	4.0	0.2	12.3	0.6	0.06

[a]Not detected

mutant leaves after a 4 h labeling experiment. The seven major classes of [^{18}O]ABA molecules are represented as a percentage of total [^{18}O]ABA (Table 4.3, columns 1-7). This allows a comparison of the ABA biosynthetic reactions in wild type and mutant tissues. Several points can be made from the labeling patterns. a) Because ABA and *t*-ABA from the same samples can have significantly different labeling patterns (Table 4.3), the law of mass action supports the hypothesis that little isomerization of ABA to *t*-ABA has occurred *in vivo* or *in vitro*. This interpretation is supported by feeding studies with apple (Rock and Zeevaart, 1990a) and measurement of ABA isomerization *in vitro* (Milborrow, 1970). b) Side chain carbonyl exchange at an aldehyde intermediate stage of ABA biosynthesis (Rock and Zeevaart, 1990a) was higher in the mutants than wild type (Table 4.3, compare column 4 *versus* column 1 between wild type and mutants). In the wild type [^{18}O]ABA pool there was relatively more doubly-labeled ABA with one ^{18}O atom on the ring and one atom in the carboxyl group (Table 4.3, column 4) than singly-labeled ABA with label on the ring (Table 4.3, column 1). This is interpreted as a high ABA-aldehyde oxidase activity which resulted in carbonyl label retention by rapid oxidation to ABA.

Conversely, the mutant ABA labeling patterns suggest there was more carbonyl oxygen exchange because there was relatively more singly-labeled ABA which was labeled on the ring (Table 4.3, column 1) than doubly-labeled ABA with one ^{18}O in the carboxyl group and one on the ring (Table 4.3, compare columns 4 *versus* 1). This observation suggests that aldehyde oxidation was slower in the mutants and is supported by previous work showing the *flc* and *sit* mutants are impaired in ABA-aldehyde oxidation (Sindhu and Walton, 1988; Sindhu *et al.*, 1990; Taylor *et al.*, 1988). c) From the MS/MS analysis it can be concluded that the mutants synthesized a higher percentage of [^{18}O]ABA which was doubly labeled in the carboxyl group than wild type leaves (Table 4.3, columns 6 and 7). When this doubly-carboxyl-labeled ABA was quantified on a gram fresh weight basis, both wild type and mutant tissues synthesized approximately equal but small amounts; significantly, *flc* and *sit* synthesized more doubly-carboxyl-labeled *t*-ABA than wild type (Table 4.3). This result correlates with endogenous *t*-ABA-alcohol levels in wild type and mutant leaves (Linforth *et al.*, 1987). Similar patterns of doubly-carboxyl-labeled ABA were seen in $^{18}O_2$ experiments of longer duration, and in [$^{18}O_2$]ABA-GE and [$^{18}O_3$]PA (data not shown).

4.4.2. ABA and *Trans*-ABA Biosynthesis in the ABA-Deficient Potato and Barley Mutants

In order to obtain supporting evidence for the hypothesis that ABA-alcohol is an intermediate in ABA biosynthesis, we analyzed the *droopy* mutant of potato (Quarrie, 1982) and the molybdenum cofactor mutant Az34 (*nar2a*) of barley (Walker-Simmons *et al.*, 1989). These two mutants have been characterized as impaired in ABA-aldehyde oxidation (Duckham *et al.*, 1989; Walker-Simmons *et al.*, 1989), and therefore might exhibit similar patterns of ABA biosynthesis as the *flc* and *sit* mutants. Table 4.4 presents ABA, *t*-ABA and catabolite levels in unstressed and 8 h water-stressed leaves of the mutants and wild types (for potato, a pseudo-wild type *Dr/dr* heterozygote was used). The *droopy* potato mutant showed the same phenotype as the *flc* and *sit* tomato mutants on the basis of *t*-ABA and *t*-ABA-GE accumulation and biosynthesis (Table 4.4). The Az34 molybdenum cofactor mutant of barley did not accumulate *t*-ABA or *t*-ABA-GE (Table 4.4).

Analysis by MS/MS of [^{18}O]ABA and [^{18}O]*t*-ABA from an 8 h labeling experiment with the potato and barley mutants showed similarities and differences from the tomato mutant labeling patterns

Table 4.4. Quantitation of ABA, *trans*-ABA and Catabolites in Heterozygous (Normal) and Homozygous (Mutant) *droopy* Potato and in Wild Type and the Molybdenum Cofactor Mutant (Az34) of Barley Before and After 8 h Water Stress

Samples were quantified by GC-NCI-SIM. Potato measurements are the mean of three experiments (± SE); barley measurements are the average of two experiments.

Species / Genotype	ABA	*t*-ABA	ABA-GE	*t*-ABA-GE	PA
			ng / g fr wt		
Potato					
Heterozygous *Dr/dr*					
Unstressed	33.5 ± 8.7	0.9 ± 0.2	2.8 ± 0.6	2.3 ± 1.0	206.0 ± 38.6
Stressed 8 h	333.1 ± 133.6	4.0 ± 1.5	16.7 ± 3.0	2.7 ± 0.7	1805.7 ± 438.2
Homozygous *dr/dr*					
Unstressed	8.0 ± 1.8	24.8 ± 5.7	1.5 ± 0.2	17.5 ± 5.8	71.5 ± 12.6
Stressed 8 h	9.0[a] ± 1.9	33.6[a] ± 8.2	2.2 ± 0.2	71.9 ± 20.2	92.5 ± 22.2

Table 4.4 (cont'd.)

Barley					
"Steptoe" wild type					
Unstressed	3.0	0.1	3.8	1.0	18.4[b]
Stressed 8 h	116.3	3.1	8.9[b]	6.7[b]	897.2[b]
Az 34 (*nar2a*)					
Unstressed	1.0	0.1	5.2	1.1	17.2[b]
Stressed 8 h	13.0	0.4	5.5[b]	1.0[b]	96.4[b]

[a]Four experiments [b]One experiment

(Table 4.5). Both mutants showed increases in the percentage of doubly-carboxyl-labeled ABA and *t*-ABA compared to their respective wild types (Table 4.5, columns 6 and 7). However, carbonyl exchange at an aldehyde intermediate stage of biosynthesis did not appear affected in either the *droopy* potato or Az34 MoCo mutant of barley (Table 4.5, compare columns 4 *versus* 1 between wild type and mutant ABA), in contrast with the tomato mutants (Table 4.3). For *t*-ABA, carbonyl exchange was high in both wild type and mutant tissue of potato and barley (Table 4.5, compare columns 4 *versus* 1 for *t*-ABA).

4.4.3. ABA-Alcohol Oxidation in the *Flacca* and *Sitiens* Mutants

In order to directly test whether ABA-alcohol is a precursor to doubly-carboxyl-labeled ABA, we fed $[^2H_{3\text{-}6}](\pm)$ABA-aldehyde and $[^2H_{3\text{-}6}](\pm)$ABA-alcohol to wild type and *flc* leaves in $^{18}O_2$ for 8 h and measured by MS/MS the extent of ^{18}O incorporation into $[^2H_{3\text{-}6}]$ABA. From the results presented in Table 4.6, it is clear that *flc* is impaired in the oxidation of ABA-aldehyde, as previously shown (Sindhu *et al.*, 1990; Taylor *et al.*, 1988). In the $[^2H_{3\text{-}6}](\pm)$ABA-alcohol feed, the high oxidation rate in wild type was probably due to conversion of ABA-alcohol to ABA-aldehyde, which occurs non-enzymatically *in*

Table 4.5. Extent and Position of ABA and *trans*-ABA ^{18}O-Labeling in Water-Stressed Leaves of Heterozygous (Normal) and Homozygous (Mutant) *droopy* Potato and in Wild Type and the Molybdenum Cofactor Mutant (Az34) of Barley in $^{18}O_2$ *for 8 h*

All classes of [^{18}O]ABA, except columns 3 and 6, are completely labeled at the 1'-hydroxyl position. Samples were analyzed by GC-NCI-SIM and GC-NCI-CAD-MS/MS.

Species / Genotype	Percent of total [^{18}O]ABA						
	unlabeled in carboxyl		one ^{18}O atom in carboxyl			two 18O atoms in carboxyl	
	one ^{18}O in ring	two ^{18}O in ring	zero ^{18}O in ring	one ^{18}O in ring	two ^{18}O in ring	zero ^{18}O in ring	one ^{18}O in ring
	1	2	3	4	5	6	7
Potato							
Heterozygous *Dr/dr*							
ABA	0.9	trace	93.6	4.8	0.3	0.4	trace
t-ABA	7.6	N.D.[a]	92.4	N.D.	N.D.	N.D.	N.D.

Table 4.5 (cont'd.)

Homozygous *dr/dr*							
ABA	2.5	N.D.	64.6	7.4	trace	25.1	0.3
t-**ABA**	6.8	0.1	86.9	3.8	trace	2.3	trace
Barley							
Wild type "Steptoe"							
ABA	1.4	0.1	77.7	16.5	1.4	2.4	0.2
t-**ABA**	4.5	trace	94.5	0.9	N.D.	0.1	N.D.
Az 34 *(nar2a)*							
ABA	4.8	0.7	64.2	19.0	0.7	9.9	0.7
t-**ABA**	12.7	N.D.	68.0	12.1	N.D.	7.2	N.D.

[a]Not detected

Table 4.6. Quantitation of Labeled ABA from Wild Type and *Flacca* Tomato Leaves Fed Deuterated ABA-Aldehyde or ABA-Alcohol 8 h in $^{18}O_2$

Unstressed leaves were dipped in a 4 x 10^{-5} M solution of deuterated substrate (97.2% [$^2H_{3-6}$]) plus 0.05% Tween 20 and 0.2% ethanol (v/v) and immediately placed in $^{18}O_2$ (20 % [v/v] with N_2 as remainder). Samples were quantified by GC-NCI-SIM and ^{18}O incorporation in the carboxyl group confirmed by MS/MS.

Substrate / Genotype	Products		Percent ^{18}O in side chain
	[$^2H_{3-6}$]ABA	[$^{18}O^2H_{3-6}$]ABA	
	ng / g fr wt / 8 h		
[$^2H_{3-6}$]ABA-aldehyde			
Rheinlands Ruhm	1451.7	9.8	0.7%
Flacca	11.8	2.5	17.6%
[$^2H_{3-6}$]ABA-alcohol			
Rheinlands Ruhm	726.5	20.1	2.7%
Flacca	23.4	12.7	35.3%

vitro (C.D. Rock, unpublished observations). Leaves of *flc* converted a higher percentage of [$^{2}H_{3-6}$](±)ABA-alcohol, than of [$^{2}H_{3-6}$](±)ABA-aldehyde, to [$^{18}O^{2}H_{3-6}$]ABA (Table 4.6), which supports the hypothesis that ABA-alcohol is converted to ABA by oxidation with molecular oxygen.

In order to test the involvement of a P-450 monooxygenase as the molecular mechanism of ABA-alcohol oxidation in tomato, we utilized carbon monoxide, a specific inhibitor of heme P-450 monooxygenases (Ortiz de Montellano and Reich, 1986). The oxidation of ABA-alcohol was measured by GC-NCI-SIM of [$^{2}H_{3-6}$]ABA extracted from *sit* leaves incubated with [$^{2}H_{3-6}$](±)ABA-alcohol in the presence or absence of carbon monoxide or oxygen. The results are presented in Table 4.7. In the absence of molecular oxygen, there was no conversion to [$^{2}H_{3-6}$]ABA (Table 4.7). In the presence of 10% or 50% (v/v) CO, conversion to [$^{2}H_{3-6}$]ABA was inhibited 58% and 81% of control values, respectively. Similar results were obtained *in vitro* with a cell-free pumpkin endosperm extract (F. Fantauzzo and C. Rock, unpublished results) analogous to that of Gillard and Walton (1976). We further tested the monooxygenase hypothesis by measuring [^{18}O]ABA labeling patterns in *sit* leaves

Table 4.7. Inhibition by Carbon Monoxide of ABA-Alcohol Oxidation in *Sitiens* Leaves

Sitiens leaves were dipped in 1 x 10^{-5} M [$^2H_{3-6}$]ABA-alcohol plus 0.05% (v/v) Tween 20, 0.2% ethanol and incubated in the dark for 8 h in air, N_2, or air plus 10% or 50% (v/v) carbon monoxide. Samples were quantified by GC-NCI-SIM. Mean of three experiments (± SE).

Treatment	[$^2H_6$]ABA	Percent Inhibition
	ng / g fr wt / 8 h	
Air	11.9 ± 2.8	
N_2	N.D.[a]	100%
10% CO	5.0 ± 0.7	58%
50% CO	2.2 ± 0.5	81%

[a]Not detected, two experiments

incubated under $^{18}O_2$ or $^{18}O_2$ plus 50% carbon monoxide. If doubly-carboxyl-labeled ABA is synthesized by a monooxygenase, the presence of CO in this experiment should specifically inhibit the labeling of this class of [^{18}O]ABA molecules. The results in Table 4.8 confirm this prediction. The percentage of doubly-carboxyl-labeled ABA and *t*-ABA (Table 4.8, columns 6 and 7) was significantly decreased by CO treatment. When ABA and *t*-ABA from this experiment were quantified, more than 70% inhibition of doubly-carboxyl-labeled ABA and *t*-ABA biosynthesis was observed (Table 4.8). The results of these experiments support the conclusion that a cytochrome P-450 monooxygenase is responsible for ABA-alcohol oxidation *in vivo*.

4.5. DISCUSSION

Based on the results presented here, we conclude that ABA-alcohol is an intermediate in ABA biosynthesis in a shunt pathway from ABA-aldehyde that involves reduction of ABA-aldehyde to ABA-alcohol and oxidation of ABA-alcohol to ABA via a cytochrome P-450 monooxygenase (Figure 4.2). A number of species convert

Table 4.8. Extent and Position of ABA and *trans*-ABA ^{18}O Labeling in Water-Stressed Leaves of the ABA-Deficient Tomato Mutant Sitiens Incubated in $^{18}O_2$ in the Presence or Absence of 50% Carbon Monoxide for 8 h

All classes of [^{18}O]ABA, except columns 3 and 6, were completely labeled at the 1'-hydroxyl position. Samples were analyzed by GC-NCI-SIM and MS/MS. Results from one of two experiments.

	Percent of Total [^{18}O]ABA							
	Unlabeled in Carboxyl		One ^{18}O Atom in Carboxyl			Two ^{18}O Atoms in Carboxyl		
Treatment	One ^{18}O In Ring 1	Two ^{18}O In Ring 2	Zero ^{18}O In Ring 3	One ^{18}O In Ring 4	Two ^{18}O In Ring 5	Zero ^{18}O In Ring 6	One ^{18}O In Ring 7	Doubly-Carboxyl-Labeled ABA
								ng / g fr wt / 8 h
20% ; 80% (v/v) $^{18}O_2$; N_2								
ABA	7.9	trace	48.2	9.9	0.8	30.9	2.3	1.64
t-ABA	20.8	N.D.[a]	60.9	3.6	N.D.	14.6	N.D.	0.08
20% ; 30% ; 50% (v/v/v) $^{18}O_2$; N_2 ; CO								
ABA	9.5	0.4	59.2	11.8	0.1	19.0	0.1	0.44
t-ABA	34.7	0.1	63.4	0.5	N.D.	1.2	N.D.	0.002

[a]Not detected

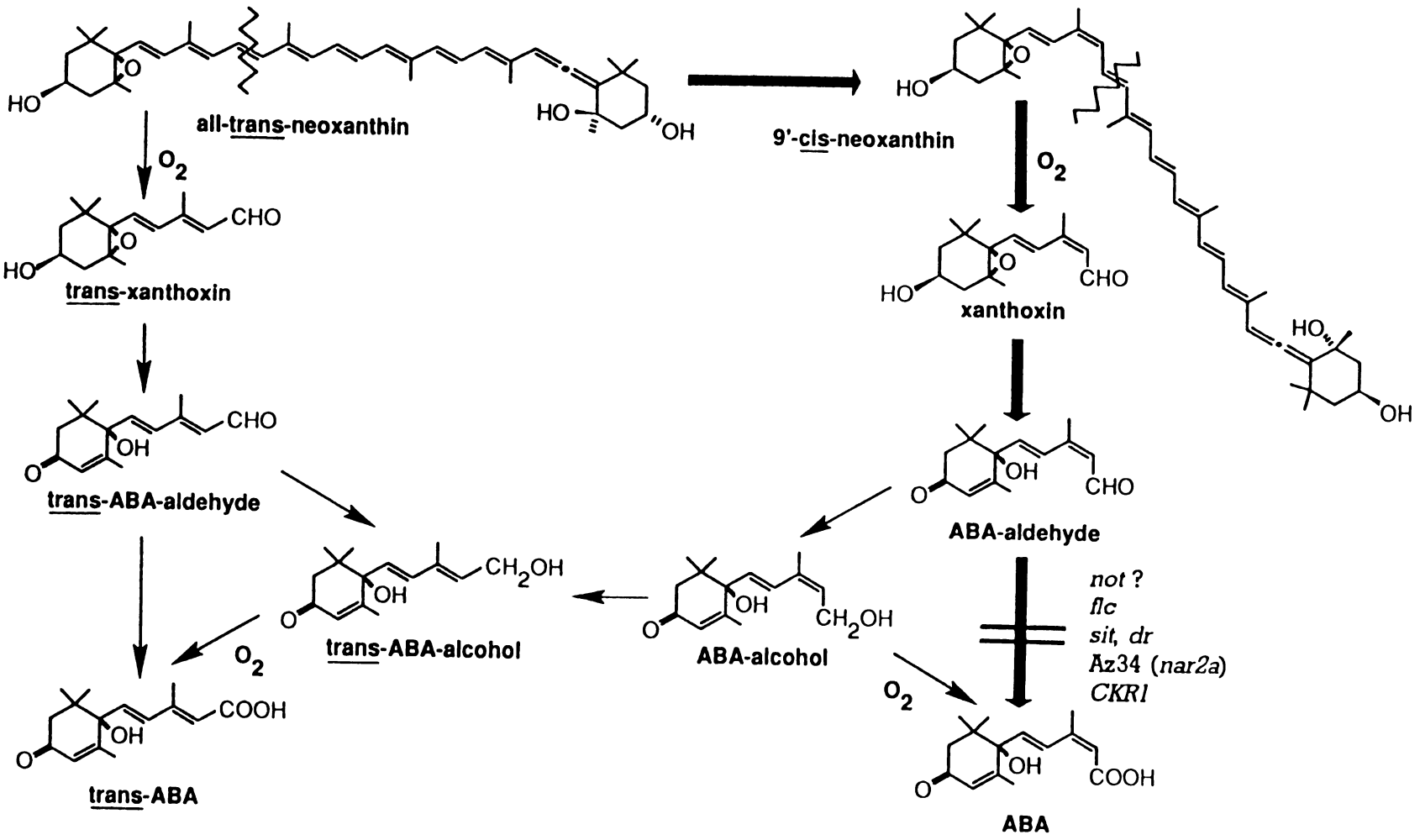
all-trans-neoxanthin
9'-cis-neoxanthin
trans-xanthoxin
xanthoxin
trans-ABA-aldehyde
ABA-aldehyde
trans-ABA-alcohol
ABA-alcohol
trans-ABA
ABA
O2
not ?
flc
sit, dr
Az34 (nar2a)
CKR1

Figure 4.2. Proposed pathways of ABA and *trans*-ABA biosynthesis from neoxanthin isomers (violaxanthin is also a cleavage substrate). The major pathway of ABA biosynthesis is shown with bold arrows. The ABA-aldehyde oxidase mutants are listed; the biochemical lesion in the *notabilis* mutant has not been clearly established.

exogenous ABA-aldehyde to ABA-alcohol (Duckham *et al.*, 1989). The *flc* and *sit* tomato mutants and *droopy* potato, which is probably homologous to *sit* (Duckham *et al.*, 1989), also isomerize a significant amount of ABA-aldehyde to *t*-ABA-alcohol (Duckham *et al.*, 1989; Linforth *et al.*, 1990). This isomerization and accumulation in the *flc* and *sit* mutants of tomato (Linforth *et al.*, 1987) gives rise to *t*-ABA and *t*-ABA-GE (Table 4.1) as a result of *t*-ABA-alcohol oxidation (Figure 4.2). This conclusion is supported by results of ^{18}O labeling studies which show a higher proportion of doubly-carboxyl-labeled ABA and *t*-ABA in the mutants of tomato (Table 4.3), barley, and potato (Table 4.5) blocked in ABA-aldehyde oxidation. Because ABA-alcohol from *flc* and *sit* is labeled in the primary alcohol group in ^{18}O labeling experiments (Linforth *et al.*, 1987; Rock and Zeevaart, unpublished results), we conclude that reduction of ABA-aldehyde results in at least partial trapping the ^{18}O present in the side chain, which is then oxidized by molecular oxygen to give doubly-carboxyl-labeled ABA in ^{18}O labeling experiments. The oxidation with $^{18}O_2$ of $[^2H_{3\text{-}6}](\pm)$ABA-alcohol to $[^{18}O^2H_{3\text{-}6}]$ABA (Table 4.6), plus the *in vivo* inhibition by CO of $[^2H_{3\text{-}6}](\pm)$ABA-alcohol oxidation (Table 4.7) and ABA with two ^{18}O atoms in the carboxyl (Table 4.8) indicate that a

cytochrome P-450 monooxygenase is the catalyst for ABA-alcohol oxidation in tomato.

The labeling data (Table 4.3) and feeding studies (Table 4.6) indicate that the shunt pathway of ABA-alcohol oxidation is not enhanced in the *flc* and *sit* tomato mutants to maximize ABA biosynthesis. We conclude that this pathway is a minor source of ABA in plants, but is physiologically significant in mutants which are impaired in ABA-aldehyde oxidation. Taken together with the quantitation data of Table 4.2, which show that wild type tomato synthesizes more *t*-ABA and *t*-ABA-GE than the *flc* and *sit* mutants, it can be concluded that oxidation of *t*-ABA-alcohol only accounts for about 10-15 percent of total *t*-ABA biosynthesis. We propose that the remainder of *t*-ABA is synthesized by a parallel pathway from all-*trans*-epoxy-carotenoids (Figure 4.2).

Duckham *et al.* (1989) proposed that synthesis of [$^2H_1$]*cis*-ABA-alcohol from [$^2H_1$](±)ABA-aldehyde was an artifact produced by conversion of the unnatural (-)ABA-aldehyde enantiomer in *flacca* and *sitiens* feeding experiments. Our data indicate that (+)-*cis*-ABA-alcohol is an endogenous metabolite of plants because (+) ABA is the naturally occurring enantiomer (Milborrow, 1970). *Cis*-ABA-

alcohol is likely the biosynthetic precursor to *t*-ABA-alcohol.

^{18}O-Labeling patterns in ABA and *t*-ABA from tomato suggest that the loss of ABA-aldehyde oxidase activity in the *flc* and *sit* mutants (Sindhu *et al.*, 1990) also results in an increase in ABA-aldehyde carbonyl oxygen enchange (Table 4.3, compare columns 4 *versus* 1 between wild type and mutants). The *not* mutant also shows this increased carbonyl exchange phenotype, although it has been shown not to be impaired in xanthoxin oxidation (Parry *et al.*, 1988) and only slightly reduced in ABA-aldehyde oxidation (Taylor *et al.*, 1988). Based on our data (Table 4.3) and those of Taylor *et al.* (1988), ABA-aldehyde oxidase may be affected by the *not* mutation. Taylor and Tarr (1984) crossed the tomato mutants and obtained all the possible double mutants; all these recombinants showed phenotypic interactions between the gene products of *not*, *flc* and *sit*. The function of these genes in ABA-aldehyde oxidation are unknown. Because the *not* mutant is extremely leaky, and the mechanisms involved in [^{18}O]ABA labeling have not been completely elucidated, and carbonyl exchange patterns are somewhat variable (compare Tables 4.3 and 4.8, columns 4 *versus* 1), we cannot conclude from our data that the site of action of the *not* mutation is

ABA-aldehyde oxidase.

The *droopy* mutant, which is probably homologous to *sit* based on map location (Duckham *et al.*, 1989), synthesizes large amounts of *t*-ABA; the MoCo mutant of barley does not (Table 4.4). The *droopy* potato and barley Az34 mutants do not exhibit decreased side chain carboxyl group labeling in [^{18}O]ABA (Table 4.5, compare columns 4 *versus* 1 between wild type and mutant ABA), as is seen in the tomato mutants. In contrast to tomato wild type *t-ABA* (Table 4.3), potato and barley wild types exchange more carbonyl label than they retain in *t*-ABA (Table 4.5, compare columns 4 *versus* 1 for *t*-ABA). Because doubly-labeled ABA with one ^{18}O atom on the ring and one in the side chain carboxyl (Tables 4.3 and 4.5, column 4) can be synthesized from either ring-labeled ABA-alcohol or doubly-labeled ABA-aldehyde, it is difficult to interpret the ABA and *t*-ABA labeling patterns in terms of individual enzyme activities, unless the precursor pool sizes and labeling patterns are known. The recently discovered *CKR1* mutant of *N. plumbaginifolia* is impaired in ABA-aldehyde oxidation, and may be useful to study the mechanism of carbonyl label retention in [^{18}O]ABA. It is not known if the mutations studied here affect the concentrations of ABA-aldehyde oxidase, or

the enzyme's catalytic activity, or ABA-aldehyde isomerization, or the reduction of ABA-aldehyde to ABA-alcohol. Purification and characterization of the wild type and mutant enzyme activities involved in the late steps of ABA biosynthesis may resolve some of these questions.

4.6. LITERATURE CITED

Creelman RA, Gage DA, Stults JT, Zeevaart JAD (1987) Abscisic acid biosynthesis in leaves and roots of *Xanthium strumarium*. Plant Physiol **85**: 726-732

Creelman RA, Zeevaart JAD (1984) Incorporation of oxygen into abscisic acid and phaseic acid from molecular oxygen. Plant Physiol **75**: 166-169

Duckham SC, Taylor IB, Linforth RST, Al-Naieb RJ, Marples BA, Bowman WR (1989) The metabolism of *cis* ABA-aldehyde by the wilty mutants of potato, pea and *Arabidopsis thaliana*. J Exp Bot **40**: 901-905

Gamble PE, Mullet JE (1986) Inhibition of carotenoid accumulation and abscisic acid biosynthesis in fluridone-treated dark-grown barley. Eur J Biochem **160**: 117-121

Gillard DF, Walton DC (1976) Abscisic acid metabolism by a cell-free preparation from *Echinocystis lobata* liquid endosperm. Plant Physiol **58**: 790-795

Heath TG, Gage DA, Zeevaart JAD, Watson JT (1990) Role of molecular oxygen in fragmentation processes of abscisic acid methyl ester in electron capture negative ionization. Org Mass Spectrom **25**: 655-663

Koornneef M, Jorna ML, Brinkhorst-van der Swan DLC, Karssen CM (1982) The isolation of abscisic acid (ABA) deficient mutants by selection of induced revertants in non-germinating gibberellin sensitive lines of *Arabidopsis thaliana* (L.) Heynh. Theor Appl Genet **61**: 385-393

Li Y, Walton DC (1990) Violaxanthin is an abscisic acid precursor in water-stressed dark-grown bean leaves. Plant Physiol **92**: 551-559

Linforth RST, Bowman WR, Griffin DA, Marples BA, Taylor IB (1987) 2-*trans*-ABA-alcohol accumulation in the wilty tomato mutants *flacca* and *sitiens*. Plant Cell Environ **10**: 599-606

Linforth RST, Taylor IB, Duckham SC, Al-Naib RJ, Bowman WR, Marples BA (1990) The metabolism and biological activity of ABA analogues in normal and *flacca* mutant tomato plants. New Phytol **115**: 517-521

Milborrow BV (1970) The metabolism of abscisic acid. J Exp Bot **21**: 17-29

Moore R, Smith JD (1985) Graviresponsiveness and abscisic acid content of roots of carotenoid-deficient mutants of *Zea mays* L. Planta **164**: 126-128

Neill SJ, Horgan R (1985) Abscisic acid production and water relations in wilty tomato mutants subjected to water deficiency. J Exp Bot **36**: 1222-1231

Neill SJ, Horgan R, Parry AD (1986) The carotenoid and abscisic acid content of viviparous kernels and seedlings of *Zea mays* L. Planta **169**: 87-96

Netting AG, Milborrow BV, Vaughan GT, Lidgard RO (1988) The fragmentation of methyl abscisate and its 2*E* isomer in methane positive and negative chemical ionization mass spectrometry. Biomed Environ Mass Spectrom **15**: 375-389

Ortiz de Montellano PR, Reich NO (1986) Inhibition of cytochrome P-

450 enzymes. *In* PR Ortiz del Montellano, ed, Cytochrome P-450: Structure, Mechanism, and Biochemistry. Plenum, New York, pp 273-314

Parry AD, Babiano MJ, Horgan R (1990a) The role of *cis*-carotenoids in abscisic acid biosynthesis. Planta **182**: 118-128

Parry AD, Blonstein AD, Babiano MJ, King PJ, Horgan R (1991) Abscisic-acid metabolism in a wilty mutant of *Nicotiana plumbaginifolia*. Planta **183**: 237-243

Parry AD, Neill SJ, Horgan R (1988) Xanthoxin levels and metabolism in the wild-type and wilty mutants of tomato. Planta **173**: 397-404

Parry AD, Neill SJ, Horgan R (1990b) Measurement of xanthoxin in higher plant tissues using ^{13}C labelled internal standards. Phytochemistry **29**: 1033-1039

Quarrie SA (1982) Droopy: a wilty mutant of potato deficient in abscisic acid. Plant Cell Environ **5**: 23-26

Rock CD, Zeevaart JAD (1990a) Abscisic (ABA)-aldehyde is a precursor to, and 1',4'-*trans*-diol a catabolite of, ABA in apple. Plant Physiol **93**: 915-923

Rock CD, Zeevaart JAD (1990b) ABA-alcohol is an intermediate in abscisic acid biosynthesis. Plant Physiol **93**: S5

Rock CD, Zeevaart JAD (1991) The *aba* mutant of *Arabidopsis thaliana* is impaired in epoxy-carotenoid biosynthesis. Proc Natl Acad Sci USA, submitted

Rock CD, Heath TG, Zeevaart JAD (1991) *Trans*-ABA biosynthesis and xanthoxin metabolism in wild type and the *aba* mutant of *Arabidopsis thaliana*. J Exp Bot, submitted

Sindhu RK, Griffin DH, Walton DC (1990) Abscisic aldehyde is an intermediate in the enzymatic conversion of xanthoxin to abscisic acid in *Phaseolus vulgaris* L. leaves. Plant Physiol **93**:

689-694

Sindhu RK, Walton DC (1988) Xanthoxin metabolism in cell-free preparations from wild type and wilty mutants of tomato. Plant Physiol **88**: 178-182

Tal M, Nevo Y (1973) Abnormal stomatal behavior and root resistance, and hormonal imbalance in three wilty mutants of tomato. Biochem Genet **8**: 291-300

Taylor IB, Linforth RST, Al-Naieb RJ, Bowman WR, Marples BA (1988) The wilty mutants *flacca* and *sitiens* are impaired in the oxidation of ABA-aldehyde to ABA. Plant Cell Environ **11**: 739-745

Taylor IB, Tarr AR (1984) Phenotypic interactions between abscisic acid deficient tomato mutants. Theor Appl Genet **68**: 115-119

Walker-Simmons M, Kudra DA, Warner RL (1989) Reduced accumulation of ABA during water stress in a molybdenum cofactor mutant of barley. Plant Physiol **90**: 728-733

Zeevaart JAD, Creelman RA (1988) Metabolism and physiology of abscisic acid. Annu Rev Plant Physiol Plant Mol Biol **39**: 439-473

Zeevaart JAD, Heath TG, Gage DA (1989) Evidence for a universal pathway of abscisic acid biosynthesis in higher plants from ^{18}O incorporation patterns. Plant Physiol **91**: 1594-1601

CHAPTER 5

THE *aba* MUTANT OF *ARABIDOPSIS THALIANA* IS IMPAIRED IN EPOXY-CAROTENOID BIOSYNTHESIS

5.1. ABSTRACT

The three mutant alleles of the *ABA* locus of *Arabidopsis thaliana* result in plants that are deficient in the plant growth regulator abscisic acid (ABA). We have used $^{18}O_2$ to label ABA in water-stressed leaves of mutant and wild type *Arabidopsis*. Analysis by selected ion monitoring and tandem mass spectrometry of [^{18}O]ABA and its catabolites, phaseic acid and ABA-glucose ester, indicates that the *aba* genotypes are impaired in ABA biosynthesis and have a small ABA precursor pool of compounds which contain oxygens on the ring, presumably oxygenated carotenoids (xanthophylls). Quantitation of the carotenoids from *aba* and wild type leaves establishes that the *aba* alleles cause a deficiency of the epoxy-carotenoids violaxanthin and neoxanthin and an accumulation of their biosynthetic precursor, zeaxanthin. These results provide evidence that ABA is synthesized via oxidative cleavage of epoxy-carotenoids (the "indirect pathway"). This is the first report of a carotenoid mutant in higher plants which undergoes normal greening. The *aba* alleles provide an opportunity to study the physiological role of epoxy-carotenoids in photosynthesis.

5.2. INTRODUCTION

Abscisic acid (ABA) is a sesquiterpenoid plant growth regulator involved in many physiological and developmental processes such as transpiration, germination and dormancy, and adaptation to environmental stresses, *e.g.* drought and chilling, and pathogen attack (Peña-Cortés *et al.*, 1989; for review see Zeevaart and Creelman, 1988). Although the structure of ABA (Figure 5.1D) has been known for 25 years (Ohkuma *et al.*, 1965), the biosynthetic pathway in higher plants has not been fully elucidated. The evidence favoring the indirect pathway from xanthophylls, as opposed to the direct pathway from farnesyl pyrophosphate (Milborrow, 1974), can be summarized as follows. 1) The *viviparous* mutants of maize, *vp-2, vp-5, vp-7,* and *vp-9,* are blocked in the early stages of carotenoid biosynthesis and are ABA-deficient (Moore and Smith, 1985; Neill *et al.*, 1985). 2) The carotenoid biosynthesis inhibitors fluridone and norflurazon also inhibit ABA biosynthesis (Gamble and Mullet, 1986; Moore and Smith, 1984). 3) $^{18}O_2$-Labeling experiments with water-stressed leaves show ^{18}O incorporation into the side chain carboxyl group of ABA, but little

Figure 5.1. The structures of: A) zeaxanthin; B) *trans*-violaxanthin; C) 9'-*cis*-neoxanthin; D) (S)-(+)-abscisic acid.

A

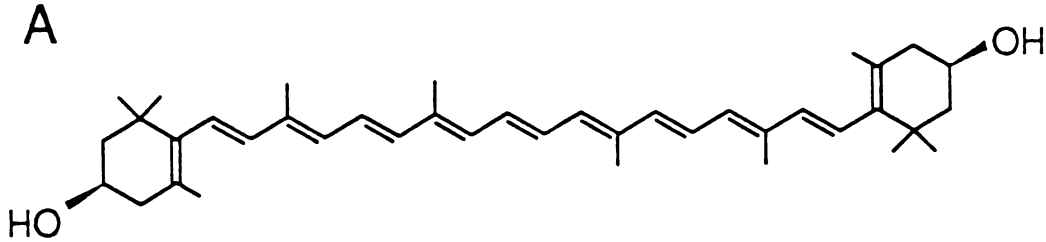

B

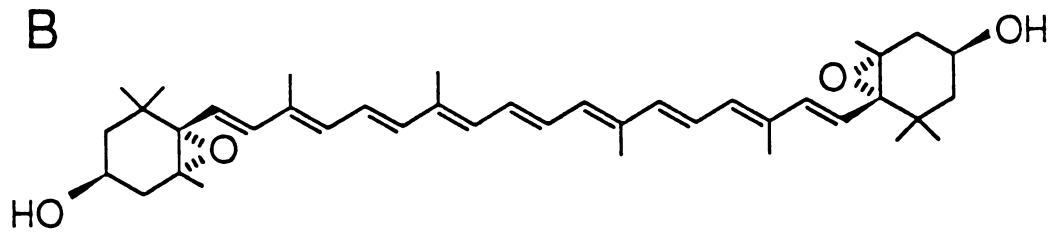

C

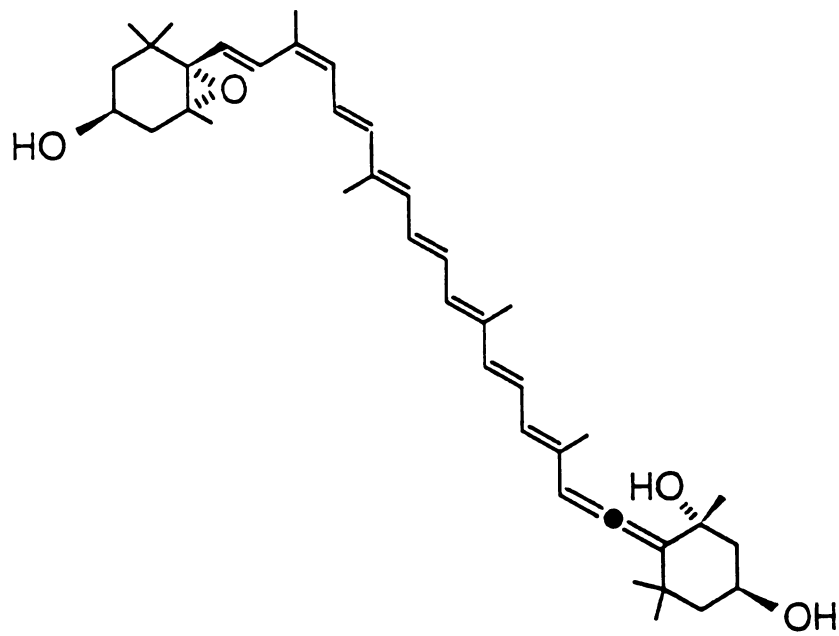

D

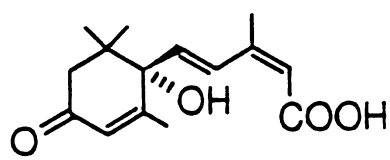

incorporation in the oxygen functions on the ring (Creelman *et al.*, 1987; Rock and Zeevaart, 1990; Zeevaart *et al.*, 1989), indicating that there is a large ABA precursor pool (presumably xanthophylls) which contains oxygens on the ring (see Figure 5.1). 4) Xanthoxin, a C_{15}- metabolite of epoxy-carotenoids, is found in plants (Parry *et al.*, 1990b) and is readily converted to ABA *in vivo* (Parry *et al.*, 1988; Taylor and Burden, 1973) and *in vitro* (Sindhu *et al.*, 1990). 5) A 1:1 correlation on a molar basis between decreases in *trans*-violaxanthin and 9'-*cis*-neoxanthin (Figure 5.1) levels and concomitant increases in ABA and its catabolites has been shown for dark-grown, water-stressed bean leaves (Li and Walton, 1990; Parry *et al.*, 1990a). In contrast to higher plants, phytopathogenic fungi synthesize ABA via a direct pathway from farnesyl pyrophosphate (Neill *et al.*, 1984; Okamoto *et al.*, 1988).

Koornneef *et al.* (1982) isolated three alleles, (*aba-1, -3, -4*), of a single locus (*ABA*) from *Arabidopsis thaliana* and showed a correlation between ABA deficiency in seeds of the *aba* genotypes and the phenotypic severity of leaf transpiration rates, reduced growth, and reduced seed dormancy. Application of ABA to the mutant plants restored the normal phenotype. Here we report ^{18}O

labeling studies and quantitation of ABA and carotenoids in leaves of wild type and the three *aba* genotypes. The results show a correlation between ABA deficiency associated with the *aba* alleles and epoxy-carotenoid deficiency.

5.3. MATERIALS AND METHODS

5.3.1. Plant Material

Seeds of *Arabidopsis thaliana* ecotype Landsberg *erecta* (collection number W20) and the mutant genotypes *aba-3* [isolation mutant G4 (Koornneef *et al.*, 1982); collection number W122], *aba-1* (A26; W21), and *aba-4* (A73; W123) were obtained from Dr. Maarten Koornneef, Agricultural University, Wageningen, The Netherlands. The genetic nomenclature recommended at the Third International *Arabidopsis* Meeting (East Lansing, MI, April 1987) is used (see Bleecker *et al.*, 1988). The *aba-1* genotype also included the recessive markers *ttg* (transparent testa glabra) and *yi* (yellow inflorescence). Seeds were germinated on 1% agar in Petri dishes for 2 weeks following storage at 4°C for two days to break dormancy. Seedlings were transplanted to trays containing a

mixture of perlite/vermiculite/peat moss (1:1:1, v/v/v). Plants were grown in a high humidity growth chamber maintained on a diurnal cycle of 9 h light (300 $\mu mol \cdot m^{-2} \cdot s^{-1}$) at 23° C and 15 h dark at 20° C. When stem elongation started, approximately 7 weeks after germination, rosette leaves were harvested and frozen in liquid N_2. For water stress experiments, detached rosettes were dehydrated with a hair dryer until 14% of the fresh weight was lost. The stressed material was immediately incubated in 20% $^{18}O_2$: 80% N_2 (v/v) or air at room temperature in the dark for 4 or 8 h and frozen in liquid N_2. The $^{18}O_2$ (97-98% enrichment) was from Cambridge Isotopes Laboratories (Woburn, MA).

5.3.2. ABA, ABA-Glucose Ester (ABA-GE), and Phaseic Acid (PA) Analysis

Frozen tissue was extracted overnight at 4° C with acetone containing 0.01% (w/v) 2,6-di-*tert*-butyl-4-methylphenol and 0.25% (v/v) glacial acetic acid. To each extract was added 20,000 dpm [^{3}H]ABA, [^{3}H]ABA-GE, and [^{3}H]PA (Cornish and Zeevaart, 1984) to quantify losses during purification. The samples were homogenized with a Polytron (Brinkmann, Westbury, NY) and filtered, and 10 ml 1.0 M potassium phosphate buffer (pH 8.2) was added. The acetone

was evaporated at 35° C using a rotovapor (Brinkmann), and the aqueous solution was passed through a cellulose filter to remove precipitated material. The pH was adjusted to 3.0 with 6 M HCl and ABA, ABA-GE and PA were partitioned five times into an equal volume of ethyl acetate. The combined organic fraction was evaporated and the residue chromatographed by reverse phase HPLC with a μBondapak C_{18} semipreparative 0.78 x 30 cm column (Waters, Milford, MA). A convex gradient (Waters no. 5) was run in 20 min from zero to 50% ethanol [plus 1% (v/v) acetic acid in water] at a flow rate of 2.5 ml/min. The eluant was monitored by UV absorbance at 262 nm. The fractions containing ABA-GE isomers plus PA (17-19 min) and ABA isomers (20.5-24 min) were collected and dried. The ABA-GE was hydrolyzed to the free acid by 2 M NH_4OH for 2 hr at 60° C and dried. Free ABA (from ABA-GE) was then separated from PA with a Nova-Pak C_{18} 0.39 x 15 cm analytical column (Waters) using a 20 min linear gradient from 10% to 60% methanol [in water containing 1% (v/v) glacial acetic acid] at a flow rate of 1.5 ml/min. The retention times of PA and ABA were 17 min and 22 min, respectively. Typical recoveries for ABA and PA were > 70% and > 50% for ABA-GE.

The ABA, ABA-GE (free acid) and PA samples were methylated with ethereal diazomethane, and a portion of each sample was quantified by GC-selected ion monitoring with a JEOL AH-505 double focussing mass spectrometer equipped with a Hewlett-Packard 5890A gas chromatograph and a 30 m, 0.259 mm internal diameter DB-23 capillary column (J. & W. Scientific, Rancho Cordova, CA) with He as the carrier gas. Flow rate was 1 ml/min. The GC oven temperature was programmed from 80° C to 200° C at 40°/min, then from 200° C to 250° C at 10°/min. Standard curves of ABA-methyl ester and PA-methyl ester with ABA-ethyl ester as an internal standard were constructed for quantitation. ABA-Methyl ester ions were monitored at m/z= 278, 280, 282, and 284 for ^{18}O-labeled samples and at m/z= 294, 296, 298, 300, and 302 for PA-methyl ester. Corrections were made for the natural abundance of stable isotopes by subtracting the theoretical contribution from the measured ion abundance. Tandem mass spectrometry was performed on a Finnegan TSQ-70 triple-quadrupole mass spectrometer as previously described (Rock and Zeevaart, 1990).

5.3.3. Carotenoid Determinations

Carotenoids were extracted according to Britton (1985) with

modifications. Frozen tissue (approximately 1 g) was extracted overnight at 4° C in 40 ml methanol containing 1% (w/v) sodium bicarbonate plus 0.1% (w/v) 2,6-di-*tert*-butyl-4-methylphenol and homogenized. Samples were manipulated in dim light to avoid isomerization of carotenoids. The extract was filtered, and the chlorophyll a and b concentrations were determined according to Holden (1976). The samples were diluted tenfold with water, NaCl was added to saturation, and the samples were repeatedly partitioned with 40 ml diethyl ether until no color remained in the aqueous fraction. The ether was evaporated, and the samples were saponified with 10% (w/v) KOH (in methanol) for 3 h at room temperature under a stream of N_2. The samples were again diluted tenfold and partitioned with diethyl ether. The ethereal extracts were stored overnight at -70° C, and ice crystals were removed by filtration. The extracts were evaporated, and the residue was resuspended in 90% hexanes, 10% ethyl acetate (v/v) and chromatographed by normal phase HPLC with a μPorasil semi-preparative 0.78 x 30 cm column (Waters) using a linear gradient from 10% to 100% ethyl acetate in 65 min at a flow rate of 2.5 ml/min. The major carotenoids were collected and identified by their

absorbance maxima, fine structure spectra, and acid shifts of absorbance maxima (Braumann and Grimme, 1981; Britton, 1985). *Cis* isomers were characterized by rechromatography of iodine-catalyzed *trans* isomers and by spectrophotometric analysis and predicted equilibrium stoichiometries (Khachik *et al.*, 1986; Molnár and Szabolcs, 1980). In addition, the identities of violaxanthin, neoxanthin and antheraxanthin isomers were confirmed by their retention times in reverse phase HPLC systems (Li and Walton, 1990; Parry *et al.*, 1990a).

Carotenoids were quantified by integration of the area under the absorbance curve at 450 nm. A standard curve of ß-carotene was constructed, and corrections were made for differences in specific extinction coefficients (Braumann and Grimme, 1981; Britton, 1985; our unpublished data).

5.4. RESULTS

5.4.1. ABA Biosynthetic Capacity is Negatively Correlated with the Phenotypic Severity Associated with the *aba* Alleles

The *aba* alleles differ in their phenotypic severity of increased

leaf transpiration, reduced growth, and reduced seed dormancy, which is correlated with reduced endogenous levels of ABA (Koornneef *et al.*, 1982). Plants homozygous for the *aba-3* allele have close to normal growth rates, while *aba-1* and *aba-4* plants are more pronounced in their negative effects on plant size and vigor (Koornneef *et al.*, 1982; our unpublished data). Biosynthesis of ABA in leaves of wild type Landsberg *erecta* and *aba* genotypes was determined by ^{18}O-labeling and quantitation of *de novo* [^{18}O]ABA and metabolites. The results (Table 5.1) show that the phenotypic severity of the alleles was correlated with reduced ABA biosynthesis. Although leaves of plants homozygous for the least severe allele, *aba-3,* accumulated ABA and catabolites which were about 50% of wild type turgid levels (our unpublished data), *aba-3* plants synthesized ABA and its catabolites, PA and ABA-GE, at about 3% of the wild type capacity in ^{18}O-labeling experiments (Table 5.1). Leaves of plants homozygous for the more severe alleles, *aba-1* and *aba-4,* had correspondingly lower ABA biosynthetic capacities (Table 5.1).

Table 5.1. Quantitation of ^{18}O-Labeled ABA and Catabolites from Water-Stressed Leaves of Wild Type and the Three *aba* Genotypes of *Arabidopsis* after Incubation for 4 or 8 hr in $^{18}O_2$

Mutants are listed in increasing order of phenotypic severity (Koornneef *et al.*, 1982). Samples were quantified as their methyl ester derivatives by GC-selected ion monitoring. Average of two experiments.

Genotype	^{18}O-Labeled Metabolites			
	ABA	ABA-GE	PA	Total
	ng / g fresh weight / time			
Landsberg *erecta*				
4 hr	28.1	0.2	104.2	132.5
8 hr	45.1	0.6	123.4	169.1
aba-3				
4 hr	1.6	trace	1.1	2.7
8 hr	2.9	0.1	1.5	4.5

Table 5.1 (cont'd.)

aba-1				
4 hr	0.7	trace	0.4	1.1
8 hr	1.2	0.1	0.8	2.1
aba-4				
4 hr	0.3	0.1	N.A.*	--
8 hr	1.0	0.1	N.A.	--

*N.A. = Not analyzed.

5.4.2. ABA Precursor Pool Size is Correlated with ABA Biosynthesis in *aba* Genotypes

The position and extent of ^{18}O incorporation into the ABA molecule can be determined by analysis of ^{18}O-labeled ABA by tandem mass spectrometry (Rock and Zeevaart, 1990; Zeevaart *et al.*, 1989). Comparison of ^{18}O incorporation, by wild type and *aba* plants, into the ring-attached oxygens of ABA (Table 5.2) indicates a correlation between ABA biosynthesis (Table 5.1) and turnover of the ABA precursor pool containing oxygens on the ring (presumably xanthophylls). Leaves of plants homozygous for the most severe allele, *aba-4,* had the highest percentage of ^{18}O incorporation into the ring-attached oxygens of [^{18}O]ABA. After 4 hr of water stress in an $^{18}O_2$ atmosphere, almost 60% of [^{18}O]ABA from *aba-4* plants was labeled in the ring 1'-hydroxyl group (Table 5.2), whereas in the wild type Landsberg tissue only 4% of the [^{18}O]ABA contained ^{18}O at this position. Plants homozygous for the less severe *aba* alleles had intermediate levels of ^{18}O ring incorporation (Table 5.2), which indicates that ABA precursor pool turnover was correlated with phenotypic severity of the alleles (Koornneef *et al.*, 1982). In the wild type Landsberg *erecta* plants, incorporation of ^{18}O in the

Table 5.2. ^{18}O Incorporation into the Ring-Attached Oxygens of ABA from Water-Stressed Leaves of Wild Type and the Three *aba* Genotypes of *Arabidopsis* after Incubation in $^{18}O_2$ for 4 or 8 h

Mutants are listed in order of increasing phenotypic severity (Koornneef *et al.*, 1982). Samples were analyzed as their methyl ester derivatives by GC-selected ion monitoring and tandem mass spectrometry (Rock and Zeevaart, 1990). The label was always present in the 1'-hydroxyl group (Zeevaart *et al.*, 1989); in addition, 5-10% of the 1'-hydroxyl-labeled ABA was also labeled in the 4'-keto group.

Genotype/ $^{18}O_2$ Incubation Time	Percent of total [^{18}O]ABA labeled in the ring-attached oxygens
Landsberg *erecta*	
4 hr	4.3%
8 hr	8.7%
aba-3	
4 hr	6.9%
8 hr	8.0%
aba-1	
4 hr	29.8%
8 hr	27.4%
aba-4	
4 hr	58.6%
8 hr	60.2%

ring-attached oxygens was six to fifteen times greater, on a fresh weight basis, than the incorporation by the *aba* plants. [This calculation is the product of [^{18}O]ABA levels (Table 5.1) and the respective percentage of [^{18}O]ABA which is ring-labeled (Table 5.2)]. Thus, the ABA precursor pool containing oxygens on the ring is much smaller in the *aba* plants than in wild type plants.

5.4.3. Epoxy-Carotenoid Deficiency and Zeaxanthin Accumulation are Correlated with the Small ABA Precursor Pool in *aba* Genotypes

The results of the $^{18}O_2$ incorporation studies with the *aba* genotypes (Tables 5.1 and 5.2) suggested that the xanthophyll levels of *aba* plants are reduced. Figure 5.2 shows chromatograms of carotenoids from leaves of wild type and *aba-4* plants. It is clear that *aba-4* plants had reduced levels of the major epoxy-carotenoids *trans*-violaxanthin and 9'-*cis*-neoxanthin (Figure 5.2, peaks 5 and 7), and that this mutant accumulated zeaxanthin (peak 3). Quantitation of carotenoids and chlorophylls from leaves of Landsberg *erecta* and the three *aba* genotypes is presented in Table 3. Zeaxanthin, the biosynthetic precursor to the epoxy-carotenoids antheraxanthin, violaxanthin, and neoxanthin (Jones and Porter, 1986), accumulated in leaves of all the *aba* genotypes. ß-Carotene, the precursor to

Figure 5.2. HPLC chromatograms of carotenoids extracted from leaves of wild type Landsberg *erecta* and the *aba-4* genotype of *Arabidopsis thaliana*. Numbered peaks are: 1, ß-carotene; 2, lutein; 3, zeaxanthin; 4, antheraxanthin; 5, *trans*-violaxanthin; 6, 9-*cis*-violaxanthin; 7, 9'-*cis*-neoxanthin.

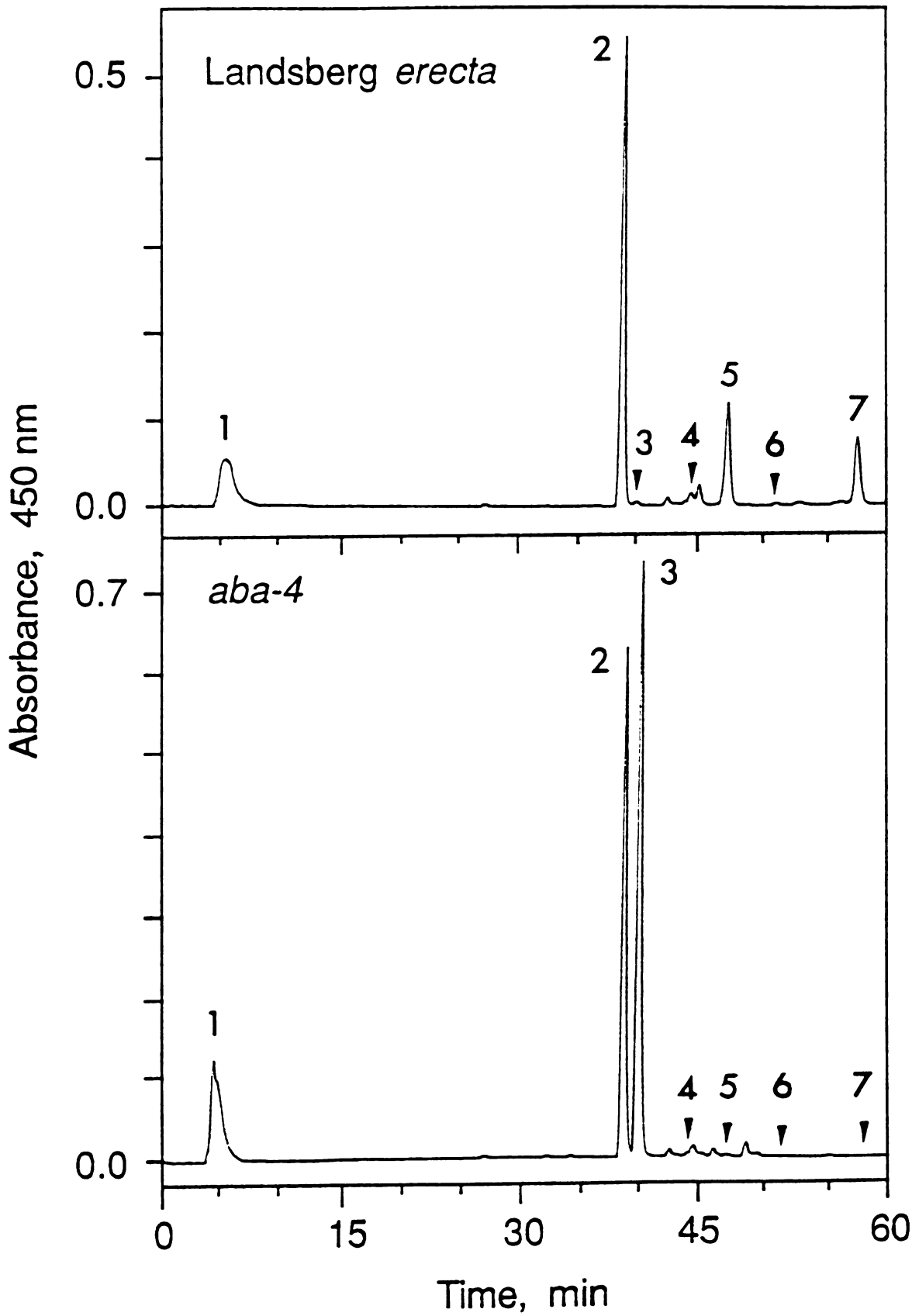
Landsberg erecta
aba-4
Absorbance, 450 nm
0.5
0.0
0.7
0.0
1
2
3
4
5
6
7
0
15
30
45
60
Time, min

zeaxanthin, also accumulated in *aba-4* plants (Table 5.3). There was a reduction of *trans*-violaxanthin and 9'-*cis*-neoxanthin in all *aba* plants. Lutein, the most abundant xanthophyll in wild type leaves and a product of the α-carotene branch pathway (Jones and Porter, 1986), was significantly reduced in the *aba* genotypes. Furthermore, the quantitative differences in zeaxanthin and ß-carotene accumulation (Table 5.3) are correlated with the phenotypic severity (Koornneef *et al.*, 1982) of the different *aba* alleles. From these results we conclude that the ABA precursor pool containing oxygens on the ring is composed of the epoxy-carotenoids violaxanthin and neoxanthin.

Total carotenoids and chlorophylls were not significantly different in wild-type and *aba* plants on a gram fresh weight basis (Table 5.3). However, the lower chlorophyll b level in *aba-4* plants is of interest because chlorophyll b and epoxy-carotenoids are associated predominantly with the light-harvesting photosynthetic complexes (Siefermann-Harms, 1985), and epoxy-carotenoids are neccessary for assembly of photosystem II light-harvesting complexes *in vitro* (Plumley and Schmidt, 1987).

Table 5.3. Quantitation of Carotenoids and Chlorophylls from Leaves of Wild Type and the Three *aba* Genotypes of *Arabidopsis*

Mutant alleles are listed in increasing order of phenotypic severity (Koornneef *et al.*, 1982). Leaves from two to six plants were extracted with methanol and chlorophyll and carotenoids measured as described in Materials and Methods. Mean of five experiments, two measurements each (± SE) except chlorophyll, six experiments.

Genotype	ß-Carotene	Lutein*	Zeaxanthin*	Antheraxanthin	*Trans*-Violaxanthin	9-*Cis*-Violaxanthin	*Trans*-Neoxanthin	9'-*Cis*-Neoxanthin	Σ Carotenoids	Chlorophyll	Chlorophyll a/b
					µg / g fresh weight						
Landsberg	23.8	58.0	1.2	0.9	17.2	0.6	1.5	20.0	122.3	1120	2.63
erecta	± 3.64	± 4.31	± 0.34	± 0.13	± 0.92	± 0.05	± 0.29	± 2.15	± 8.68	± 65	± 0.20
aba-3	24.7	39.0†	40.0†	1.1	0.4†	0.3	N.D.†,‡	0.2†	105.0	1070	2.40
	± 3.38	± 2.62	± 2.36	± 0.12	± 0.03	± 0.04		± 0.02	± 8.16	± 55	± 0.14
aba-1	25.1	38.4†	44.7†	0.9	0.4†	0.3	N.D.†	0.1†	109.4	1150	2.58
	± 1.67	± 1.28	± 2.32	± 0.11	± 0.03	± 0.06		± 0.02	± 4.26	± 58	± 0.24
aba-4	33.0§	46.1¶	52.2†	0.6	0.3†	0.2	N.D.†	0.2†	133.4	1250	3.00
	± 3.72	± 4.94	± 5.46	± 0.14	± 0.06	± 0.04		± 0.07	± 12.68	± 27	± 0.22

*Includes *cis* isomers. †Mutant significantly different from wild type, $P < 0.02$ (two sided "t" test). ‡N.D. = not detected. §Mutant significantly greater than wild type, $P < 0.08$ (one sided "t" test). ¶Mutant significantly different from wild type, $P < 0.12$.

5.5. DISCUSSION

The data presented here (Tables 5.2, 5.3) provide strong correlative evidence for the indirect pathway of ABA biosynthesis from violaxanthin and neoxanthin. If a direct pathway from farnesyl pyrophosphate exists in *Arabidopsis*, it is of negligible physiological importance. From extrapolation of the data in Tables 5.1 and 5.3, we predict that a complete loss of epoxy-carotenoids would result in absence of ABA and would be lethal.

The correlations between phenotypic severity (Koornneef *et al.*, 1982), reduced ABA biosynthesis (Tables 5.1, 5.2) and reduced epoxy-carotenoid content (Table 5.3) suggest that the *ABA* locus affects an enzyme which functions in the epoxidation of xanthophylls. Such an enzyme has been identified in chloroplast envelopes (Costes *et al.*, 1979) and as a component of the xanthophyll cycle (Siefermann and Yamamoto, 1975), which is involved in the dissipation by zeaxanthin of excess energy in photosynthesis (Demmig *et al.*, 1987; Demmig-Adams *et al.*, 1990). The data presented here imply that one and the same epoxidase is involved in the xanthophyll cycle and in epoxy-carotenoid biosynthesis. The mutations in the different alleles are presumably leaky, and the

residual epoxidase activity determines the rate-limiting step of violaxanthin and neoxanthin biosynthesis, and consequently of ABA biosynthesis, in *aba* plants.

Because *aba* plants have increased ABA precursor pool turnover (Table 5.2), these genotypes may be useful to study the regulation of epoxy-carotenoid and ABA biosynthesis. The involvement of violaxanthin, neoxanthin, and zeaxanthin in photosynthetic processes makes the *aba* alleles of *Arabidopsis* a promising experimental tool to investigate the function of epoxy-carotenoids and the xanthophyll cycle in plants.

5.6. LITERATURE CITED

Braumann T, Grimme LH (1981) Reversed-phase high performance liquid chromatography of chlorophylls and carotenoids. Biochim Biophys Acta **637**: 8-17

Britton G (1985) General carotenoid methods. Meth Enzymol **111**: 113-149

Bleecker AB, Estelle MA, Somerville C, Kende H (1988) Insensitivity to ethylene conferred by a dominant mutation in *Arabidopsis thaliana*. Science **241**: 1086-1089

Cornish K, Zeevaart JAD (1984) Abscisic acid metabolism in relation to water stress and leaf age in *Xanthium strumarium*. Plant Physiol **76**: 1029-1035

Costes C, Burghoffer C, Joyard J, Block M, Douce R (1979) Occurrence and biosynthesis of violaxanthin in isolated spinach chloroplast envelopes. FEBS Lett **103**: 17-21

Creelman RA, Gage DA, Stults JT, Zeevaart JAD (1987) Abscisic acid biosynthesis in leaves and roots of *Xanthium strumarium*. Plant Physiol **85**: 726-732

Demmig B, Winter K, Krüger A, Czygan F-C (1987) Photoinhibition and zeaxanthin formation in intact leaves: a possible role of the xanthophyll cycle in the dissipation of excess light energy. Plant Physiol **84**: 218-224

Demmig-Adams B, Adams WW III, Heber U, Neimanis S, Winter K, Krüger A, Czygan F-C, Bilger W, Björkman O (1990) Inhibition of zeaxanthin formation and of rapid changes in radiationless energy dissipation by dithiothreitol in spinach leaves and chloroplasts. Plant Physiol **92**: 293-301

Gamble PE, Mullet JE (1986) Inhibition of carotenoid accumulation and abscisic acid biosynthesis in fluridone-treated dark-grown barley. Eur J Biochem **160**: 117-121

Holden M (1976) Chlorophylls. *In* TW Goodwin, ed, Chemistry and Biochemistry of Plant Pigments, Vol 2. Academic, New York. pp 1-37

Jones BL, Porter JW (1986) Biosynthesis of carotenes in higher plants. CRC Crit Rev Plant Sci **3**: 295-324

Khachik F, Beecher GR, Whittaker NF (1986) Separation, identification, and quantification of the major carotenoid and chlorophyll constituents in extracts of several green vegetables by liquid chromatography. J Agric Food Chem **34**: 603-616

Koornneef M, Jorna ML, Brinkhorst-van der Swan DLC, Karssen CM (1982) The isolation of abscisic acid (ABA) deficient mutants by selection of induced revertants in non-germinating gibberellin sensitive lines of *Arabidopsis thaliana* (L.) Heynh. Theor Appl Genet **61**: 385-393

Li Y, Walton DC (1990) Violaxanthin is an abscisic acid precursor in water-stressed dark-grown bean leaves. Plant Physiol **92**: 551-559

Milborrow BV (1974) The chemistry and physiology of abscisic acid. Annu Rev Plant Physiol **25**: 259-307

Molnár P, Szabolcs J (1980) Occurrence of 15-*cis*-violaxanthin in *Viola tricolor*. Phytochemistry **19**: 623-627

Moore R, Smith JD (1984) Growth, graviresponsiveness and abscisic acid content of *Zea mays* seedlings treated with fluridone. Planta **162**: 342-344

Moore R, Smith JD (1985) Graviresponsiveness and abscisic acid content of roots of carotenoid-deficient mutants of *Zea mays* L. Planta **164**: 126-128

Neill SJ, Horgan R, Parry AD (1986) The carotenoid and abscisic acid content of viviparous kernels and seedlings of *Zea mays* L. Planta **169**: 87-96

Neill SJ, Horgan R, Walton DC (1984) Biosynthesis of abscisic acid. *In* A Crozier, JR Hillman, eds, The Biosynthesis and Metabolism of Plant Hormones. Cambridge Univ, Cambridge, UK, pp 43-70

Ohkuma K, Addicott FT, Smith OE, Thiessen WE (1965) The structure of abscisin II. Tetrahedron Lett **29**: 2529-2535

Okamoto M, Hirai N, Koshimizu K (1988) Biosynthesis of abscisic acid. Mem Coll Agric Kyoto Univ **132**: 79-115

Parry AD, Babiano MJ, Horgan R (1990a) The role of *cis*-carotenoids in abscisic acid biosynthesis. Planta **182**: 118-128

Parry AD, Neill SJ, Horgan R (1988) Xanthoxin levels and metabolism in the wild-type and wilty mutants of tomato. Planta **173**: 397-404

Parry AD, Neill SJ, Horgan R (1990b) Measurement of xanthoxin in

higher plant tissues using ^{13}C labelled internal standards. Phytochemistry **29**: 1033-1039

Peña-Cortés H, Sánchez-Serrano JJ, Mertens R, Willmitzer L, Prat S (1989) Abscisic acid is involved in the wound-induced expression of the proteinase inhibitor II gene in potato and tomato. Proc Natl Acad Sci USA **86**: 9851-9855

Plumley FG, Schmidt GW (1987) Reconstitution of chlorophyll a/b light-harvesting complexes: xanthophyll-dependent assembly and energy transfer. Proc Natl Acad Sci USA **84**: 146-150

Rock CD, Zeevaart JAD (1990) Abscisic (ABA)-aldehyde is a precursor to, and 1',4'-*trans*-ABA-diol a catabolite of, ABA in apple. Plant Physiol **93**: 915-923

Siefermann D, Yamamoto HY (1975) Properties of NADPH and oxygen-dependent zeaxanthin epoxidation in isolated chloroplasts. Arch Biochem Biophys **171** 70-77

Siefermann-Harms D (1985) Carotenoids in photosynthesis. I. Localization in photosynthetic membranes and light-harvesting function. Biochim Biophys Acta **811**: 325-355

Sindhu RK, Griffin DH, Walton DC (1990) Abscisic aldehyde is an intermediate in the enzymatic conversion of xanthoxin to abscisic acid in *Phaseolus vulgaris* L. leaves. Plant Physiol **93**: 689-694

Taylor HF, Burden RS (1973) Preparation and metabolism of 2-[^{14}C]-*cis,trans*-xanthoxin. J Exp Bot **24**: 873-880

Zeevaart JAD, Creelman RA (1988) Metabolism and physiology of abscisic acid. Annu Rev Plant Physiol Plant Mol Biol **39**: 439-473

Zeevaart JAD, Heath TG, Gage DA (1989) Evidence for a universal pathway of abscisic acid biosynthesis in higher plants from ^{18}O incorporation patterns. Plant Physiol **91**: 1594-1601

CHAPTER 6

2-*TRANS*-ABSCISIC ACID BIOSYNTHESIS AND THE METABOLISM OF ABA-ALDEHYDE AND XANTHOXIN IN WILD TYPE AND THE *aba* MUTANT OF *ARABIDOPSIS THALIANA*

6.1. ABSTRACT

Abscisic acid (ABA) and 2-*trans*-ABA (*t*-ABA) biosynthesis were studied in wild type Landsberg *erecta* and the three allelic *aba* mutants of *Arabidopsis thaliana* (L.) Heynh., which are impaired in epoxy-carotenoid biosynthesis. Labeling experiments with $^{18}O_2$ and mass spectrometric analysis of [^{18}O]ABA and its catabolites ABA-glucose ester (ABA-GE) and phaseic acid (PA), and *t*-ABA and *t*-ABA-GE, showed that *t*-ABA biosynthesis was less affected than ABA biosynthesis by mutations at the *ABA* locus. The *aba-4* allele caused the most severe impairment of ABA biosynthesis compared with the other two mutant alleles *aba-1* and *aba-3*, yet *aba-4* plants synthesized as much *t*-ABA as wild type Landsberg *erecta* plants. Feeding experiments with RS-[$^2H_6$]ABA-aldehyde isomers and unlabeled xanthoxin suggest that *t*-xanthoxin and *t*-ABA-aldehyde are precursors to ABA and *t*-ABA in *Arabidopsis*.

6.2. INTRODUCTION

The abscisic acid (ABA)-deficient mutants of *Arabidopsis thaliana* (L.) Heynh. and tomato (*Lycopersicon esculentum* Mill.) have been paramount to the understanding of ABA biosynthesis. Recently, it has been shown that the *aba* alleles of *Arabidopsis* are impaired in epoxy-carotenoid biosynthesis (Rock and Zeevaart, 1991), which provides strong evidence for the indirect pathway of ABA biosynthesis from the epoxy-carotenoids violaxanthin and neoxanthin, through 2-*cis*-xanthoxin and 2-*cis*-ABA-aldehyde to ABA (for review see Zeevaart and Creelman, 1988). The *flacca* and *sitiens* mutants of tomato are impaired in ABA-aldehyde oxidation (Sindhu and Walton, 1988; Taylor *et al.*, 1988) and accumulate *t*-ABA-alcohol (Linforth *et al.*, 1987). ABA-deficient mutants in potato (*Solanum tuberosum*, group *Phureja*; Duckham *et al.*, 1989), *Nicotiana plumbaginifolia* (Parry *et al.*, 1991), and barley (*Hordeum vulgare*; Walker-Simmons *et al.*, 1989) have also been characterized as impaired in ABA-aldehyde oxidation. We have demonstrated that the *flacca* and *sitiens* mutants of tomato synthesize a significant percentage of ABA from ABA-alcohol via a shunt pathway from ABA-

aldehyde (Rock *et al.*, 1991). In these mutants, most *t*-ABA and the catabolite *t*-ABA-GE are synthesized from *t*-ABA-alcohol.

With the exception of the shunt pathway from *t*-ABA-alcohol, little work has been done on the biosynthesis of *t*-ABA, since this isomer is biologically inactive (Walton, 1983). Since *trans*-ABA is rapidly esterified to *t*-ABA-GE (Milborrow, 1970), it may have been overlooked in ABA biosynthesis studies. Apple fruits can accumulate significant amounts of *t*-ABA during ripening (Bangerth, 1983), and this *t*-ABA is not the result of isomerization of ABA (Rock and Zeevaart, 1990). 2-*Trans*-xanthoxin, a metabolite of epoxy-carotenoids and precursor to *trans*-ABA (Taylor and Burden, 1973), is the predominant isomer found in plants (Parry *et al.*, 1988, 1990). The identification of [^{18}O]*t*-ABA-aldehyde in ^{18}O labeling studies with apple fruits suggested the existence of a parallel pathway of *t*-ABA biosynthesis from epoxy-carotenoids through *t*-xanthoxin and *t*-ABA-aldehyde (Rock and Zeevaart, 1990).

Here we report results of feeding and ^{18}O labeling studies with leaves of wild type Landsberg *erecta* and the three *aba* genotypes of *Arabidopsis thaliana*. The results suggest that *t*-ABA is synthesized via a pathway distinct from *t*-ABA-alcohol oxidation. Quantitation of

ABA, *t*-ABA and catabolites indicates that plants homozygous for the most ABA-deficient allele, *aba-4*, are capable of synthesizing significant amounts of *t*-ABA.

6.3. MATERIALS AND METHODS

6.3.1. Plant Material

Seeds of *Arabidopsis thaliana* (L.) Heynh., ecotype Landsberg *erecta* (collection number W20) and the mutant genotypes *aba-3* [isolation mutant G4 (Koornneef *et al.*, 1982); collection number W122], *aba-1* (A26; W21), and *aba-4* (A73; W123) were obtained from Dr. M. Koornneef, Agricultural University, Wageningen, The Netherlands. The *aba-1* genotype also carried the recessive markers *ttg* (transparent testa/glabrous) and *yi* (yellow inflorescence). Seeds were germinated on 1% agar in Petri dishes for 2 wks following storage at 4°C for two d to break dormancy. Seedlings were transplanted to trays containing a mixture of perlite/vermiculite/peat moss (1:1:1, v/v/v). Plants were grown in a high humidity growth chamber and maintained on a diurnal cycle of 9 h light (300 $\mu E \cdot m^{-2} \cdot s^{-1}$), 23° C and 15 h dark, 20° C. When stem

elongation started, approximately 7 weeks after germination, rosette leaves were harvested and frozen in liquid N_2 or used for feeding and $^{18}O_2$ labeling experiments. For ABA biosynthesis studies the tissue was water-stressed with a hair dryer until 14% of the fresh weight was lost. The tissue was incubated in 20% $^{18}O_2$: 80% N_2 (v/v)(Creelman and Zeevaart, 1984) or in air, at room temperature in the dark for 24 h, and frozen in liquid N_2. $^{18}O_2$ (97-98% enrichment) was purchased from Cambridge Isotopes Laboratories (Woburn, MA, USA).

6.3.2. Feeding Experiments

RS-[$^2H_{3-6}$]ABA-aldehyde [97.2% (w/w)] was synthesized as described (Rock and Zeevaart, 1990). 2-*Cis*- and *trans*-xanthoxin were obtained by potassium permanganate oxidation of violaxanthin (Burden and Taylor, 1970), extracted from leaves of *Xanthium strumarium* (Britton, 1985) and purified via an open ODS column as described by Sindhu and Walton (1987). Reaction products were chromatographed by normal phase HPLC on a μPorasil semipreparative 0.78 x 30 cm column (Waters, Milford, MA, USA) with a linear gradient from 10 to 60% (v/v) ethyl acetate in hexanes in 23 min at a flow rate of 2.5 cm^3 min^{-1} and the eluant monitored by

UV absorbance at 280 nm. Xanthoxin isomers and butenone were collected from 28 to 31 min and dried under a stream of N_2. The xanthoxin isomers were separated from butenone by reverse phase HPLC on a μBondapak semipreparative 0.78 x 30 cm column (Waters) with a linear gradient of 20-60% (v/v) ethanol (in water) in 25 min at a flow rate of 2.5 cm^3 min^{-1}. Butenone eluted at 12 min and xanthoxin isomers at 18 min. Samples were taken to dryness under a stream of N_2. Xanthoxin and ABA-aldehyde isomers were separated and purified by reverse phase HPLC using a 4 μm Novapak C_{18} Radial-PAK 0.8 x 10 cm cartridge (Waters) and a linear gradient from 20% to 60% (v/v) methanol (in water) in 45 min at a flow rate of 2.5 cm^3 min^{-1}. *Trans*-ABA-aldehyde eluted from 22.7 to 23.5 min, and *cis*-ABA-aldehyde from 25.5 to 26.8 min. *Trans*-xanthoxin eluted from 29.8 to 31 min, and *cis*-xanthoxin from 32 min to 33.3 min. Substrate purity was confirmed by GC-flame ionization detection, and the isomers were quantified by UV absorbance (Burden and Taylor, 1970; Rock and Zeevaart, 1990). A 2.5 μg cm^{-3} aqueous solution (1 x 10^{-2} mol m^{-3}) of substrate containing 0.05% (v/v) Tween 20 was vacuum infiltrated into leaf tissue from seven to 16 plants of wild type or *aba* genotypes, respectively, to give similar

fresh weights. The tissue was placed in air, or 20% $^{18}O_2$: 80% N_2 (v/v) for xanthoxin experiments, incubated in darkness for 8 h, and then frozen.

6.3.3. Extraction, Purification, and Quantitation of Metabolites

ABA, *t*-ABA, ABA-GE, *t*-ABA-GE, and phaseic acid (PA) were extracted and purified by reverse phase HPLC as described (Rock and Zeevaart, 1991). The 2-*trans* isomers of ABA and ABA-GE had slightly shorter retention times in this HPLC system than the corresponding 2-*cis*-isomers. Samples were methylated with ethereal diazomethane and quantified by GC-negative chemical ionization-selected ion monitoring as described (Chapters 4, 5). ABA-aldehyde was extracted and quantified by the isotope dilution method as described by Rock and Zeevaart (1990). Tandem mass spectrometry (MS/MS) was performed on a Finnegan TSQ-70 triple-quadrupole mass spectrometer as previously described (Rock and Zeevaart, 1990).

o

m

pla

les

erec

take

leave

in wil

the *ab*

6.4. RESULTS

6.4.1. ABA and *Trans*-ABA Biosynthesis and Metabolism

Initial characterization of the *aba* genotypes established a negative correlation between transpiration rates and ABA accumulation in seeds and immature green siliques (Koornneef *et al.*, 1982); the three *aba* genotypes also showed a correlation between ABA levels, reduced growth rates, and reduced seed dormancy. Table 6.1 confirms this result for leaf tissue. There was a negative correlation between phenotypic severity of the *aba* alleles and ABA, *t*-ABA and catabolite levels in unstressed tissue, with the exception of *t*-ABA and *t*-ABA-GE accumulation in plants homozygous for the most severe allele *aba-4*. *Trans*-ABA levels in unstressed *aba-4* plants were higher than in wild type, and *t*-ABA-GE was only slightly less than in wild type (Table 6.1). After 24 h water stress, Landsberg *erecta* accumulated ABA and its catabolites ABA-GE and PA, when taken together, to levels about six times higher than unstressed leaves (Table 6.1). The combined contents of *t*-ABA and *t*-ABA-GE in wild type increased only about two-fold (Table 6.1). In leaves of the *aba* genotypes, ABA and the major catabolite PA increased

Table 6.1. Quantitation of ABA, *trans*-ABA and Catabolites from Leaves of *Arabi*
Genotypes P, f

Table 6.1. Quantitation of ABA, *trans*-ABA and Catabolites from Leaves of *Arabidopsis* Wild Type and *aba* Genotypes Before and After 24 h Water Stress

Mutants are listed in order of increasing phenotypic severity. Samples were quantified by GC-negative chemical ionization-selected ion monitoring.

Genotype/Treatment	ng (g fresh weight)$^{-1}$ (mean ± standard error, n= 3-7)				
	ABA	*t*-ABA	ABA-GE	*t*-ABA-GE	PA
Landsberg *erecta*					
Unstressed	7.1 ± 1.38	0.9 ± 0.31	5.7 ± 2.20	3.9 ± 1.30	23.6 ± 5.50
Stressed 24 h	39.8 ± 13.64	0.8 ± 0.12	6.7 ± 2.42	11.2 ± 2.98	190.3 ± 80.48
aba-3					
Unstressed	2.8 ± 0.84	0.6 ± 0.08	4.0 ± 2.30	1.3 ± 0.43	3.7 ± 1.51
Stressed 24 h[a]	3.3	0.4	1.6	1.4	4.0
aba-1					
Unstressed	2.2 ± 0.58	0.1 ± 0.04	5.8 ± 4.12	2.1 ± 0.57	1.6 ± 0.51
Stressed 24 h[a]	2.5	0.8	1.0	0.8	1.6
aba-4					
Unstressed	1.9 ± 0.19	1.4 ± 0.14	2.1 ± 0.41	2.8 ± 1.66	2.2[a]
Stressed 24 h[a]	3.6	4.0	3.2	9.2	2.4

[a]Average of two experiments.

la

GC

199

6.2

cata

genc

ABA

corre

associ

the acc

was due

slightly in response to 24 h water stress. ABA-GE levels were more variable in both wild type and mutant tissue (Table 6.1). Consistent with the relatively high levels of *t*-ABA and *t*-ABA-GE in unstressed *aba-4* tissue, leaves of this mutant allele also accumulated a significant amount of *t*-ABA and *t*-ABA-GE after 24 h water stress (Table 6.1). Thus, although ABA biosynthesis is impaired by the *aba* mutation, in the case of the *aba-4* genotype, *t*-ABA biosynthesis is not reduced as compared to Landsberg wild type.

The capacity for ABA biosynthesis can be measured by ^{18}O-labeling studies and quantification of [^{18}O]ABA and catabolites by GC-negative chemical ionization-mass spectrometry (Rock *et al.*, 1991; Rock and Zeevaart, 1990, 1991; Zeevaart *et al.*, 1989). Table 6.2 presents the quantification of ^{18}O-labeled ABA, *t*-ABA and catabolites from water-stressed leaves of wild type and *aba* genotypes in $^{18}O_2$ for 24 h. Consistent with the results of Table 6.1, ABA biosynthesis was reduced in the *aba* genotypes and negatively correlated with phenotypic severity (Koornneef *et al.*, 1982) associated with the individual *aba* alleles (Table 6.2). Furthermore, the accumulation of *t*-ABA and *t*-ABA-GE in *aba-4* plants (Table 6.1) was due to *de novo* synthesis of *t*-ABA and *t*-ABA-GE (Table 6.2).

Table 6.2. Quantitation of ^{18}O-Labeled ABA, *trans*-ABA and Catabolite [illegible]

type and *aba* Genot[illegible]

Table 6.2. Quantitation of ^{18}O-Labeled ABA, *trans*-ABA and Catabolites from Water-Stressed Leaves of *Arabidopsis* wild type and *aba* Genotypes after 24 hr in $^{18}O_2$

Mutants are listed in order of increasing phenotypic severity. Samples were quantified by GC-negative chemical ionization-selected ion monitoring. Average of two experiments.

Genotypes	ng (g fresh weight)$^{-1}$ (24 h)$^{-1}$					Ratio *cis* /*trans* metabolites
	[^{18}O]ABA	[^{18}O]*t*-ABA	[^{18}O]ABA-GE	[^{18}O]*t*-ABA-GE	[^{18}O]PA[a]	
Landsberg *erecta*	32.2	0.3	2.0	2.4	145.6	66.6
aba-3	2.6	0.3	0.2	0.3	1.1	6.5
aba-1	1.8	0.4	trace	N.D.[b]	N.D.	4.5
aba-4	1.7	1.4	0.4	1.4	N.D.	0.8

[a] [^{18}O]PA with two or more ^{18}O atoms, *i.e.*, synthesized from [^{18}O]ABA.

[b] Not detected.

i

c

re

m

^{18}C

oxi

and

(epo

carb

When *t*-ABA biosynthesis ([^{18}O]*t*-ABA plus [^{18}O]*t*-ABA-GE) in wild type and *aba* plants was expressed as a fraction of ABA biosynthesis ([^{18}O]ABA + [^{18}O]ABA-GE + [^{18}O]PA) , a positive correlation between relative *t*-ABA biosynthesis and phenotypic severity was observed (Table 6.2, ratio *cis/trans* metabolites). Thus, consistent with the elevated *t*-ABA levels in *aba-4* plants (Table 6.1), ^{18}O labeling studies also showed that the *aba* alleles had less effect on *t*-ABA than ABA biosynthesis (Table 6.2).

The fragmentation by NCI of Me-ABA has been elucidated (Heath *et al.*, 1990; Netting *et al.*, 1988). By MS/MS of [^{18}O]ABA from *in vivo* labeling experiments it is possible to quantify the incorporation of ^{18}O into each oxygen atom of ABA: the side chain carboxyl, the ring 4'-keto, and the 1'-hydroxyl group. Four possible reactions in ABA biosynthesis have been characterized by this method of analysis (Rock *et al.*, 1991; Rock and Zeevaart, 1990): 1) ^{18}O incorporation into the side chain carboxyl group as a result of oxidative cleavage of epoxy-carotenoids, such as 9-*cis*-violaxanthin and 9'-*cis*-neoxanthin. 2) Turnover of the large ABA precursor pool (epoxy-carotenoids), resulting not only in ^{18}O incorporation into the carboxyl group, but also into the oxygens on the ring of [^{18}O]ABA.

3) Synthesis of ABA from ABA-alcohol in a minor shunt pathway from ABA-aldehyde, which yields doubly-carboxyl-labeled [^{18}O]ABA via incorporation of ^{18}O from a second molecular oxygen. 4) Side chain carbonyl oxygen exchange with water at an aldehyde intermediate stage of ABA biosynthesis, resulting in loss of side chain carboxyl label in [^{18}O]ABA. Analysis by MS/MS of [^{18}O]ABA and [^{18}O]*t*-ABA from stressed wild type and *aba-4* plants in $^{18}O_2$ for 24 hr is presented in Table 6.3. The [^{18}O]ABA molecules are qualitatively distinguished by the number of ^{18}O atoms and their position of incorporation, giving rise to five major classes of [^{18}O]ABA (columns 1-5). The percentage of total [^{18}O]ABA in each class allows a comparison of the ABA biosynthetic pathways in the wild type and *aba-4* genotypes. Landsberg *erecta* showed the typical pattern of ^{18}O incorporation in ABA from stressed leaves. The bulk of [^{18}O]ABA was singly labeled, and the label was present in the carboxyl group. This pattern of incorporation is due to the large epoxy-carotenoid pool which turns over slowly; ^{18}O is incorporated into the side chain of ABA during oxidative cleavage of the xanthophyll precursor (Rock and Zeevaart, 1990; Zeevaart *et al.*, 1989). In plants homozygous for the *aba-4* allele, 65 percent of the [^{18}O]ABA was labeled in the

Table 6.3. Extent and Position of ^{18}O-Labeling in ABA and *trans*-ABA from Water-Stressed Leaves of Wild Type and the *aba-4* Genotype Incubated in $^{18}O_2$ for 24 h

Samples were analyzed by GC-tandem mass spectrometry (MS/MS). All classes of [^{18}O]ABA, except columns 3 and 5, are completely labeled at the 1'-hydroxyl position. Triply-labeled [^{18}O]ABA was less than 0.5% of total [^{18}O]ABA and is not listed.

Genotype	Percent of total [^{18}O]ABA				
	Unlabeled in carboxyl		One ^{18}O atom in carboxyl		Two ^{18}O atoms in carboxyl
	One ^{18}O in ring 1	Two ^{18}O in ring 2	Zero ^{18}O in ring 3	One ^{18}O in ring 4	Zero ^{18}O in ring 5
Landsberg *erecta*					
ABA	2.1	0.1	84.7	12.1	0.6
t-ABA	11.1	0.2	76.6	11.3	0.8
aba-4					
ABA	32.1	0.4	28.4	33.0	1.2
t-ABA	55.4	0.4	19.6	23.0	0.4

f

n

ur

ex

ald

Zee

ator

oxygens on the ring, while in wild type only 14 percent of the [^{18}O]ABA was labeled on the ring (Table 6.3, compare columns 1 plus 4 between wild type and mutant). This result indicates that the epoxy-carotenoid precursor pool was turning over rapidly in the mutant, consistent with the observed low levels of epoxy-carotenoids (Rock and Zeevaart, 1991). In both wild type and *aba* genotypes, *t*-ABA from the same material contained a higher percentage of ^{18}O label in the ring positions than ABA (Table 6.3, compare columns 1 plus 4 between ABA and *t*-ABA). Based on the law of mass action, the large differences in labeling patterns between [^{18}O]ABA and [^{18}O]*t*-ABA from the same samples indicate that isomerization of ABA was not the source of *t*-ABA. This conclusion is supported by feeding studies with apple (Rock and Zeevaart, 1990) and measurements of ABA isomerization *in vitro* (Milborrow, 1970).

Isotope exchange studies have shown that [^{18}O]ABA which is unlabeled in the side chain carboxyl group can arise in ^{18}O-labeling experiments by carbonyl oxygen exchange with the medium at an aldehyde intermediate stage of ABA biosynthesis (Rock and Zeevaart, 1990). Thus, xanthoxin or ABA-aldehyde with two ^{18}O atoms could be oxidized to doubly-labeled ABA (*e.g.*, Table 6.3,

column 4), or could exchange the carbonyl label and then be oxidized to ABA that is only labeled on the ring (Table 6.3, column 1). The data in Table 6.3 suggest that carbonyl exchange was slightly higher in the *aba-4* plants than in wild type, because ABA from Landsberg *erecta* tissue retained almost six times more label in the side chain than it lost the label, but the *aba-4* plants lost a greater percentage of side chain label (Table 6.3, compare columns 4 *versus* 1 between wild type and mutant). [^{18}O] *Trans*-ABA from both wild type and *aba-4* plants showed a higher degree of aldehyde carbonyl exchange than [^{18}O]ABA from the same sample (Table 6.3, compare columns 4 and 1 between ABA and *t*-ABA).

[^{18}O]ABA with two ^{18}O-atoms in the carboxyl group (Table 6.3, column 5) is synthesized from [^{18}O]ABA-alcohol with incorporation of ^{18}O by a minor shunt pathway from ABA-aldehyde (Rock *et al.*, 1991). The minor shunt pathway of ABA biosynthesis from ABA-alcohol was not affected in the *aba-4* genotype (Table 6.3, compare column 5 between wild type and mutant). This is unlike the *flacca* and *sitiens* mutants of tomato, which are blocked in ABA-aldehyde oxidation (Sindhu and Walton, 1988; Taylor *et al.*, 1988) and synthesize a significant percentage of ABA and *t*-ABA via ABA-alcohol and *t*-ABA-

alcohol, respectively (Rock *et al.*, 1991).

6.4.2. ABA-Aldehyde and Xanthoxin Metabolism in *aba* Mutant Alleles

In order to determine if the *ABA* locus affects aldehyde oxidation, C-2 isomers of RS-[$^2H_6$]ABA-aldehyde were fed to leaves of wild type and *aba* genotypes. In agreement with the work of Duckham *et al.* (1989), mutations at the *ABA* locus do not affect ABA-aldehyde oxidation (Table 6.4). There was evidence for isomerization of ABA-aldehyde and *t*-ABA-aldehyde to their respective C-2 isomers with subsequent oxidation to *t*-ABA and ABA, followed by conjugation to their glucose esters (Table 6.4). This is interpreted to mean that there was little or no interconversion between ABA-GE and *t*-ABA-GE, which is supported by results of feeding studies with apple fruits (Rock and Zeevaart, 1990) and tomato shoots (Milborrow, 1970).

Xanthoxin is a postulated intermediate in ABA biosynthesis between epoxy-carotenoid cleavage and ABA-aldehyde oxidation (Sindhu *et al.*, 1990; Zeevaart and Creelman, 1988). In order to test whether the *ABA* locus affects xanthoxin metabolism, C-2 isomers of xanthoxin were fed to wild type and *aba* genotypes in the presence

Table 6.4. Conversion of [$^2H_6$]ABA-Aldehyde Isomers to ABA, *trans*-ABA and Catabolites in Leaves of *Arabidopsis* Wild Type and *aba* Genotypes

A 2.5 μg cm^{-3} (1 x 10^{-2} mol m^{-3}) solution of RS-[$^2H_6$]ABA-aldehyde isomer (*cis* = 85% *cis*, *trans* = 96% *trans* isomer) containing 0.05% Tween 20 (vol/vol) was vacuum infiltrated into the leaf tissue and incubated in the dark for 8 h. Samples were quantified by GC-negative chemical ionization-selected ion monitoring. Results from one of three similar experiments.

Genotype / Substrate	ng (g fresh weight)$^{-1}$ (8 h)$^{-1}$				
	[$^2H_{3-6}$]ABA	[$^2H_{3-6}$] *t*-ABA	[$^2H_{3-6}$]ABA-GE	[$^2H_{3-6}$] *t*-ABA-GE	[$^2H_{1-3}$]PA
Landsberg *erecta*					
cis-ABA-aldehyde	1099.3	92.1	11.0	7.7	2711.5
trans-ABA-aldehyde	45.8	361.1	0.6	4.5	222.8
aba-1					
cis-ABA-aldehyde	668.2	44.2	12.7	3.2	3630.1
trans-ABA-aldehyde	21.1	401.6	0.6	6.4	67.0
aba-4					
cis-ABA-aldehyde	1791.4	180.2	23.0	5.2	4756.8
trans-ABA-aldehyde	49.6	1390.0	1.0	31.5	94.0

of $^{18}O_2$. The presence of $^{18}O_2$ during the xanthoxin feed allowed subtraction of any ABA synthesized from endogenous substrates during the experiment, because this ABA was ^{18}O-labeled. Exogenous xanthoxin would not incorporate ^{18}O during oxidation to ABA except via ABA-alcohol (Rock *et al.*, 1991), which is a minor pathway in *Arabidopsis* and amounts to only about 2% of the total ABA (Table 6.3, see below). The results presented in Table 6.5 show that the conversion of xanthoxin to ABA was not affected by the *ABA* locus. There was considerable isomerisation of *t*-xanthoxin, which was metabolized to ABA and then PA (Table 6.5). *Cis*-xanthoxin was also isomerised, but to a lesser extent than *t*-xanthoxin. It has been shown that *t*-xanthoxin is converted to *t*-ABA in tomato plants (Taylor and Burden, 1973; Parry *et al.*, 1988). Only small quantities of [^{18}O]ABA and [^{18}O]*t*-ABA were detected in the xanthoxin isomer feeding experiments (data not shown); if ABA and *t*-ABA were synthesized from ABA-alcohol and *t*-ABA-alcohol, a significant amount of ABA from exogenous xanthoxin would have been ^{18}O-labeled (Rock *et al.*, 1991). The apparent higher xanthoxin and ABA-aldehyde oxidizing activity of the mutant tissue may be a result of the smaller size of the mutant leaves, which resulted in

Table 6.5. Conversion of Xanthoxin Isomers to ABA, *trans*-ABA and Catabolites in Leaves of *Arabidopsis* Wild Type and *aba* Genotypes in $^{18}O_2$

A 2.5 μg cm^{-3} (1 x 10^{-2} mol m^{-3}) solution of *cis*- or *trans*-xanthoxin (both isomers 94% pure) containing 0.05% Tween 20 (vol/vol) was vacuum infiltrated into leaf tissue, which was then put under 20% $^{18}O_2$: 80% N_2 for 8 h. ABA, *t*-ABA, and catabolites were quantified by GC-negative chemical ionization-selected ion monitoring and endogenous (time = 0 h) and *de novo* ABA and catabolites (= ^{18}O-labeled after 8 h) were subtracted from the total to give the amounts of ABA and catabolites synthesized from applied xanthoxin. Results from one of three experiments with similar results.

Genotype/Substrate	ng (g fresh weight)$^{-1}$ (8 h)$^{-1}$				
	ABA	*t*-ABA	ABA-GE	*t*-ABA-GE	PA
Landsberg *erecta*					
cis-xanthoxin	14.1	60.0	0.0[a]	1.7	705.8
trans-xanthoxin	3.3	61.0	0.0	1.4	492.7
aba-1					
cis-xanthoxin	38.5	29.2	0.0	0.9	2788.7
trans-xanthoxin	8.8	94.7	0.0	0.0	431.5
aba-4					
cis-xanthoxin	128.2	104.4	7.6	1.0	3716.6
trans-xanthoxin	67.1	242.0	1.5	12.9	2302.0

[a]After correction for endogenous material.

complete infiltration of substrate into the tissue (C.D. Rock, unpublished observations).

6.5. DISCUSSION

The results presented here suggest that *t*-ABA in *Arabidopsis* is synthesized primarily through a pathway which is distinct from *t*-ABA-alcohol oxidation (Rock *et al.*, 1991). In the presence of $^{18}O_2$, ABA-alcohol and *t*-ABA-alcohol can be oxidized to ABA and *t*-ABA, respectively (Figure 6.1), with incorporation of ^{18}O into the carboxyl group (Rock *et al.*, 1991). In *Arabidopsis*, this pathway accounts for only slighly more than 1 percent of the total [^{18}O]ABA and [^{18}O]*t*-ABA, based on abundance of doubly-carboxyl-labeled ABA and *t*-ABA (Table 6.3, column 5). Feeding experiments by Duckham *et al.* (1989) with deuterated ABA-aldehyde did not result in significant synthesis of *t*-ABA-alcohol in *Arabidopsis*. The results of our ABA-aldehyde isomer feeding experiments (Table 6.4) support the conclusion that isomerization of ABA-aldehyde to give *t*-ABA-alcohol and *t*-ABA is only a few percent of the total ABA biosynthesis. The most likely source of *t*-ABA, therefore, is via a parallel pathway from

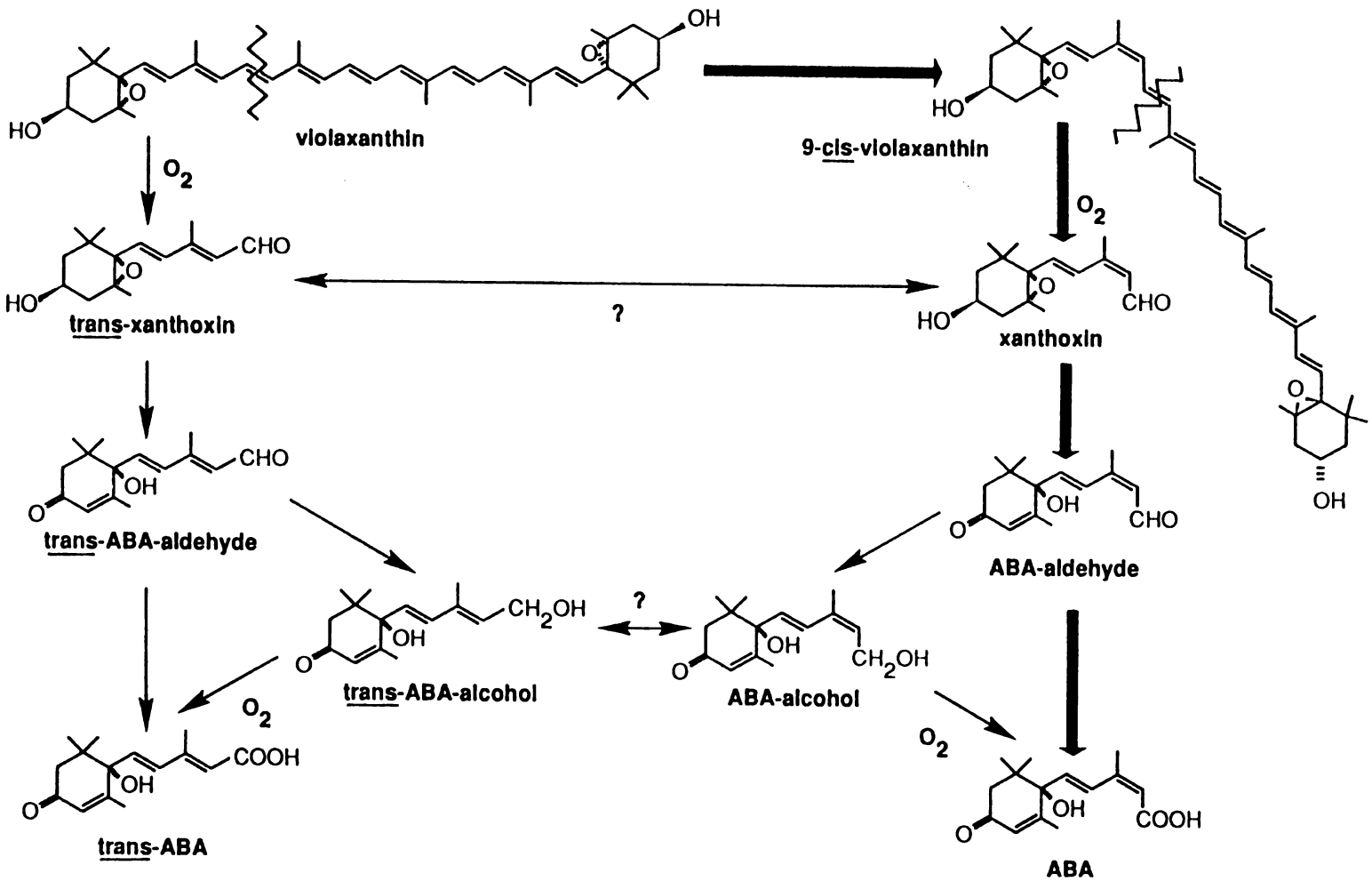
violaxanthin
9-cis-violaxanthin
O2
trans-xanthoxin
?
xanthoxin
trans-ABA-aldehyde
ABA-aldehyde
trans-ABA-alcohol
?
ABA-alcohol
O2
O2
trans-ABA
ABA

Figure 6.1. Proposed pathways of abscisic acid and *trans*-abscisic acid biosynthesis from violaxanthin (neoxanthin is also a substrate for cleavage. The major pathway is denoted by heavy arrows; unknown reactions are shown with question marks.

all-*trans*-epoxy-carotenoids (Rock *et al.*, 1991; Rock and Zeevaart, 1990; Figure 6.1).

There was greater isomerization in the *t*-xanthoxin and RS-[$^2H_6$]*t*-ABA-aldehyde feeding experiments than in the *cis* isomer experiments (Tables 6.4 and 6.5). These observations suggest that *t*-xanthoxin and *t*-ABA-aldehyde may be precursors to ABA in *Arabidopsis* (Figure 6.1). Similar feeding experiments with xanthoxin isomers in tomato shoots by Taylor and Burden (1973) and Parry *et al.* (1988) showed some isomerisation and conversion to ABA isomers; however, labeled ABA catabolites were not quantified in these experiments. High *t*-xanthoxin : xanthoxin ratios have been found in all tissues and species so far examined (Parry *et al.*, 1988, 1990). Xanthoxin and *t*-xanthoxin interconvert non-enzymatically *in vitro* with an equilibrium that favors the *trans* isomer (Parry *et al.*, 1990). Although precautions were taken to minimize isomerization, we cannot rule out artifactual isomerization of xanthoxin isomers during the feeding experiments. Our results suggest that *t*-xanthoxin was isomerized *in vivo* to xanthoxin to a greater extent than xanthoxin to *t*-xanthoxin, which is against the expected direction of the isomerization reaction (xanthoxin --> *t*-xanthoxin; Parry *et al.*,

1990). In the present study, endogenous ABA-aldehyde and *t*-ABA-aldehyde were present in leaves of wild type and *aba* genotypes (data not shown). Thus, a parallel pathway from all-*trans*-epoxy-carotenoids may give rise to *t*-ABA and ABA in *Arabidopsis* (Figure 6.1).

The cause(s) of the relatively high *t*-ABA biosynthetic capacities in the *aba* genotypes (Table 6.2) are not understood. One possible explanation is that epoxy-carotenoid deficiency in the *aba* genotypes results in an altered regulation of the parallel pathways to ABA and *t*-ABA. The cleavage enzyme may utilize *trans*-violaxanthin as a substrate when 9-*cis*-violaxanthin is limiting; isomerisation of the resultant *t*-xanthoxin would contribute to ABA biosynthesis, but would also result in greater *t*-ABA biosynthetic rates. The observation that *trans*-epoxy-carotenoids are more reduced in the *aba* genotypes than 9-*cis*-epoxy-carotenoids (Rock and Zeevaart, 1991) is not inconsistent with this hypothesis. Isolation and characterization of the enzymes involved in ABA biosynthesis may resolve questions of substrate specificity and the multiple pathways of ABA and *t*-ABA biosynthesis.

6.6. LITERATURE CITED

Bangerth F (1982) Changes in the ratio of cis-trans to trans-trans abscisic acid during ripening of apple fruits. Planta **155**: 199-203.

Britton G., 1985. General carotenoid methods. Meth Enzymol **111**: 113-149

Burden RS, Taylor HF (1970) The structure and chemical transformations of xanthoxin. Tetrahed Lett **47**: 4071-4074

Creelman RA, Zeevaart JAD (1984) Incorporation of oxygen into abscisic acid and phaseic acid from molecular oxygen. Plant Physiol **75**: 166-169

Duckham SC, Taylor IB, Linforth RST, Al-Naieb RJ, Marples BA, Bowman WR (1989) The metabolism of *cis* ABA-aldehyde by the wilty mutants of potato, pea and *Arabidopsis thaliana*. J Exp Bot **40**: 901-905

Heath TG, Gage DA, Zeevaart JAD, Watson JT (1990) Role of molecular oxygen in fragmentation processes of abscisic acid methyl ester in electron capture negative ionization. Organ Mass Spectrom **25**: 655-663

Koornneef M, Jorna ML, Brinkhorst-van der Swan DLC, Karssen CM (1982) The isolation of abscisic acid (ABA) deficient mutants by selection of induced revertants in non-germinating gibberellin sensitive lines of *Arabidopsis thaliana* (L.) Heynh. Theor Appl Genet **61**: 385-393

Linforth RST, Bowman WR, Griffin DA, Marples BA, Taylor IB (1987) 2-*trans*-ABA-alcohol accumulation in the wilty tomato mutants *flacca* and *sitiens*. Plant Cell Environ **10**: 599-606

Milborrow BV (1970) The metabolism of abscisic acid. J Exp Bot **21**: 17-29

Netting AG, Milborrow BV, Vaughan GT, Lidgard RO (1988) The fragmentation of methyl abscisate and its 2*E* isomer in methane positive and negative chemical ionization mass spectrometry. Biomed Environ Mass Spectrom **15**: 375-389

Parry AD, Blonstein AD, Babiano MJ, King PJ, Horgan R (1991) Abscisic-acid metabolism in a wilty mutant of *Nicotiana plumbaginifolia*. Planta **183**: 237-243

Parry AD, Neill SJ, Horgan R (1988) Xanthoxin levels and metabolism in the wild-type and wilty mutants of tomato. Planta **173**: 397-404

Parry AD, Neill SJ, Horgan R (1990) Measurement of xanthoxin in higher plant tissues using ^{13}C labelled internal standards. Phytochemistry **29**: 1033-1039

Rock CD, Heath TG, Gage DA, Zeevaart JAD (1991) Abscisic (ABA)-alcohol is an intermediate in ABA biosynthesis in a shunt pathway from ABA-aldehyde. Plant Physiol, submitted

Rock CD, Zeevaart JAD (1990) Abscisic(ABA)-aldehyde is a precursor to, and 1',4'-*trans*-diol a catabolite of, ABA in apple. Plant Physiol **93**: 915-923

Rock CD, Zeevaart JAD (1991) The *aba* mutant of *Arabidopsis thaliana* is impaired in epoxy-carotenoid biosynthesis. Proc Natl Acad Sci USA, submitted

Sindhu RK, Griffin DH, Walton DC (1990) Abscisic aldehyde is an intermediate in the enzymatic conversion of xanthoxin to abscisic acid in *Phaseolus vulgaris* L. leaves. Plant Physiol **93**: 689-694

Sindhu RK, Walton DC (1987) Conversion of xanthoxin to abscisic acid by cell-free preparations from bean leaves. Plant Physiol **85**: 916-921

Sindhu RK, Walton DC (1988) Xanthoxin metabolism in cell-free preparations from wild type and wilty mutants of tomato. Plant

Physiol **88**: 178-182

Taylor HF, Burden RS (1973) Preparation and metabolism of 2-[^{14}C]-*cis,trans*-xanthoxin. J Exp Bot **24**: 873-880

Taylor IB, Linforth RST, Al-Naieb RJ, Bowman WR, Marples BA (1988) The wilty mutants *flacca* and *sitiens* are impaired in the oxidation of ABA-aldehyde to ABA. Plant Cell Environ **11**: 739-745

Walker-Simmons M, Kudra DA, Warner L (1989) Reduced accumulation of ABA during water stress in a molybdenum cofactor mutant of barley. Plant Physiol **90**: 728-333

Walton DC (1983) Structure-activity relationships of abscisic acid analogs and metabolites. *In* FT Addicott, ed, Abscisic Acid. Praeger, New York, pp 113-146

Zeevaart JAD, Creelman RA (1988) Metabolism and physiology of abscisic acid. Annu Rev Plant Physiol Plant Mol Biol **39**: 439-473

Zeevaart JAD, Heath TG, Gage DA (1989) Evidence for a universal pathway of abscisic acid biosynthesis in higher plants from ^{18}O incorporation patterns. Plant Physiol **91**: 1594-1601

CHAPTER 7

^{18}O INCORPORATION INTO VIOLAXANTHIN AND ABSCISIC ACID VIA THE XANTHOPHYLL CYCLE SUPPORTS VIOLAXANTHIN AS A PRECURSOR OF ABSCISIC ACID

7.1. INTRODUCTION

The xanthophylls have been shown to function in a number of physiological processes of importance to plants, such as scavenging of oxygen radicals produced by photooxidation (Cogdell, 1989), photosynthetic light harvesting (Siefermann-Harms, 1985), assembly of light harvesting complexes (Plumley and Schmidt, 1984; Humbeck *et al.*, 1989), ABA biosynthesis (Rock and Zeevaart, 1991), and dissipation of excess light energy through the "xanthophyll cycle" (Demmig *et al.*, 1987; Demmig-Adams *et al.*, 1990). The xanthophyll cycle is the reversible, light-induced deepoxidation/epoxidation of the epoxy-carotenoids violaxanthin and antheraxanthin in the thylakoid membrane (Figure 7.1)(Siefermann-Harms, 1977; Yamamoto, 1979). The product of deepoxidation is zeaxanthin, which has recently been shown to function in the protection of the photosynthetic apparatus by non-photochemical quenching of high-chlorophyll fluorescence, thus preventing photoinhibition by high photon flux densities (Demmig *et al.*, 1987; Demmig-Adams *et al.*, 1990). In order to study the biosynthetic relationship of xanthophylls and ABA, we have utilized the xanthophyll cycle to specifically

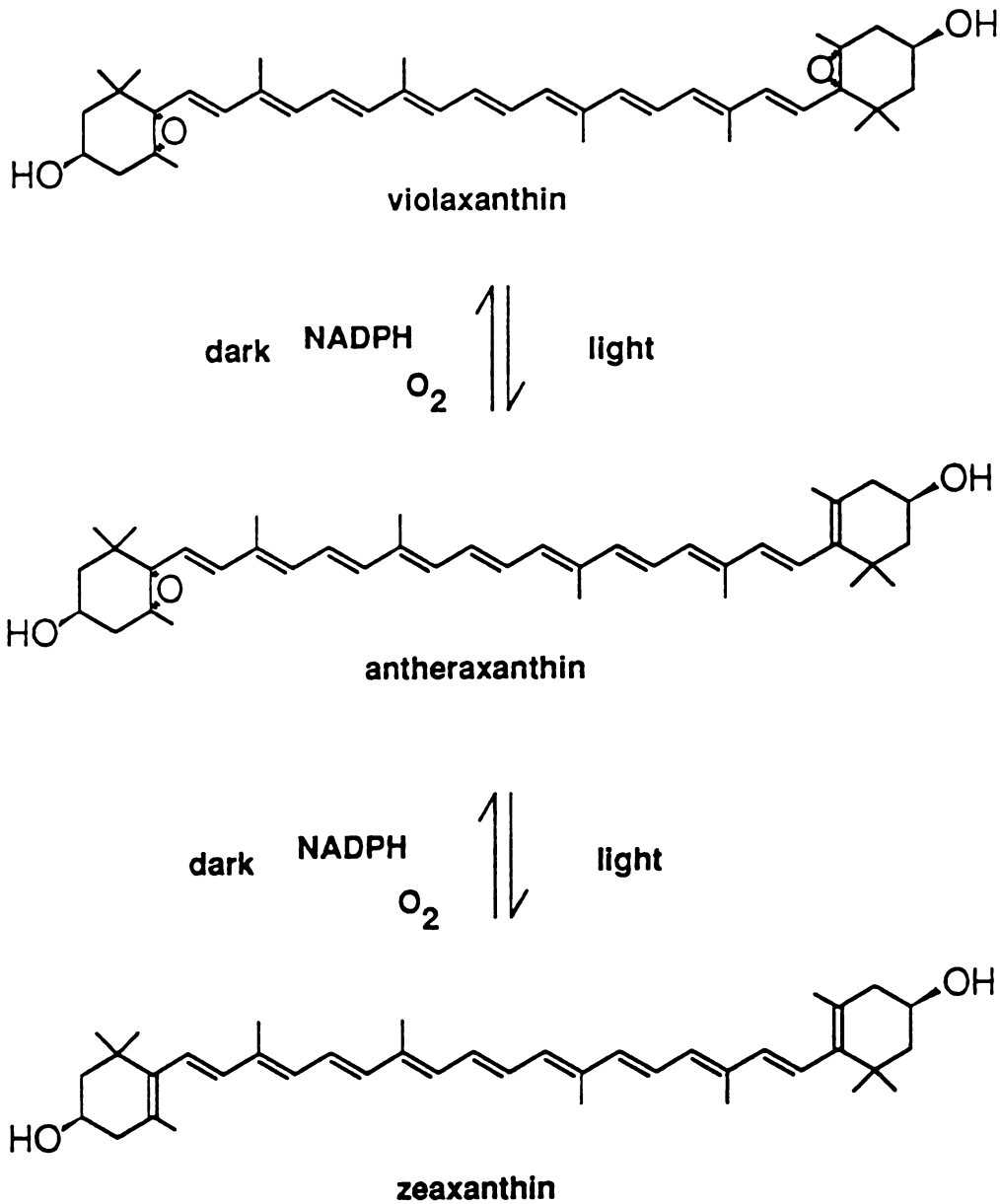

Figure 7.1. The xanthophyll cycle (after Yamamoto, 1979).

pulse-label the epoxide group of violaxanthin and antheraxanthin with ^{18}O and follow ^{18}O incorporation into the 1'-hydroxyl position of [^{18}O]ABA synthesized after water-stress in air. Results of a similar experiment with bean leaves have been reported by Li and Walton (1987).

7.2. MATERIALS AND METHODS

Spinach (*Spinacia oleracea* L., Savoy Hybrid 612, Harris Seed Co., Rochester, NY) was grown as described (Zeevaart, 1971). Fully expanded leaves were excised and immediately weighed and frozen in liquid N_2 for determination of the initial ABA content. About 80 g fresh weight of leaves were arranged in a monolayer in a custom-designed 28 cm x 38 cm x 1 cm vacuum-tight plexiglas case fitted with an O-ring and lined with wet paper towels. The case was sealed with C-clamps and evacuated and flushed with N_2 four times. The case was illuminated through an icewater bath with a 400 W halogen lamp ("multivapor," General Electric) at a photon flux density of 900 $\mu E \cdot m^{-2} \cdot s^{-1}$ for 50 min; this was the length of time found to give the maximum conversion of violaxanthin to zeaxanthin

(data not shown). The case was evacuated and $^{18}O_2$ (97-98% enrichment, Cambridge Isotope Laboratories, Woburn MA) introduced to 20% (v/v) and filled with N_2. The tissue was incubated for 4 h in the dark in $^{18}O_2$, then removed to air and a portion frozen for ABA and xanthophyll determinations. This length of time was sufficient for complete regeneration of the violaxanthin pool (data not shown). The remainder of the sample was water-stressed with a hair dryer until 14% of the fresh weight had been lost, then incubated in air for 2 h and frozen. A control experiment was performed with leaves which were treated as described above, except N_2 was substituted for $^{18}O_2$ after irradiation, and $^{18}O_2$ was substituted for air after water stress.

ABA and xanthophylls were extracted and purified as described (Rock and Zeevaart, 1991). ABA was quantified as the methyl ester derivative by GC-ECD using a standard curve of ABA-Me with dieldrin as an internal standard. Incorporation in [^{18}O]ABA-Me was measured by GC-NCI-SIM and MS/MS as described in Rock and Zeevaart (1990) and corrected for ^{13}C isotope contributions. Incorporation of ^{18}O in *trans*-violaxanthin, 9'-*cis*-neoxanthin, antheraxanthin, zeaxanthin, and lutein was measured by positive ion

FAB-MS on a JEOL-HX110 double focussing mass spectrometer by direct probe in a matrix of nitrobenzyl alcohol (Vetter and Meister, 1985). Nominal mass molecular ions of violaxanthin and neoxanthin gave m/z = 600.4, antheraxanthin m/z = 584.4, lutein, and zeaxanthin, m/z = 568.4. These compounds showed the typical xanthophyll fragment ions of m/z = M^+-80, m/z = 221, and m/z = 181 (Budzikiewicz *et al.*, 1970). The percent ^{18}O incorporation was calculated after correcting for ^{13}C isotope abundance and proton adduct formation, described in Appendix D).

7.3. RESULTS AND DISCUSSION

In order to establish a biosynthetic relationship between xanthophylls and ABA, the amounts of ^{18}O-labeled precursor and product and the position of ^{18}O label must be determined. Figure 7.2 shows the molecular ion (M^+) obtained by FAB-MS of all-*trans*-violaxanthin before and after running the xanthophyll cycle for 4 h in $^{18}O_2$. About 80% of ^{18}O-labeled violaxanthin was doubly-labeled (see Appendix D, Table D.4).

The ^{18}O enrichment of xanthophylls pulse-labeled via the

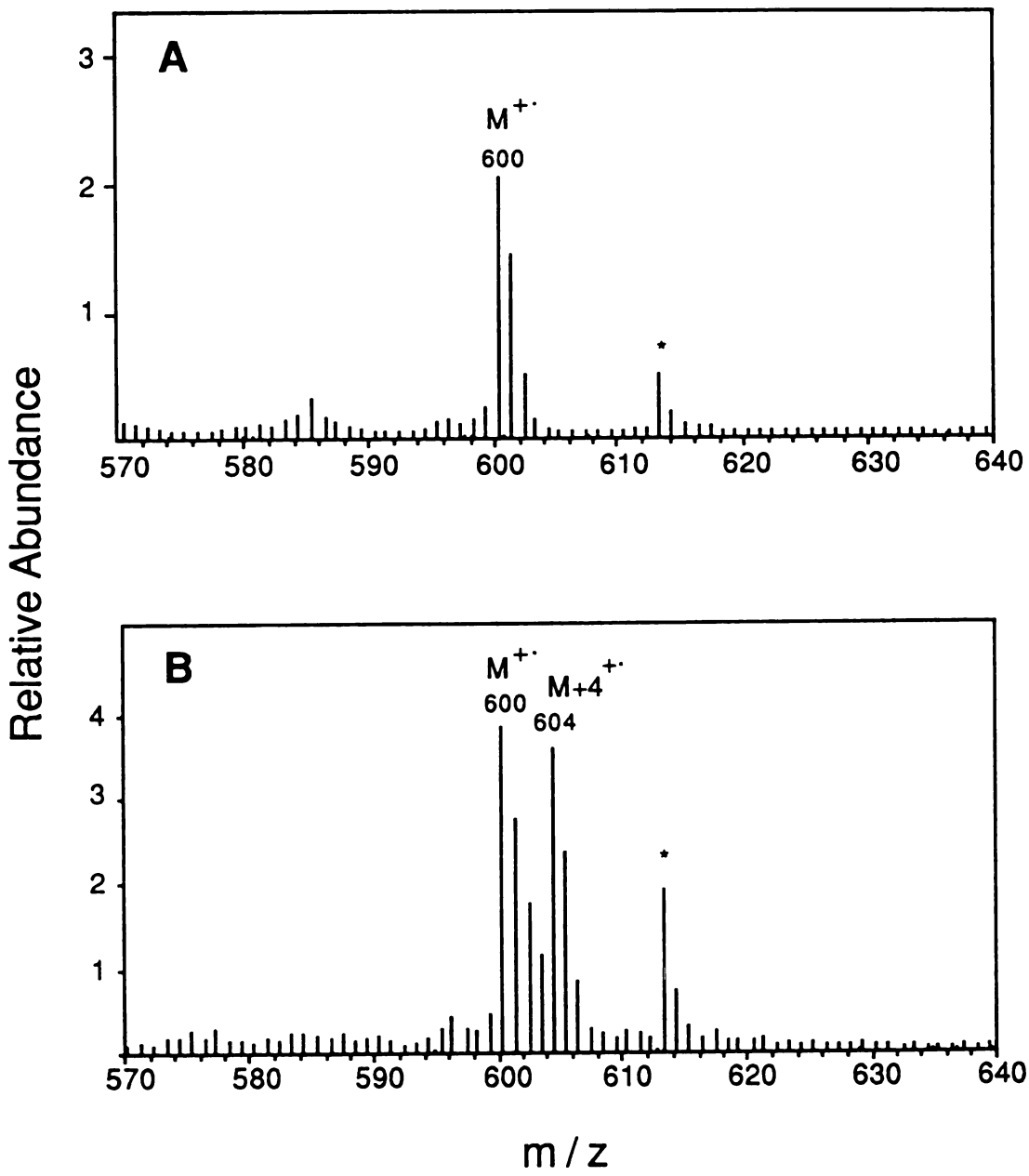

Figure 7.2. Positive ion FAB-mass spectra of the molecular ion cluster of all-*trans*-violaxanthin from unlabeled (A), and ^{18}O-labeled (B) spinach leaves run through the xanthophyll cycle, 4 h in $^{18}O_2$. The asterisk (*) indicates a matrix ion.

xanthophyll cycle is presented in Table 7.1. This analysis reflects the synthesis and turnover rates of the compounds under conditions where violaxanthin and antheraxanthin are de-epoxidated in N_2 in the light and re-epoxidated in 20% $^{18}O_2$ in the dark. Violaxanthin and antheraxanthin were highly enriched with ^{18}O (Table 7.1). The lack of complete labeling in violaxanthin was presumably due to inaccessability of a fraction of the violaxanthin pool to the xanthophyll cycle enzymes (Siefermann and Yamamoto, 1974). The greater enrichment of antheraxanthin compared to violaxanthin (Table 7.1) was due to its smaller pool size and more rapid turnover (data not shown) as an intermediate between zeaxanthin and violaxanthin. Zeaxanthin showed some ^{18}O incorporation into the ring hydroxyl functions (Table 7.1), presumably as a result of *de novo* synthesis from ß-carotene. Antheraxanthin and violaxanthin showed a similarly small enrichment of two and three ^{18}O atoms, or three and four ^{18}O atoms, respectively, as zeaxanthin (see Appendix D, Table D.4). Neoxanthin and lutein are not substrates in the xanthophyll cycle (Yamamoto and Higashi, 1978) and were not ^{18}O-labeled (Table 7.1).

Analysis of [^{18}O]ABA by MS/MS allows determination of the

Table 7.1. ^{18}O Enrichment of Xanthophylls from Spinach Leaves After Running the Xanthophyll Cycle in $^{18}O_2$ for 4 h

Xanthophylls were purified by normal phase HPLC and analyzed by FAB-MS.

Compound	^{18}O Enrichment (percent of molecules)
Trans-violaxanthin	51%
Trans-antheraxanthin	75%
Trans-zeaxanthin	3%
9'-*cis*-neoxanthin	< 1%
Trans-lutein	ND[a]

[a] Not detected

position and extent of ^{18}O label (Rock and Zeevaart, 1990). In Table 7.2 the levels of [^{18}O]ABA and the percentage of [^{18}O]ABA in each oxygen function are presented. When [^{18}O]ABA was analyzed from tissue frozen immediately after ^{18}O labeling, only 20% of the [^{18}O]ABA was labeled in the 1'-hydroxyl function (Table 7.2). In this treatment the bulk of [^{18}O]ABA was carboxyl-labeled (Table 7.2); it is the typical labeling pattern of ABA (Creelman *et al.*, 1987). When the^{18}O xanthophyll cycle material was water-stressed and allowed to synthesize ABA in air after the 4 h $^{18}O_2$ pulse-labeling of violaxanthin, a large increase in the percentage of ^{18}O incorporation into the 1'-hydroxyl was observed (Table 7.2). However, very little [^{18}O]ABA was synthesized by the stressed tissue, only about 5 ng/g fr wt/4 h (Table 7.2, "[^{18}O]ABA" column). It can be deduced that the [^{18}O]ABA synthesized after water stress was nearly entirely labeled in the 1'-hydroxyl position and unlabeled in the carboxyl group to effect the drastic change in labeling patterns from a small amount of additional [^{18}O]ABA. A second conclusion which can be drawn from the results in Table 7.2 is that the bulk of ABA synthesized (about 80%) was unlabeled (compare "Total ABA" *versus* "[^{18}O]ABA" columns). The control experiment with 2 h water-stress in $^{18}O_2$ gave the expected

Table 7.2. Position and Extent of ABA Labeling in Spinach Leaves After Running the Xanthophyll Cycle in $^{18}O_2$ for 4 h

Detached leaves were irradiated in N_2 for 50 min to convert violaxanthin to zeaxanthin, then placed in 20%:80% (v/v) $^{18}O_2$: N_2 for 4 h, and then either frozen or stressed in air for 2 h before freezing. An experiment showing stress-induced ^{18}O incorporation into ABA is included. Samples were quantified as their methyl ester derivatives by GC-SIM and GC-MS/MS (Rock and Zeevaart, 1990).

Treatment	Total ABA	[^{18}O]ABA	Percent [^{18}O]ABA by position		
			4'-keto	1'-hydroxyl	carboxyl
	ng/ g fw	*ng/ g fw/time*			
Control	18.0				
4 hr in $^{18}O_2$,					
no stress	33.0	18.8	2.7	19.8	77.5
4 hr in $^{18}O_2$, 2 hr					
stress in air	125.0	24.0	3.5	63.0	33.5
4 hr in N_2, 2 hr					
stress in $^{18}O_2$	224.0	152.0	1.4	1.0	97.6

high percentage incorporation into the side chain carboxyl group and a high rate of [^{18}O]ABA biosynthesis (Table 7.2). Labeling of the 4'-keto function of ABA (Table 7.2) was consistent with low incorporation into the ring-hydroxyl functions of violaxanthin (Appendix D, Table D.4).

We interpret the results of Tables 7.1 and 7.2 as evidence in support of violaxanthin as a precursor to ABA. Both violaxanthin and 9'-*cis*-neoxanthin are present in spinach leaves at levels approximately 100-fold greater (Khachik *et al.*, 1986) than ABA (Table 7.2). The high percentage of 1'-hydroxyl-labeled [^{18}O]ABA in the pulse chase experiment (Table 7.2) provides evidence for a biosynthetic link between violaxanthin and ABA. Antheraxanthin can also be an ABA precursor based on ^{18}O enrichment (Table 7.1). However, the large, transient changes in antheraxanthin levels in leaves exposed to a high photon flux density suggest it functions solely as an intermediate between violaxanthin and zeaxanthin (data not shown). The lack of ^{18}O incorporation in 9'-*cis*-neoxanthin (Table 7.1) correlates with the lack of [^{18}O]ABA biosynthesis two hours later (Table 7.2). Therefore, 9'-*cis*-neoxanthin could be the source of the unlabeled ABA. This interpretation is supported by

similar results with bean leaves (Li and Walton, 1987). Alternatively, unlabeled violaxanthin could be the source of *de novo* unlabeled ABA.

Subcellular sequestering of xanthophylls (Siefermann and Yamamoto, 1974; Siefermann-Harms *et al.*, 1978; Siefermann-Harms, 1985) suggests that the ABA precursor pool of xanthophylls may not be the same as the xanthophyll cycle pool. However, it is clear that these two pools are connected, based on ^{18}O incorporation into the 1'-hydroxyl position of ABA after labeling violaxanthin through the xanthophyll cycle (Tables 7.1 and 7.2). 9-*Cis*-violaxanthin is probably an intermediate in ABA biosynthesis from violaxanthin; an isomerization reaction from *trans*-violaxanthin has been postulated (Li and Walton, 1990). If the xanthophyll cycle is specific for all-*trans*-violaxanthin (Yamamoto and Higashi, 1978), then isomerization of all-*trans*-violaxanthin to 9-*cis*-violaxanthin must be rapid, considering the [^{18}O]ABA data (Table 7.2). In order to provide stronger evidence for ABA biosynthesis from ^{18}O-labeled xanthophylls, 9-*cis*-violaxanthin could be analysed by FAB-MS to determine if the ^{18}O enrichment is higher than for violaxanthin. Chloroplast envelopes have a separate pool of violaxanthin from the

thylakoids (Siefermann-Harms *et al.*, 1978) and may exhibit different ^{18}O labeling patterns in xanthophyll cycle pulse-chase experiments, providing additional information on the subcellular location of ABA biosynthesis. The rapid and specific ^{18}O labeling of *trans*-violaxanthin by the xanthophyll cycle allows examination of the biosynthetic relationship of violaxanthin to ABA and epoxy-carotenoids such as 9-*cis*-violaxanthin, neoxanthin and 9'-*cis*-neoxanthin.

7.4. LITERATURE CITED

Budzikiewicz H, Brzezinka H, Johannes B (1970) Zur Photosynthese grüner Pflanzen, 2. Mitt.: Massenspektroskopische Untersuchungen Carotinoiden. Monatshefte für Chemie **101**: 579-609.

Creelman RA, Gage DA, Stults JT, Zeevaart JAD (1987) Abscisic acid biosynthesis in leaves and roots of *Xanthium strumarium*. Plant Physiol **85**: 726-732

Cogdell R (1989) Chlorophylls. *In* TW Goodwin, ed, Plant Pigments. Academic, New York, pp 183-230

Demmig B, Winter K, Krüger A, Czygan F-C (1987) Photoinhibition and zeaxanthin formation in intact leaves: a possible role of the xanthophyll cycle in the dissipation of excess light energy. Plant Physiol **84**: 218-224

Demmig-Adams B, Adams WW III, Heber U, Neimanis S, Winter K,

Krüger A, Czygan F-C, Bilger W, Björkman O (1990) Inhibition of zeaxanthin formation and of rapid changes in radiationless energy dissipation by dithiothreitol in spinach leaves and chloroplasts. Plant Physiol **92**: 293-301

Humbeck K, Römer S, Senger H (1989) Evidence for an essential role of carotenoids in the assembly of an active photosystem II. Planta **179**: 242-250

Khachik F, Beecher GR, Whittaker NF (1986) Separation, identification, and quantification of the major carotenoid and chlorophyll constituents in extracts of several green vegetables by liquid chromatography. J Agric Food Chem **34**: 603-616

Li Y, Walton DC (1987) Xanthophylls and abscisic acid biosynthesis in water-stressed bean leaves. Plant Physiol **85**: 910-915

Li Y, Walton DC (1990) Violaxanthin is an abscisic acid precursor in water-stressed dark-grown bean leaves. Plant Physiol **92**: 551-559

Plumley FG, Schmidt GW (1987) Reconstitution of chlorophyll a/b light-harvesting complexes: xanthophyll-dependent assembly and energy transfer. Proc Natl Acad Sci USA **84**: 146-150

Rock CD, Zeevaart JAD (1990) Abscisic (ABA)-aldehyde is a precursor to, and 1',4'-*trans*-diol a catabolite of, ABA in apple. Plant Physiol **93**: 915-923

Rock CD, Zeevaart JAD (1991) The *aba* mutant of *Arabidopsis thaliana* is impaired in epoxy-carotenoid biosynthesis. Proc Natl Acad Sci USA, submitted

Siefermann D, Yamamoto HY (1974) Light-induced de-epoxidation of violaxanthin in lettuce chloroplasts. III. Reaction kinetics and effect of light intensity on de-epoxidase activity and substrate availability. Biochim Biophys Acta **357**: 144-150

Siefermann-Harms D (1977) The xanthophyll cycle in higher plants. *In* M Teveni, HK Lichtenthaler, eds, Lipids and Lipid Polymers

in Higher Plants. Springer-Verlag, New York, pp 218-230

Siefermann-Harms D (1985) Carotenoids in photosynthesis. I. Location in photosynthetic membranes and light-harvesting function. Biochim Biophys Acta **811**: 325-355

Siefermann-Harms D, Joyard J, Douce R (1978) Light-induced changes of the carotenoid levels in chloroplast envelopes. Plant Physiol **61**: 530-533

Vetter W, Meister W (1985) Fast atom bombardment mass spectrum of ß-carotene. Org Mass Spectrom **20**: 266-267

Yamamoto HY (1979) Biochemistry of the violaxanthin cycle in higher plants. Pure Appl Chem **51**: 639-648

Yamamoto HY, Higashi RM (1978) Violaxanthin de-epoxidase: lipid composition and substrate specificity. Arch Biochem Biophys **190**: 514-522

Zeevaart, JAD (1971) Effects of photoperiod on growth rate and endogenous gibberellins in the long-day rosette plant spinach. Plant Physiol **47**: 821-827

CHAPTER 8

CONCLUDING REMARKS

In vivo ^{18}O labeling and analysis of [^{18}O]ABA by tandem mass spectrometry has proven a powerful approach to elucidating the ABA biosynthetic pathway, which is shown in Figure 8.1. This approach established that ABA-aldehyde is a precursor to, and ABA-*trans*-diol a catabolite of ABA. Feeding studies with the synthetic deuterium-labeled ABA analogs ABA-alcohol, ABA-aldehyde, and ABA-*trans*-diol also contributed to understanding the biosynthetic relationships of these compounds in plants. ^{18}O Labeling and FAB-MS analysis of epoxy-carotenoids has provided additional support for the indirect pathway of ABA biosynthesis.

By applying these tools to the study of ABA biosynthesis in ABA-deficient mutants, the biosynthetic blocks in the tomato, potato, barley, and *Arabidopsis* mutants have been identified. The *flacca* and *sitiens* mutants of tomato and *aba* of *Arabidopsis* provide a clear picture of two important components of the ABA pathway: a minor shunt pathway from ABA-aldehyde --> ABA-alcohol --> ABA, and the indirect pathway of ABA biosynthesis from epoxy-carotenoids. Biosynthesis of *trans*-ABA is less clear, but the *aba* mutant provides

support for a parallel pathway from all-*trans*-epoxycarotenoids, and the tomato mutants show that ABA-aldehyde functions as a precursor to *trans*-ABA, albeit a minor pathway. The experimental approach documented here is applicable to the characterization of novel ABA-deficient mutants, which are clearly needed in order to further characterize ABA biosynthesis.

What still remains as a large gap in our understanding of ABA biosynthesis is the characterization of the "cleavage enzyme," which specifically cleaves epoxy-carotenoids and is the most likely biosynthetic step to be regulated by water stress and other environmental and developmental signals. The xanthoxin and ABA-aldehyde oxidase activities are not induced by water stress (Sindhu and Walton, 1987; Sindhu *et al.*, 1990). Another aspect of ABA biosynthesis which warrants attention is the possible role of xanthophyll isomerases (Li and Walton, 1990), which would convert all-*trans*-epoxy-carotenoids to 9-*cis*-epoxy-carotenoids. The existence of a xanthoxin isomerase, which would convert the prevalent 2-*trans*-xanthoxin to *cis*-xanthoxin, should not be discounted.

The long term objective of research into ABA biosynthesis is to

understand the role of ABA in growth and development. Characterization of the enzymes and genes involved in ABA biosynthesis will allow analysis of the molecular mechanisms which regulate plant responses to environmental and developmental signals, and provide a means to critically examine the role of ABA in physiological processes.

8.1 LITERATURE CITED

Li Y, Walton DC (1990) Violaxanthin is an abscisic acid precursor in water-stressed dark-grown bean leaves. Plant Physiol **92**: 551-559

Sindhu RK, Walton DC (1987) Conversion of xanthoxin to abscisic acid by cell-free preparations from bean leaves. Plant Physiol **85**: 916-921

Sindhu RK, Griffin DH, Walton DC (1990) Abscisic aldehyde is an intermediate in the enzymatic conversion of xanthoxin to abscisic acid in *Phaseolus vulgaris* L. leaves. Plant Physiol **93**: 689-694

APPENDICES

APPENDIX A

Table A.1. Partition Coefficients of ABA-Aldehyde, ABA-*trans*-Diol and ABA in Three Different Solvents as a Function of pH

K_d = [solute$_{aqueous}$]/[solute$_{organic}$]. Compounds [10 μg of (±)-ABA-aldehyde and (±)-ABA-*trans*-diol, or 50,000 dpm (±)-ABA (specific activity 110 Ci/mmol)] were added to 10 mL 0.2 M potassium phosphate buffer having the specified pH and partitioned once against an equal volume of solvent, which was collected and dried. The aqueous phase was then adjusted with 1 N HCl to pH 3.0 (for ABA and ABA-*trans*-diol) and partitioned five times with 5 mL ethyl acetate, which was pooled and dried. ABA-*trans*-diol was quantified by GC-electron capture detection, and ABA-aldehyde was quantified by GC-flame ionization detection with eicosane as an internal standard. ABA was measured by scintillation counting. The measured K_ds for ABA correlate well with similar determinations by Ciha *et al.*[a] and Neill and Horgan[b]. The K_d of ABA-aldehyde was not appreciably affected by pH and is smaller (compound more hydrophobic) than that of ABA. ABA-aldehyde was found to be labile in the presence of strong acid or base (data not shown). The K_d of ABA-*trans*-diol was greater than that of ABA (compound more hydrophyllic) and is strongly affected by pH.

Solvent/pH	K_d		
	ABA-aldehyde	ABA-*trans*-diol	ABA
Diethyl ether			
pH 3.5	< 0.1	0.1	0.2
pH 5.0	0.1	0.4	0.4
pH 7.5	0.1	218.0	20.6
pH 8.2	0.1	∞[c]	27.2
pH 10.0	0.1	∞	28.6

Table A.1 (cont'd.)

Solvent/ pH	ABA-aldehyde	ABA-*trans*-diol	ABA
Ethyl acetate			
pH 3.5	< 0.1	< 0.1	0.1
pH 5.0	< 0.1	0.6	0.1
pH 7.5	0.1	242.0	6.8
pH 8.2	0.1	∞	13.0
pH 10.0	< 0.1	∞	27.7
n-Hexanes			
pH 3.5	N.D.[d]	∞	76.9
pH 5.0	19.1	∞	116.3
pH 7.5	15.5	∞	100.0
pH 8.2	11.9	∞	100.0
pH 10.0	4.2	∞	125.0

[a] Ciha AJ, Brenner ML, Brun WA (1977) Rapid separation and quantification of abscisic acid from plant tissues using high performance liquid chromatography. Plant Physiol. 59: 821-826.

[b] Neill SJ, Horgan R (1987) Abscisic acid and related compounds. *In* L Rivier, A Crozier, eds, The Principles and Practice of Plant Hormone Analysis. London, Academic, pp 111-167.

[c] ∞ > 1000

[d] Not determined, recovery too low.

APPENDIX B

Table B.1. Stability of Deuterium Label in ABA-Aldehyde and ABA-*trans*-Diol at Various pHs

Compounds (10 μg) were purified by reverse phase HPLC or incubated at room temperature in the dark for six d in 0.2 M potassium phosphate buffer. The solution was adjusted to pH 7.0 for ABA-aldehdye, or pH 3.0 for ABA-*trans*-diol, and the compounds partitioned into ethyl acetate. Samples were analyzed by GC-negative chemical ionization-selected ion monitoring. Because little exchange occurred in the labeled compounds over extended periods of time at pH extremes, it was concluded that the labeled compounds are suitable for use as internal standards for quantitation and as substrates for *in vivo* feeding experiments.

Treatment	[$^2H_6$]ABA-Aldehyde		[$^2H_7$]ABA-*Trans*-Diol	
	% m/z=248	% m/z=254	% m/z= 280	% m/z=287
Stock solution	0.1	49.7	0.2	56.5
HPLC-purified	0.7	43.5	0.1	57.3
pH 2.8	1.5	35.9	0.2	58.2
pH 5.0	0.5	39.3	0.1	55.0
pH 7.5	1.9	34.1	0.1	56.2
pH 8.2	1.0	45.3	0.1	55.6

APPENDIX C

Table C.1. Correction Factors for Carotenoid Integration Data

The integration data obtained from normal phase HPLC of carotenoid extracts monitored at 450 nm were multiplied by these scalars (Beer's Law is a linear function) to correct for differences in specific extinction coefficients and absorbance at 450 nm. Differences in absorbance at $\lambda_{maximum}$ were calculated from absorbance spectra taken by a Hewlett-Packard 1040M photodiode array detector (kindly provided by Professor Derek Lamport, Michigan State University) which was online with the HPLC effluent.

Carotenoid	Scalar
ß-Carotene	1
Lutein and Isomers	1.0477
Zeaxanthin and Isomers	1.0378
Antheraxanthin	1.1313
Violaxanthin	1.2169
9-*Cis*-Violaxanthin	1.6576
Neoxanthin and 9'-*Cis*-Neoxanthin	1.8391

APPENDIX D

CALCULATIONS OF NATURAL ISOTOPE CONTRIBUTIONS TO MASS SPECTRAL DATA

D.1. Mass Spectral and SIM Data

The standard curve of ABA-Me used to quantify unlabelled and ^{18}O-labeled ABA from plant extracts by GC-SIM does not include data on the naturally abundant heavy isotopes, *i.e.* only the molecular ion abundance (m/z = 278) is integrated over the retention time of the ABA-Me peak. Therefore, to accurately quantify [$^{18}O_n$]ABA-Me (m/z = 280, 282, 284; n = 1-3) from *in vivo* labeling experiments, the theoretical contribution of naturally occurring ^{13}C and ^{18}O isotopes to the heavy classes of ABA-Me must be subtracted. Conversely, when a known amount (determined spectrophotometrically) of an ABA biosynthetic precursor is fed to plant material and the resultant ABA quantified, the heavy isotope contribution must be calculated and added to the measured quantity of ABA in order to accurately determine the biosynthetic capacity of the tissue.

The stable isotope ^{13}C currently comprises 1.115% of the atmospheric CO_2 which is fixed by photosynthesis. Because plants

discriminate against ^{13}C fixation at a level less than 3 percent (Farquhar *et al.*, 1989), the estimate of 1.115% ^{13}C is satisfactory. The probability that any ABA-Me molecule (16 carbon atoms) contains two atoms of ^{13}C can be calculated from a binomial expansion of the natural abundances of ^{12}C and ^{13}C. The percent contribution of ^{13}C at mass $(M + 2)^{\cdot}$ relative to the nominal mass is approximately equal to 0.0060 times the square of the number of carbon atoms present in the molecule (Watson, 1985). Therefore, each heavy class of ABA-Me [$(M + 2)^{\cdot}$, $(M + 4)^{\cdot}$, $(M + 6)^{\cdot}$; m/z = 280, 282, 284] has a ^{13}C contribution to its ion abundance equal to 1.536% [$= 0.006(16)^2$] of the corresponding ion abundance of the class which is two atomic mass units lighter. By subtracting from m/z = 282 the ^{13}C contribution by m/z = 280, one eliminates *bona fide* ^{18}O-labeled ABA-Me that was in fact [$^{13}C_2{}^{18}O$]ABA-Me. When quantifying [^{18}O]ABA, this underestimation of [^{18}O]ABA is small and negligible (< 1.536%). The naturally abundant ^{18}O comprises 0.2% of atmospheric oxygen and therefore contributes an additional 0.8% of the ion abundance at m/z = 278 to the abundance of ABA-Me m/z = 280 (because there are four oxygens in ABA-Me). Contributions to [$^{18}O_2$]ABA and [$^{18}O_3$]ABA due to naturally occurring ^{18}O are not included because

the ^{18}O labeling experiments preclude this effect.

As an example, Table D.1 shows the measured and transformed data of an [^{18}O]ABA sample from the experiment reported in Chapter 7 (Table 7.2). The individual classes of [^{18}O]ABA (one, two, or three ^{18}O atoms) can be expressed as a percentage of total [^{18}O]ABA, which is an important parameter when analyzing MS/MS data.

D.2. MS/MS Data

Interpretation of MS/MS data is also complicated by ^{13}C isotope effects. When parent ions are selected in a triple quadrupole mass spectrometer to determine the position of ^{18}O labeling, ABA-Me molecules containing two ^{13}C atoms are also included in the analysis. Their relative abundance in the daughter ion spectrum is a result of the abundance of ABA-Me molecules which are two atomic mass units lighter than the parent ion. When there is only slight ^{18}O enrichment in ABA-Me, the ^{13}C effects are proportionally large.

Quantification by MS/MS of [^{18}O]ABA labeling patterns is confined to ^{18}O incorporation in the side chain of ABA-Me because of the lack of proton extraction effects and the abundance of ions

Table D.1. Example of SIM Data Correction for ^{13}C and ^{18}O Natural Abundance Contributions

m / z	Measured Area (A)	Correction Term	Transformed Area
278	59.420	none	59.420
280	14.034	$A_{278}(0.02336)$	12.646
282	1.606	$A_{280}(0.01536)$	1.390
284	0.034	$A_{282}(0.01536)$	0.009

% [^{18}O]ABA of total = 19.12%

% m/z 280 of [^{18}O]ABA = 90.04%

% m/z 282 of [^{18}O]ABA = 9.90%

% m/z 284 of [^{18}O]ABA = 0.06%

produced (daughter fragment m/z = 141; see Heath *et al.*, 1990). If ^{18}O is incorporated in the side chain of [^{18}O]ABA-Me, the side chain daughter ion is shifted to m/z = 143 or 145 for one or two ^{18}O atoms, respectively. The presence of ABA-Me molecules with two ^{13}C atoms produces side chain fragment ions with m/z = 141, 142, and 143 because there is a distribution (assumed random) of the two ^{13}C atoms in the carbon skeleton of ABA-Me. Furthermore, ions at m/z = 143, 144, and 145 can be the result of one ^{18}O atom and two ^{13}C atoms in the ABA-Me molecule. This mixed labeling of ABA-Me by experiment-derived ^{18}O and naturally abundant ^{13}C is subtracted from the data to allow calculation of ^{18}O labeling patterns of the nominal mass of ABA-Me plus ^{18}O. This method assumes the labeling patterns of ^{13}C-containing ABA-Me are identical to those of unlabeled material (*i.e.*, no isotope discrimination by ABA biosynthesis enzymes).

The observed MS/MS data for m/z = 142 and 144 (one ^{13}C in the side chain) can be used to calculate the theoretical ^{13}C contributions to the ion abundance at m/z = 141, 143, and 145. The number of possible positions of two ^{13}C atoms in ABA-Me is determined by a "combinations formula" which gives the number of

different combinations of n objects taken r at a time (different orders of the same r not counted separately).

$$C_{n,r} = \frac{n!}{(n-r)!\,r!} .$$

For ABA-Me (16 carbons, $n = 16$), there are 120 different ways to have two ^{13}C atoms ($r = 2$) in the same molecule:

$$\frac{16!}{(16-2)!2!} = 120 .$$

For the side chain of ABA-Me ($n = 7$), there are 21 possible ways to have two ^{13}C atoms. For the ring moiety of ABA-Me ($n = 9$), there are 36 possible ways to have two ^{13}C atoms. Therefore, the number of possible ways to have one ^{13}C atom in the ring and one in the side chain is the difference between the total possible ways to have two ^{13}C atoms in ABA-Me (120) and the possible ways to have both ^{13}C atoms in either the ring or the side chain (21 + 36), which equals 63. The probabilities for each possible side chain labeling pattern (zero, one or two ^{13}C atoms) are calculated as follows.

1) The probability that one ^{13}C atom is in the side chain = 63/120.

2) The probability that two ^{13}C atoms are in the side chain = 21/120.

3) The probability that zero ^{13}C atoms are in the side chain (both in the ring) = 36/120.

Now the ratio of probabilities can be used as a scalar of the observed ion intensity at m/z = 142 (or 144) to calculate the theoretical contribution of ion intensity at m/z = 141 and 143 (or 143 and 145). A simple linear equation is set up, where theoretical probability equals the observations:

$$\frac{\text{Unknown contribution to ion abundance at m/z 141}}{\text{Observed ion abundance at m/z 142}} = \frac{\text{Probability of } ^{13}C \text{ contributing to m/z 141}}{\text{Probability of } ^{13}C \text{ contributing to m/z 142}}$$

or, rearranged:

Unknown contribution to ion abundance at m/z 141 =

[Observed ion abundance at m/z 142][(36/120)/(63/120)]

= 0.571[Observed ion abundance at m/z 142)].

Similarly, the unknown contribution to ion abundance at m/z 143 =

[Observed ion abundance at m/z 142][(21/120)/(63/120)]

= 0.333[Ion abundance at m/z 142].

In Table D.2 the measured data from Table 7.2 are given as an example of the corrections made to allow calculation of the extent and position of ^{18}O labeling as a percentage of total [^{18}O]ABA. Note that in this example m/z = 284 data are not included. The MS/MS data of a given mass is "weighted" by multiplying its percentage contribution to the total [^{18}O]ABA (*e.g.*, m/z 280 =90.04%, from Table D.1). The results are shown in Table D.3.

D.3. FAB-MS of Carotenoids

Because carotenoids have 40 carbon atoms and FAB-MS generates a significant amount of proton adducts (Watson, 1985), the isotope effect is a large factor when quantifying ^{18}O enrichment of carotenoids. The proton adduct effect, which is unique for each carotenoid structure (data not shown), precludes an accurate measurement of ^{18}O enrichment from data on the molecular ion cluster. Therefore, the assumption is made that loss of protons is negligible and that adduct formation is not dependent on mass (no

Table D.2. Example of MS/MS Data Correction for ^{13}C Natural Abundance Contributions

m/z	Observed			Transformed		Percent	
	m/z= 141	m/z= 142	m/z= 143	m/z= 141	m/z= 143	ring	side chain
280	125242	8711	74301	120268	71400	62.75	37.25
282	2022	N.D.[a]	20311	2022	20311	9.05	90.95

[a] Not detected.

Table D.3. Calculation of ABA Labeling Patterns from Corrected SIM and MS/MS Data

	Percent of Total [^{18}O]ABA				
	Unlabeled in Carboxyl		One ^{18}O Atom in Carboxyl		
	one in ring	two in ring	zero in ring	one in ring	two in ring
	(0.9004)(62.75)	(0.0990)(9.05)	(0.9004)(37.25)	(0.0990)(37.25)	trace
=	56.50	0.90	33.54	3.69	trace

isotope effects); ^{18}O incorporation can then be determined by empirical methods with a precision of a few percent. This is accomplished by analysis of unlabeled and ^{18}O-labeled carotenoid samples by FAB-MS under identical ionization conditions. The measured data for the molecular ion cluster are normalized (*e.g.*, as percentage of nominal mass abundance). Then two transformations of the raw data are performed: a) the correction for proton adduct formation, and b) the correction for ^{13}C isotope contributions to ^{18}O-labeled ions.

In order to correct the observed data for proton adduct formation of each carotenoid, a scalar factor, $a_{carotenoid}$, representing the fractional contribution of the molecular ion (M^+) to the ion abundance at $(M + 1)^+$, is calculated from the observed ion abundance at $(M + 1)^+$ of a given unlabeled carotenoid, minus the theoretical contribution (44.6% of M^+) from ^{13}C:

$$a_{carotenoid} = \frac{\%(M + 1)^+_{observed} - 44.6}{100} .$$

This scalar is then used to transform the measured data so that an accurate estimate of actual ^{18}O-labeled and unlabeled compounds is

obtained. For the unlabeled nominal mass the proton adduct contribution to $(M + H)^+$ is added back to $M^+_{observed}$:

$$M^{+actual} = M^+_{observed} + a_{carotenoid} M^+_{observed} .$$

For labeled masses, only ^{18}O-labeled ion abundances are desired. Therefore, the observed ion abundance from the unlabeled control is subtracted from the observed ion abundance of the labeled sample and corrected for proton adduct affects:

$$(M + x)_{labeled\ corrected,\ x=\ 2\ -->8}$$
$$= (M + x)_{labeled\ observed} - (M + x)_{unlabeled\ observed}$$
$$- a(M + x - 1)_{labeled\ corrected} .$$

The transformations proceed sequentially from $(M + 2)^+$ to $(M + 8)^+$, if the carotenoid has four oxygen atoms. Note that this correction does not apply to the $(M + H)^+$ ion; the $(M + H)^+_{labeled\ corrected}$ value is 44.6 in the $(M + 2)^+_{labeled\ corrected}$ calculation.

After the data are transformed to corrected ^{18}O ion abundances, the ^{13}C isotope contribution to the data can be subtracted (step b). It is assumed that the ^{18}O labeling patterns of ^{13}C-labeled carotenoids are identical to the nominal mass ^{18}O labeling patterns (no isotope discrimination). Thus the calculation of

carotenoid labeling patterns is simplified and comparable to the ABA calculations. Based on the theoretical ^{13}C contribution to $(M + 2)^+$ [$40^2(0.006) = 0.096$], one can subtract 9.6% of the corrected ^{18}O ion abundance at $(M + 2)^+$, $(M + 4)^+$, and $(M + 6)^+$ from the ion abundance at $(M + 4)^+$, $(M + 6)^+$, and $(M + 8)^+$, respectively [the $(M + 2)^+$ data were already corrected empirically by subtraction].

Now the actual percent ^{18}O incorporation can be calculated. Only "actual" data for M^+, $(M + 2)^+$, $(M + 4)^+$, $(M + 6)^+$, and $(M + 8)^+$ are neccessary, because only nominal masses plus experimental ^{18}O masses are included.

$$\% \text{ enrichment} = \frac{100[(M + 2) + (M + 4) + (M + 6) + (M + 8)]}{M + (M + 2) + (M + 4) + (M + 6) + (M + 8).}$$

Enrichment of individual masses can also be calculated as a percentage of total ^{18}O-labeled sample from these corrected data. An example of these calculations is given in Table D.4.

D.4. LITERATURE CITED

Heath TG, Gage DA, Zeevaart JAD, Watson JT (1990) Role of molecular oxygen in fragmentation processes of abscisic acid methyl ester in electron capture negative ionization. Org Mass Spectrom **25**: 655-663

Table D.4. Example of [^{18}O]Violaxanthin FAB-MS Data Correction for ^{13}C Natural Abundance and Proton Adduct Contributions

Sample	Observed	Corrected[a]	Actual[b]
Unlabeled Violaxanthin			
M^+	100	124.1	
$(M + H)^+$	68.7	---	
$(M + 2)^+$	22.0	---	
$(M + 3)^+$	5.8	---	
$(M + 4)^+$	1.5	---	
Labeled Violaxanthin			
M^+	100	124.1	124.1
$(M + H)^+$	72.2	44.6	
$(M + 2)^+$	46.4	13.6	13.6
$(M + 3)^+$	30.3	21.2	
$(M + 4)^+$	93.4	86.8	85.5
$(M + 5)^+$	59.6	38.7	
$(M + 6)^+$	21.6	12.3	4.0
$(M + 7)^+$	5.6	2.6	
$(M + 8)^+$	3.6	3.0	1.8

[a] Calculated as: $(M + x)_{\text{labeled corrected, x= 2 -->8}} = (M + x)_{\text{labeled observed}} - (M + x)_{\text{unlabeled observed}} - a(M + x - 1)_{\text{labeled corrected}}$ where $a_{\text{violaxanthin}} = 0.687 - 0.446 = 0.241$. See (a) in text.

[b] Calculated as $(M + x)_{\text{actual, x = 4,6,8}} = (M + x)_{\text{corrected}} - 0.096(M + x - 2)_{\text{corrected}}$. Actual percent enrichment for this sample = 45.8% (see step b, text).

Farquhar GD, Ehleringer JR, Hubick KT (1989) Carbon isotope discrimination and photosynthesis. Annu Rev Plant Physiol Plant Mol Biol **40**: 503-537

Watson JT (1985) Introduction to Mass Spectrometry, 2nd ed. Raven Press, New York